UNCONVENTIONAL RADICAL MINIEMULSION POLYMERIZATION

A Dissertation
Presented to
The Academic Faculty

by

Qi, Genggeng

In Partial Fulfillment
of the Requirements for the Degree
Doctor of Philosophy in the
School of Chemical & Biomolecular Engineering

Georgia Institute of Technology
December 2008

UNCONVENTIONAL RADICAL MINIEMULSION POLYMERIZATION

Approved by:

Dr. F. Joseph Schork, Advisor
School of Chemical & Biomolecular Engineering
Georgia Institute of Technology

Dr. Athanasios Nenes
School of Chemical & Biomolecular Engineering
Georgia Institute of Technology

Dr. Christopher W. Jones, Advisor
School of Chemical & Biomolecular Engineering
Georgia Institute of Technology

Dr. Andrew Lyon
School of Chemistry & Biochemistry
Georgia Institute of Technology

Dr. William J. Koros
School of Chemical & Biomolecular Engineering
Georgia Institute of Technology

Date Approved: October 23, 2008

Dedicated to

my parents

who have supported me all the way

ACKNOWLEDGEMENTS

I would like to thank all people who have helped and inspired me during my doctoral study.

I wish to express my most sincere gratitude to my advisors, Dr. Joseph Schork and Dr. Christopher Jones, for allowing me join the group in 2003 and for their continuous encouragement, support and guidance throughout the past five years. Their scientific intelligence and enthusiasm have inspired me to new research ideas. It is their trust and confidence that motivates me to probe into the unexplored research fields in my work. Their logical way of thinking, critical attitude and integral view on research enriched my growth as a researcher. Their thoughtful and elaborative advice was vital in the development of my presentation and writing skills.

I would like to thank Dr. William Koros, Dr. Athanasios Nenes and Dr. Andrew Lyon for serving on my committee and providing valuable suggestions during this work. I am also deeply grateful to Dr. William Koros for his time and help in settling down my post doctoral training.

I would also like to thank the Schork and Jones group members, especially Dr. James Russum and Dr. Wilfred Smulders, and two undergraduates, Michael Nolan, and Bennett Eleazer, for their able assistance and valuable suggestions in our or my work. Many thanks go out to my friends at Georgia Tech, Ying Wang, Jing Su, Zhaohui Tong, Reginard Thio, Yonghao Xiu and all others I can not fully list here.

My parents deserve special gratitude for their prayers, encouragement and trust. I have to say sorry to them since I did not get a chance to come back home and visit them in the past 5 years. I owe them too much.

Finally, the financial support from NSF and other sources is gratefully acknowledged.

TABLE OF CONTENTS

LIST OF TABLES

LIST OF FIGURES

NOMENCLATURE

a	Radius of droplets, m
$\bar{a}$	Number average radius of droplets, m
a_c	Critical radius, m
C_i	Concentration of component *i* in the medium, mol/L
$C_i^{'}$	Concentration of component *i* in bulk, mol/L
C_i^{surf}	Concentration of component *i* at the surface of droplets, mol/L
D_i	Diffusion constant of component *i* in the medium, m^2/s
J_i	Flux of composition *i* between the droplets and the medium, mol/s
$N_{0,0}$	Fraction of particles containing no radical
$N_{1,0}^m$	Fraction of particles containing one monomeric radical
$N_{1,0}^p$	Fraction of particles containing one polymeric radical
$N_{0,1}^m$	Fraction of particles containing one RAFT intermediate radical whose two arms are less than critical degree
$N_{0,1}^{mp}$	Fraction of particles containing one RAFT intermediate radical whose one arm is less than critical degree while another is larger than critical degree
$N_{0,1}^p$	Fraction of particles containing one RAFT intermediate radical whose two arms are larger than critical degree
k_{add}	Addition coefficient of a polymeric radical to RAFT agent, $L/mol \cdot s^{-1}$
k_{-add}	Addition coefficient of a monomeric radical to RAFT agent, $L/mol \cdot s^{-1}$
k_f	Exiting coefficient of a monomeric radical to the continuous phase, s^{-1}

k_{mf} Chain transfer coefficient of a polymeric radical to monomer, L/mol·s^{-1}

$k_{frag}^{\ m}$ Fragment coefficient of RAFT intermediate radicals whose two arms are shorter than critical degree, mol/L·s^{-1}

$k_{frag}^{\ mp}$ Fragment coefficient of RAFT intermediate radicals (one arm is shorter while the other is larger than critical degree) into a macro RAFT agent and a monomeric radical, mol/L·s^{-1}

$k_{-frag}^{\ mp}$ Fragment coefficient of RAFT intermediate radicals (one arm is shorter while the other is larger than critical degree) into a oligomeric RAFT agent and a polymeric radical, mol/L·s^{-1}

$k_{frag}^{\ p}$ Fragment coefficient of RAFT intermediate radicals whose two arms are larger than critical degree, mol/L·s^{-1}

k_p^1 Propagating coefficient of a monomeric radical, L/mol·s^{-1}

$[RAFT]_m$ Concentration of original or oligomeric RAFT agent, mol/L

$[RAFT]_p$ Concentration of macro RAFT agent, mol/L

V_{mi} Partial molar volume of component *i*, L/mol

x_i Molar fraction of component *i* in the droplets

x_{ic} Molar fraction of component *i* in the droplets at a_c

Greek letters

μ_i^0 Chemical potential of component *i* under the standard state

$\mu_i^{'}$ Chemical potential of component *i* in bulk

μ_i^{drop} Chemical potential of component *i* in the droplets

μ_i^{surf} Chemical potential of component *i* at the droplets' surface

ρ_{re} Reentry rate of monomeric radicals, s^{-1}

ρ Total entry rate of radicals, s^{-1}

ρ_I	Entry rate of initiator derived radicals with a chain length larger than critical degree, s^{-1}
σ	Surface tension of miniemulsions, N/m
ϕ_i	Volume fraction of component *i* in the droplets

SUMMARY

Conventional free-radical miniemulsion polymerization has been well studied since its birth in early 1970s. Conventional free-radical miniemulsion polymerizations have inherent limitations associated with uncontrolled free-radical polymerization mechanism. The goal of this work is to develop a variety of unconventional miniemulsion polymerization techniques by applying new polymerization techniques (typically in solution or bulk) to miniemulsion systems to overcome their inherent limitations and extend the application of free-radical miniemulsion polymerization.

This work focused on the exploration of kinetic and mechanistic aspects of unconventional miniemulsion polymerizations. First, enzyme initiated free-radical miniemulsion polymerization, in contrast with those conventional chemical initiated miniemulsion polymerization, is demonstrated for the first time as an answer to the challenges associated with using the hydrophobic of vinyl monomers in aqueous enzymatic reactions. A procedure for enzyme initiated free-radical miniemulsion polymerization was formulated and stable poly(styrene) latexes were successfully synthesized. The kinetics of enzyme initiated free-radical miniemulsion polymerization and the effect of reaction conditions on the polymerization was elucidated. Second, RAFT miniemulsion polymerization of hydrophobic monomers was performed in CSTR trains and the transient states, previously identified by others in our group, were elucidated. Next, RAFT miniemulsion polymerization of a partially water soluble monomer was studied. RAFT miniemulsion polymerizations of γ-methyl-α-methylene-γ-butyrolactone, a partially water soluble lactone monomer derived from renewable sources, was successfully formulated. Homogeneous nucleation was found to play an important role in the free-radical "miniemulsion" homopolymerization of MeMBL. By using styrene as a comonomer, the RAFT miniemulsion polymerizations of MeMBL and styrene were well controlled and narrowly distributed copolymers of MeMBL/styrene were produced. Following the study of the partially water monomer, RAFT inverse miniemulsion polymerization was proposed for the polymerization of hydrophilic monomers. The kinetics of RAFT inverse miniemulsion polymerization of acrylamide

exhibited the typical behavior of controlled polymerizations up to high conversions. The effects of reaction parameters on the polymerization rate and particle size were investigated. The dominant locus of radical generation for particle nucleation and the fate of desorbed monomeric radicals in inverse miniemulsion polymerizations were evaluated. Finally in this work, conclusions and implications are presented and ideas for future work are suggested.

CHAPTER 1

INTRODUCTION

1.1 Conventional Free-radical Miniemulsion Polymerizations

1.1.1 Definition of miniemulsions and conventional miniemulsion polymerizations

Emulsions are dispersions of liquid droplets (dispersed phase) in another immiscible liquid (continuous phase) created with the aid of surfactants. Most emulsions are oil-in-water systems and can be roughly classified into three categories according to their physical properties such as droplet size, turbidity and stability: macroemulsions, miniemulsions and microemulsions.[3]

Macroemulsions, as the name implies, have the largest average droplet size of the three types of emulsions, and the droplets vary from hundreds of nanometers to tens of microns. Because of the relatively large size and the coarseness of droplets, macroemulsions tend to be milky and liable to phase separation. Microemulsions, however, are thermodynamically stable transparent emulsion systems that are only heterogeneous on the molecular scale because of a relatively high amount of surfactants employed.[4] Under different conditions, different forms of micro domains instead of large droplets can be dominant in microemulsions, such as bicontinuous phases, nano-globules, micelles and liquid crystals. These domains fluctuate in size and shape by spontaneous coalescence and break-up, and have a typical equilibrium size about 10-50nm.

Conventional miniemulsions are aqueous dispersions of relatively stable oil droplets with a size range of 50-500nm prepared by strong shearing of a system containing oil, water, surfactants, and costabilizers.[5] A costabilizer is an osmotic agent to limit the diffusion degradation of miniemulsions, which will be discussed in the next section more in detail. Long chain alkanes and alcohols, e.g. hexadecane and cetyl alcohol, have proven to be good costabilizers in miniemulsions. [6-8] Polymers, chain transfer agents and comonomers can be also used as costabilizers.[9-11] The most common

type of miniemulsion polymerization is free-radical polymerization of oil soluble monomers in an aqueous continuous phase, initiated by common chemical initiators such as azo initiators or peroxides. “Conventional” is used here to describe such a class of miniemulsion polymerizations, in contrast with other types of miniemulsion polymerizations that will be discussed in the following chapters.

1.1.2 Characteristics of conventional miniemulsion polymerizations

Conventional miniemulsion polymerizations have several features similar to either macroemulsion polymerizations or microemulsion polymerizations, but even more characteristics distinguishing them from the other two types of emulsion polymerizations. Before going through these characteristics, it is important to discuss briefly the stability of emulsions and particle nucleation mechanisms in typical emulsion polymerizations.

Stability of emulsions

To achieve a good stability, emulsions have to be appropriately formulated against two main kinds of degradation: diffusional degradation and droplet coalescence. Once an oil-in-water emulsion is created, there exists a distribution of emulsion droplet sizes. The size difference results in Laplace pressure which causes a net mass transport of monomers from smaller droplets to larger ones by molecular diffusion through the continuous phase, or Ostwald ripening. [12] With the disappearance of smaller droplets, the average droplet size increases and this leads to phase separation. To avoid the diffusional degradation, a small amount of ultrahydrophobe called a costabilizer, can be added to the dispersed phase. If there is diffusion of monomers between different sized droplets, the concentration of the costabilizer would increase in the small droplets but decrease in the large ones. The osmotic pressure of the ultrahydrophobe would thus balance the Laplace pressure and stop the diffusion. Meanwhile, destabilization of emulsions can also occur by droplet collision and coalescence. Suitable amounts of surfactant can be employed in the emulsions to build electrostatic or steric forces and prevent droplet coalescence.

Particle nucleation

Monomers partition in different phases of emulsions: monomer-swollen surfactant micelles, the continuous phase, and emulsion droplets. Based on the dominant phases of nucleation, the mechanism of particle nucleation can be classified into three categories:[13]

1. Micellar nucleation

   Initiator radicals generated in the aqueous phase enter the monomer-swollen micelles, as primary or oligomeric radicals, and initiate polymerization to form monomer-swollen polymer particles.

2. Homogeneous nucleation[14]

   The initiator radicals propagate to a certain degree by reaction with monomer units and precipitate out from the continuous phase. Stabilized with a certain amount of surfactants, primary particles can form from the oligomeric radicals. The primary particles can keep growing into polymer particles by propagation of the oligomeric radical with the absorbed monomer, or coagulation with themselves.

3. Droplet nucleation

   Radicals generated in the aqueous phase enter the emulsion droplets as single or oligomeric radicals and propagate in the droplets to form particles.

With this information, we can now compare conventional miniemulsion polymerization and macroemulsion polymerization. There are significant physical difference between conventional miniemulsions and macroemulsions:

1. Average droplet size. Conventional macroemulsions consist of large monomer droplets in microns while around droplets are 50-500nm for miniemulsions.
2. Stability. The droplets in macroemulsions are typically very unstable due to coalescence and Ostwald ripening, followed by Stokes law creaming. It has been shown that this degradation of macroemulsions can be very fast.[15] For miniemulsions, the droplet distribution is relatively narrow due to strong shearing force or sonication. The shelf life of miniemulsions is much longer than macroemulsions thanks to the use of costabilizers. The small droplet size prevents Stokes law creaming.
3. Surfactant concentration. The desired surfactant concentration in a miniemulsion is below critical micelle concentration (CMC), resulting in ideally no micelles or

very few micelles in the aqueous phase. On the other hand, the surfactant concentration in macroemulsion varies significantly and can be above CMC in many cases.

Moreover, conventional miniemulsion polymerizations are distinguished from macroemulsion polymerizations based on the dominant particle nucleation mechanism. Conventional macroemulsion polymerizations usually follow a micellar nucleation mechanism and the polymerization process can be divided into three intervals. [16] In principle, all micelles become nucleated in interval I, usually at a low conversions of about 2-10 %. During Interval II, the number of monomer swollen particles keeps constant and the particles grow at a constant rate by the polymerization of monomer from the droplet reservoirs. Interval III begins when the droplets disappear (typically at 40-50% conversion) and continues to the end of the reaction. In contrast, droplet nucleation is the dominant process in miniemulsion polymerization. The droplets act as nanoreactors, therefore, the kinetics of miniemulsion polymerizations are sometimes similar to their bulk or solution counterparts. It is also worthy to note that in an miniemulsion polymerization without the intervention of a phase-transfer event, a radical in one particle has no direct access to a radical in another particle, i.e. the radicals are compartmentalized and therefore, the termination rate can be reduced in miniemulsion polymerizations. The effect of compartmentalization has profound effects on the kinetics of miniemulsion (and macroemulsion) polymerizations, which will be discussed in the following chapters in more detail.

The differences between conventional miniemulsion polymerizations and microemulsion polymerizations are even more significant. Certain physical properties of these two emulsions can be criteria to distinguish them:

1. Interfacial tension. The large amount of surfactants in microemulsions leads to complete surfactant coverage of the micro domains, and thus a very low surface tension. For conventional miniemulsions, however, a low surfactant concentration is required to minimize the potential existence of micelles in the aqueous phase. The interfacial tension is much larger than in microemulsions due to insufficient surfactant coverage of the droplet surface.

2. Average droplet size. The droplet size range of miniemulsions is from 50nm to 500nm. For microemulsions, the micro domains have a size below 100nm, usually in the range of 10-50nm.
3. Turbidity. Miniemulsions tend to have much higher turbidity than microemulsions. Miniemulsions appear milky while microemulsions are usually transparent.
4. Stability. Conventional miniemulsions are kinetically stable and generally have a shelf life from hours to several months with the help of costabilizers. Microemulsions are thermodynamically stable phasses whose shelf lives are even longer than those of miniemulsions.

Other than the physical differences, micellar nucleation and homogeneous nucleation are dominant nucleation processes for microemulsion while droplet nucleation dominates for miniemulsion.

As a summary, the characteristics of miniemulsions are summarized as follows: [17]

1. Steady-state dispersed miniemulsions are kinetically stabilized systems thanks to the use of costabilizers. High shearing forces are needed for the formation of miniemulsions.
2. The interfacial tension between the oil and water phases in a miniemulsion is significantly larger than zero. The surface coverage of the miniemulsion droplets by surfactant molecules is incomplete.
3. Particle nucleation in miniemulsions is dominated by droplet nucleation.
4. During particle formation, the growth of droplets in miniemulsions can be suppressed. In miniemulsions, the redistribution of monomer is balanced by a high osmotic pressure of the costabilizer which makes the influence of the initial structures less important.
5. Compared with microemulsions and a number of macroemulsions, the amount of surfactant required to form a miniemulsion is comparatively small to prevent the formation of micelles in the continuous phase.

1.1.3 Previous work on conventional miniemulsion polymerization

1.1.3.1 Early work (1973-mid 1980s)

A deep understanding of conventional miniemulsions and miniemulsion polymerizations has been achieved since the basic conception of miniemulsion polymerization was first proposed by John Ugelstad, John Vanderhoff and Mohamed EI Aasser in the 1970s.[18] The early work made breakthroughs in the clarification of particle nucleation processes in emulsion polymerizations and demonstrated that droplet nucleation could play an important role if the droplet size is small enough. [6, 19, 20] Other than the understanding of the particle nucleation mechanism, the early work outlined the basis of miniemulsion formulations, namely, that high shearing force should be applied to reduce the size of the monomer droplets, and that these droplets should be protected against both diffusional degradation and droplet coagulation by the use of long chain thiols, alcohols, and alkanes and proper surfactants. [19, 21, 22] In addition, various approaches for the preparation of miniemulsions was developed, such as by ultrasonication or via use of a microfluidizer.

1.1.3.2 Recent work (mid 1980s-to present)

Fundamental research on the kinetics and applications of miniemulsion polymerizations made significant progress in this period.

Most of work was focused on the kinetic study of batch miniemulsion homopolymerizations with styrene as the monomer. The droplet nucleation mechanism and robustness of the miniemulsion polymerizations were thoroughly investigated. Polymers were found to be one candidate for use as costabilizer and could enhance the nucleation of droplets. It was first found by Schork that the addition of a monomer soluble polymer to an emulsion can slow the effects of Ostwald ripening and impart diffusional stability to the droplets.[11] Droplet nucleation was the dominant nucleation mechanism in the polymer-stabilized miniemulsion polymerizations.[11] As a result of the robust droplet nucleation, the polymerization rates and the particle number in miniemulsion polymerizations were found to be less sensitive to variations in the recipe or retarders compared with macroemulsion polymerization controls. Miller et al. carried out styrene miniemulsion polymerizations using different costabilizers and a small amount of poly(styrene) as a second costabilizer. [23-26] It was found that by adding the small amount of poly(styrene), the polymerization rate increased as a result of an

increased final particle number. The final number of polymer particles in the miniemulsion polymerization stabilized with cetyl alcohol and 1wt% of poly(styrene) was insensitive to the initiator concentration, while an increase in particle number was observed when cetyl alcohol was used alone. The authors attributed the enhancement in nucleation rate to the higher efficiency of the droplets containing polymer in capturing aqueous phase radicals. These hypotheses were checked by Blythe et al. who showed that the nucleation and polymerization rate enhancement were not affected by the molecular weight of the polymer. [27-30] These results ruled out the effect of the internal viscosity on the entry efficiency. In addition, neither the number of particles nor the polymerization rate was affected by the polymer end group ($–SO_3$, $–SO_4$, -H), indicating that the enhanced droplet nucleation was not due to the disruption of the condensed phase by the polymer. Therefore, it was proposed that the dominating cause of enhanced droplet nucleation was the preservation of monomer droplets by the presence of the polymer.

Other than the homopolymerizations, various copolymerizations were also performed in miniemulsion. It was found that the copolymer composition can be different in miniemulsion and macroemulsion copolymerizations because of different nucleation mechanisms. Reimers et al. carried out miniemulsion copolymerizations of methyl methacrylate (MMA) with other highly hydrophobic monomers, e.g. p-methylstyrene (pMS), and compared the kinetic behavior with that of macroemulsion copolymerization controls.[10] Although both the miniemulsion and the macroemulsion copolymerizations of pMS and MMA tended to follow the integrated copolymer equation, a copolymer richer in the pMS was formed in miniemulsion polymerization while a copolymer richer in the methyl methacrylate from macroemulsion polymerization. Droplets would have a higher concentration of pMS throughout the reaction which yields a copolymer with a higher pMS fraction by droplet nucleation. In contrast, micellar nucleation should lead to a copolymer with higher methyl methacrylate content, because it can cross the aqueous phase more readily. As the water solubility of the comonomer decreases, the difference in incorporation of the hydrophobic monomer between the mini- and macroemulsion polymerization becomes more pronounced. Delgado et al. made a comprehensive study the miniemulsion copolymerization of vinyl acetate and butyl acrylate and developed a mathematical model for the polymerization taking account of the effect of particle

equilibrium swelling. [31-34] Delgado also found a higher BA content in the copolymer from the miniemulsion copolymerization than the equivalent macroemulsion.[31]

The particle nucleation mechanism can be also affected by the comonomer in the miniemulsion copolymerization. When a partially water soluble monomer, e.g. 2-hydroxyethyl methacrylate (HEMA), was used with styrene, the fraction of polymer particles formed by droplet nucleation decreased by increasing the amount of HEMA though the total number of particles formed by droplet nucleation increased because HEMA presents some surface activity and yields a higher number of droplets.[35] When a completely water-soluble monomer such as acrylic acid (AA) was used, the extent of homogeneous nucleation, surprisingly, decreased as the concentration of acrylic acid increased, presumably because the water solubility of the oligomers increased with the AA content.[36] Oil-soluble initiator promotes nucleation in monomer droplets whereas homogeneous nucleation predominates in the system initiated with a water-soluble initiator. [31-34]

The continuous free-radical miniemulsion polymerization was preliminarily studied in this period. Continuous systems are attractive because of their high throughput and low operating and labor costs. Additionally, at steady state, continuous processes can produce polymers with more consistent composition compared to batch or semibatch systems. Barnette et al. performed the pioneering study on the continuous miniemulsion polymerization of methyl methacrylate in single CSTR.[7, 37] Unlike oscillation of conversion usually observed in continuous macroemulsion polymerizations, the continuous miniemulsion polymerization maintained a steady state of monomer conversion. Through the investigation of the miniemulsion polymerization of vinyl acetate in a CSTR, Aizpurua et al. confirmed the lack of oscillation phenomenon.[30,31] Samer et al compared the kinetic behavior of miniemulsion copolymerization of methyl methacrylate with 2-ethylhexylacrylate(EHA) in one CSTR and the batch miniemulsion polymerization.[38] The batch miniemulsion copolymerization did incorporate more of the less water soluble monomer EHA than a batch macroemulsion. However, this expected behavior was not observed in the CSTR, probably due to the presence of monomer-starved polymerizing particle in the reactor. Other than in CSTR, free-radical miniemulsion polymerization was carried out in PFR. The study of Samer et al. showed

that with the same residence time, the choice of reactors, either CSTR or PFR, had negligible effect on the polymerization rate because of droplet nucleation.[39] Since the fouling and mixing issues were greatly eliminated due to droplet nucleation, PFR miniemulsion polymerization was proved to be an approach to produce relatively high solid content latexes. [40, 41]

1.2 Selected New Techniques in the Last Decade

Various new techniques emerged in the last decade, such as enzymatic polymerizations, and controlled polymerizations. Applying these new techniques to miniemulsion systems will endow conventional miniemulsion polymerizations numerous novel or unique features and contribute to the birth of different unconventional miniemulsion polymerizations.

1.2.1 Enzymatic polymerizations

Enzymatic polymerizations are defined as chemical polymer syntheses in vitro via non-biosynthetic (non-metabolic) pathways catalyzed by an isolated enzyme.[42] There were a few reports about enzymatic oligomerization in the 1980s. [43-45] However, it was not until the mid 1990s when several families of enzymes highly efficient for the polymerization of unnatural substrates were found, that interest in the area of enzyme-catalyzed polymerizations grew rapidly. [42, 46, 47]

Compared with common chemical initiated polymerizations, enzyme-catalyzed polymerizations have several advantages as follows:

1. Mild polymerization conditions with regard to temperature, pressure, and pH, which can often lead to energy efficiency;
2. High enantio-, regio-, and chemoselectivities as well as regulation of stereochemistry providing development of new reactions to functional compounds for pharmaceuticals and agrichemicals; [48-50]
3. Environmentally friendly synthetic processes. All naturally occurring polymers are produced in vivo by enzymatic catalysis. Enzymatic polymerizations can greatly contribute to global sustainability by using renewable resources as starting substrates of functional polymeric materials.

4. A proven new synthetic strategy for useful polymers otherwise difficult to produce by conventional chemical catalysts, such as polysaccharides.[49]

Natural enzymes can be divided into six classes: oxido-reductases, transferases, hydrolases, lyases, isomerases and ligases.[51] Among the six classes, three have been reported to catalyze or induce polymerization in vitro, i.e. oxido-reductases, transferases, and hydrolases. Most oxido-reductases contain metal catalytic centrers, such as iron(III) (horse radish peroxidase, HRP), copper(I) (laccase), and manganese(II), (manganese peroxidase). Several oxido-reductases, e.g. HRP, can easily polymerize a wide range of phenol and aniline derivatives by the decomposition of hydrogen peroxide at the expense of aromatic proton donors. [52-57] In addition to polyphenols and polyanilines, HRP can also induce polymerization of vinyl monomers, such as styrene and methyl methacrylate, with the help of hydrogen peroxide. [58, 59] Transferases, such as phosphorylase and glycosyl transferase, catalyze group transfer reactions. The primary example of the potential of a transferase is the synthesis of amylase from D-glucosyl phosphate and oligomers with a minimum length of four glucosyl-residues as a primer by using potato phosphorylase.[60] Lipases, among different hydrolases, are the most-investigated enzymes for in vitro synthesis since they are known to catalyze reactions in organic media without any cocatalyst. The lipase-catalyzed polymerizations have been well reviewed in several papers. [61-64]

To date, almost all of enzymatic polymerizations were carried out in homogeneous media in which the enzymes are either dissolved or suspended. Very limited efforts have been taken for enzymatic polymerizations in heterogeneous systems. Prior to this work, there was only one paper published about enzyme-catalyzed ring opening polymerization of lactones in miniemulsion.[65]

1.2.2 Controlled free-radical polymerizations

Controlled free-radical polymerization is a special form of addition polymerization where most of polymer chains maintain their livingness, i.e. the ability to continue adding monomer units, after the polymerization. Generally, controlled polymerizations include the following features:

1. Polymer chain livingness, i.e. the ability to grow after the initial monomer charge is exhausted.
2. Pseudo-first order kinetics.
3. Linear relationship between the number average molar mass of the polymer and the monomer conversion.
4. Narrow molecular weight polydispersity (Mw/Mn)

Controlled polymerization has become a popular method for synthesizing polymers since the polymer structure can be tailored thanks to the polymer chain livingness. Block copolymers can be synthesized easily by incorporating a polymer block in different stages. Additional advantages of controlled polymerization are predetermined molar mass, narrow polydispersity and control over end-groups of polymer products.

Since anionic polymerization, the first kind of controlled polymerization technique, was discovered in 1956, [66, 67] various controlled polymerizations have been proposed. In the last decade, three new important controlled polymerizations was developed:

1. Stable free-radical mediated polymerization (SFRP) [68, 69]
2. Atom transfer radical polymerization (ATRP) [70]
3. Reversible Addition Fragmentation chain Transfer (RAFT) polymerization[71, 72]

Among these controlled polymerizations, RAFT polymerization is especially suitable for miniemulsion since RAFT polymerization has a faster polymerization rate than SFRP and ATRP from a mechanistic perspective, as will be discussed below. At the same time, RAFT polymerization is superior to the other controlled polymerization methods due to the mild reaction conditions and decreased sensitivity to water and other contaminants.

1.2.2.1 Concept of RAFT polymerization

The concept of RAFT comes from two different pieces of work first reported in the late 1980s. The Australian Commonwealth Scientific and Research Organization (CSIRO) group reported the use of poly(methyl methacrylate) macromonomers as chain transfer agents in radical polymerization in 1986. [68, 73] The process was named addition fragmentation chain transfer (AFCT). A variety of AFCT agents were reported later,[74-76]

however, the polymers prepared from these processes showed high polydispersity in most cases. It was not until 1998 that the CSIRO group found with thiocarbonyl thio derivatives gave polymers with predictable molecular weights and very narrow polydispersities using a wide range of monomers. Furthermore, the polymer end groups remained active at the end of the reaction. [71, 77]

Almost at the same time, Zard et al. report polymerizations using a degenerative transfer of radical species to a xanthate (MADIX is used to describe this kind of polymerization). [78] In fact, RAFT and MADIX are almost the same, only slightly differing in the activating group on the chain transfer agents.

1.2.2.2 RAFT agent and mechanism of RAFT polymerizations

A RAFT agent is a special chain transfer agent with a high chain transfer constant. Unlike other common chain transfer agents, the chain transfer reaction of the RAFT agent is reversible and rapid. Most RAFT agents have a general structure as shown in Figure 1.1:

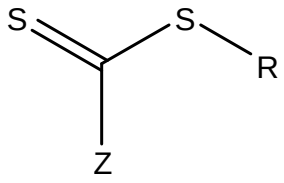

R: leaving group

Z: activating group

Figure 1.1 General structure of RAFT agents

The function of Z group is to facilitate the reaction of free radicals with the C=S bond. The R group has to be a good leaving group and capable of reinitiating the polymerization. Radical stability, polarity, and steric factors all contribute to the leaving ability of the R-group. [79, 80]

RAFT polymerizations are based on reversible chain transfer mechanism. [71, 72]

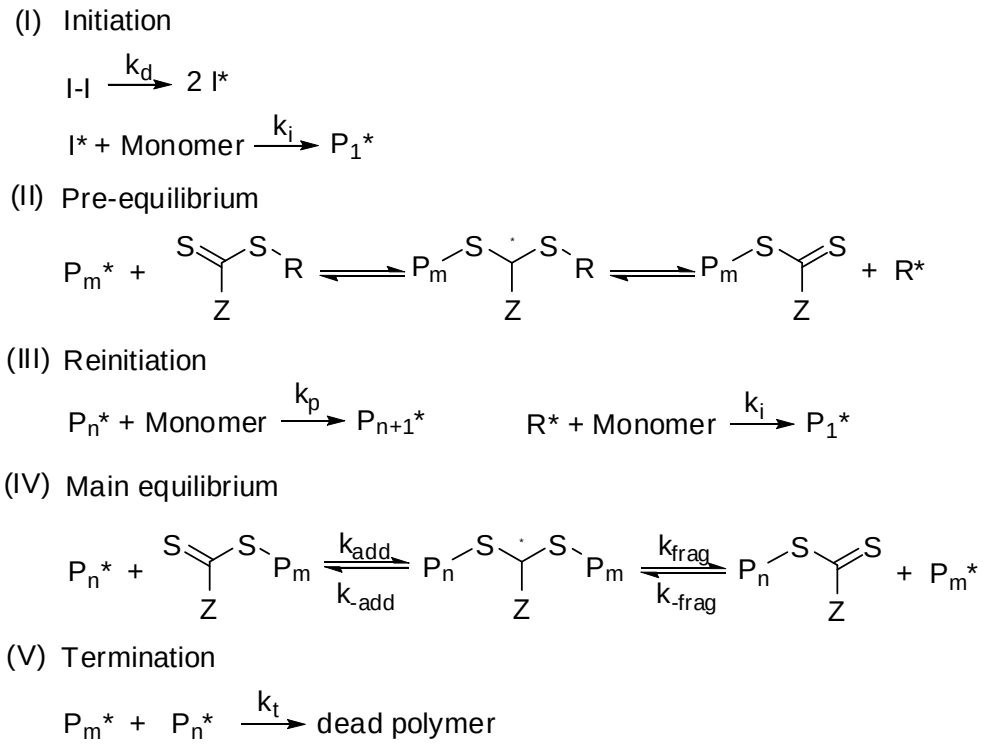

Figure 1.2 Mechanism of RAFT polymerizations

A conventional free-radical initiator generates radicals in step I. These radicals or oligomeric radicals derived from the initiator radicals by adding a few of monomer units attack the C=S bond of RAFT agent and form RAFT intermediate radicals reversibly. The intermediate radicals can reversibly fragment back to a RAFT agent and a leaving group R. In third step, the R group reinitiates the polymerization and grows into a polymeric radical. In the main equilibrium step, the growing polymeric chains undergo a chain transfer reaction with macro RAFT agents (the R group is substituted by other polymeric chains). If the chain transfer reaction is rapid enough, all the polymeric chains will grow at the same time, and as a result, RAFT polymerizations have pseudo first order kinetics. It is worthy to note that most of the final polymer chains have a RAFT functional group at the chain end; therefore, the polymers are "living" and can be used as a macro RAFT for chain extension.

It is worthwhile to note that RAFT differs in mechanism from the other two controlled polymerization techniques, i.e. SFRP and ATRP. RAFT is based on chain

transfer reactions between propagating radicals and RAFT agents. Therefore, the radical concentration, ideally, will not decrease in the presence of RAFT agents since another radical is produced once a radical is consumed by the addition reaction to a RAFT agent. However, SFRP and ATRP operate via reversible termination of growing radicals, which result in a much lower radical concentration compared to the RAFT process. The mechanistic difference leads to a much slower polymerization rate in SFRP and ATRP compared to RAFT under similar reaction conditions. This is one reason we prefer RAFT polymerization to SFRP and ATRP in a miniemulsion system. Of course, retardation and inhibition were also found in a few of RAFT systems, e.g. using cumyl dithiobenzoate as RAFT agent.[81] The causes of these phenomena are still under investigation and are being rigorously debated in the literature. [79-82]

1.2.2.3 RAFT polymerization in miniemulsions

In the past ten years, great efforts have been taken in the application of RAFT chemistry to miniemulsion polymerizations. RAFT miniemulsion polymerizations are significantly different from conventional miniemulsion polymerizations (as mentioned in section 1.1.3) in regard to polymerization kinetics, molecular weight distribution and colloidal stability, etc. this is why RAFT miniemulsion polymerizations are classified as one kind of unconventional miniemulsion polymerizations here. [83-95]

Lansalot et al. studied the role of RAFT agent structure on styrene miniemulsion.[90] The presence of the RAFT agent slowed the polymerization rate for miniemulsion polymerization significantly. The author suggested the exit of the RAFT agent-leaving group to the aqueous phase could be the reason for the retardation. This assumption was supported by the fact that no retardation compared to the conventional miniemulsion was observed when using a macro-PEPDTA agent whose R group can not exit. A detailed kinetic study of RAFT miniemulsion polymerization of styrene was reported by Luo et al.[94] Polymerization rate was found to be determined by both the chain transfer constant and the concentration of RAFT agent. Retardation was found to be an inherent feature of RAFT miniemulsions as a result of compartmentalization.

Recently continuous RAFT miniemulsion polymerizations have been developed mainly at Georgia Tech. Smulders et al. reported the controlled styrene miniemulsion

polymerization in a CSTR and a CSTR train.[2] In spite of a relatively high polydispersity (PDI) of polymer in a single CSTR, the PDI can decrease by increasing the number of CSTRs. [2, 96] Unexpected transient states, an increase or fluctuation of conversion over prolonged times rather than a steady state was observed in the CSTR trains. Living gradient copolymers of styrene and n-butyl acrylate (BA) were synthesized in the CSTR train by feeding a macroemulsion of BA to a RAFT miniemulsion of styrene.[1] Continuous RAFT miniemulsion polymerizations have also been carried out in tubular reactor. Well defined polymer latexes, e.g. poly(styrene) and poly(vinyl acetate), were successfully produced in the tubular reactor using a surfactant combination of SDS and Triton X-405. [97, 98] While the kinetics in the tubular reactors should be compared to batch controls theoretically, the RAFT miniemulsion polymerizations in the tubes were found to have a small but consistently higher rate. Meanwhile, the PDIs in the tubes were consistently higher than in the comparable batch experiments. These differences were attributed to axial dispersion within the tubes and fluid slippage at the tube wall.[99] The effect of residence time distributions and the flow regime in the tubular reactor on the RAFT miniemulsion polymerization were also explored by using a hydrophobic dye as tracer.[99] It was found that axial dispersion was generally quite large in the tubes. Laminar flow was not observed even when the Reynolds numbers used were below 10. This strong axial dispersion was believed to be responsible for the broader molecular weight distributions in the tubular reactor.

1.2.3 Inverse miniemulsion polymerizations

Conventional emulsion polymerization can only be carried out with monomers that are essentially water-insoluble. However, one can invert the whole process, using an organic solvent as the continuous phase, and water soluble monomer dissolved in water as the dispersed phase (i.e. inverse emulsion polymerization). In this case, water-in-oil surfactants are used to create the emulsion. Either hydrophilic or hydrophobic initiators can be used. Such systems are used commercially to produce very high molecular weight water-soluble polymers, e.g. poly(acrylamide), poly(acrylic acid), which can be used for flocculants, and other applications.[3] The pioneering work on this system was done by Vanderhoff et al. in 1962, where submicron particles were obtained.[100] Segregation of

polymerizing free radicals in these particles contributes to the very high molecular weights necessary for flocculants applications. Particle nucleation in these systems is thought to be both micellar and droplet nucleation. High shear may be applied to reduce the droplet size. Thus, the classic "inverse emulsion polymerization" appears more like inverse miniemulsion polymerization due to the homogenization step and droplet nucleation.

Inverse miniemulsion polymerization has been developed to a limited extent more recently. These systems are distinguished by the features of inverse emulsion polymerization (organic continuous phase, aqueous dispersed phase), but add in features of miniemulsion polymerization (high levels of shear and use of a costabilizer to prevent Ostwald ripening). Inverse miniemulsion polymerization has not been investigated to near the level of traditional O/W miniemulsion polymerization, but surpasses inverse emulsion polymerization due to greater colloidal stability.[101] Both inverse systems allow the formation of homogeneous particles consisting of various water soluble polymers such as poly(acrylamide) and poly(acrylic acid).

Few investigations have been carried out inverse miniemulsion polymerization. Landfester et al. recently reported the inverse miniemulsion polymerization.[102] They showed that the principles of aqueous miniemulsions can be transferred to nonaqueous media. Relatively stable inverse miniemulsions could be achieved by adding salt as the costabilizer. Copolymerization of monomers with different polarities was also carried out.[103] Initiators soluble in either the oil or water phase, or residing at the interface were used, and the locus of initiation was found to have a large influence on the quality of the obtained copolymers. Wang et al. investigated the kinetics of polymerization of hydrophilic monomers by both direct miniemulsion and inverse miniemulsion.[104] They proposed a mechanism for inverse miniemulsions and further pointed out that dispersants can be crucial factor in determining the mechanism. Capek studied inverse miniemulsion polymerization of acrylamide.[105] The inverse miniemulsion polymerizations were surprisingly fast, reaching final conversion within several minutes. Two different

intervals of polymerization rate were observed and were attributed to the combination of the gel effect and nucleation mode.

1.3 Goal and Outline of the Work

The goal of the work is to develop various unconventional miniemulsion polymerizations by the introduction of new techniques to conventional miniemulsion systems; at the same time, explore the kinetics and mechanism of these unconventional miniemulsion polymerizations. The outline of the work is shown in Figure 1.3. In Chapter 2, enzyme initiated free-radical miniemulsion polymerization is proposed for the first time to solve the problems in using enzymes and common vinyl monomers, resulting from the hydrophobicity of the vinyl monomers. Chapter 3-5 discuss different types of RAFT miniemulsion polymerizations, arranged in the order of increasing monomer hydorphilicity. The transient states of RAFT polymerization in CSTR trains, as mentioned in section 1.2.2.3, are studied in Chapter 3. Potential reasons and solutions for the transient states were given. In Chapter 4, RAFT miniemulsion polymerization of a partially water soluble lactone monomers derived from renewable sources is successfully formulated. The kinetics of free-radical emulsion and RAFT miniemulsion polymerizations of the novel monomer are studied. In Chapter 5, the RAFT inverse miniemulsion polymerization technique is developed for the first time. A well defined stable inverse hydrogel latex is achieved. The kinetics and special features of the RAFT inverse miniemulsion polymerization are investigated. Finally, a summary and suggestions for future work are addressed in Chapter 6.

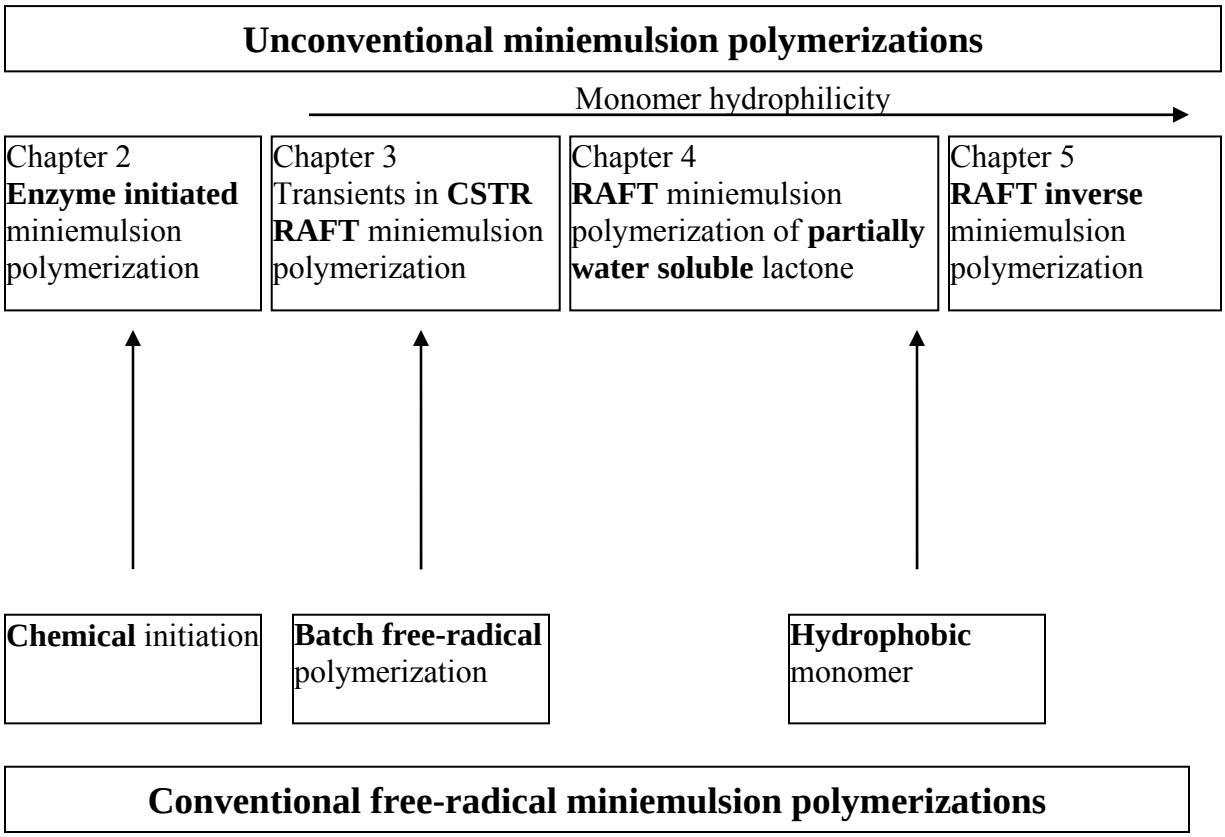

Figure 1.3 Relationships between unconventional and conventional miniemulsion polymerizations in this work

CHAPTER 2

ENZYME-INITIATED MINIEMULSION POLYMERIZATION*

2.1 Introduction

Enzyme-catalyzed polymerization in vitro has gained considerable attention in the last two decades as an efficient tool in the preparation of various polymers. [46, 60] The high selectivity, mild reaction conditions and environmental compatibility inherent in enzymatic reactions have made this approach a very attractive alternative in the synthesis of complex, stereoselective and bioactive compounds, which are often difficult to obtain by conventional chemical routes. To date, polymers such as poly(saccharides), poly(esters), poly(phenols) and poly(anilines) have been the synthesized by enzyme-catalyzed polymerizations.[106-117] The enzymatic polymerization of hydrophobic vinyl monomers such as styrene, however, have scarcely been reported.[118, 119]

Oxidoreductases, especially horse radish peroxidase (HRP), are known to have the ability to catalyze the oxidation of phenols, anilines and their derivatives. [107, 113-117] The potential of using HRP and other oxidases to catalyze the free-radical polymerization of vinyl monomers was first reported by Derango et al. [120] The polymers were formed in the presence of a large excess of hydrogen peroxide. They claimed that the oxo-Iron(IV) π-radical cation generated by HRP and H_2O_2 may contribute to the polymerization. Poly(acrylamide), poly(methyl methacrylate) and poly(styrene) were synthesized by HRP and other oxidases with β-diketones as initiators. [118, 119, 121-125] It was found that no polymer was produced if a low ratio of H_2O_2:monomer was used in the absence of β-diketones. Thus another mechanism was proposed where β-diketone radicals generated by HRP-catalyzed oxidation of the β-diketone by H_2O_2 may initiate the polymerizations. [118]

One reason why enzymatic polymerizations of vinyl monomers have not been thoroughly investigated could be that the majority of common vinyl monomers are barely

* Portions of this chapter have been published in *Biomacromolecules*, 2006, 7, 2927-2930.

soluble in water, which is the traditional reaction medium for the application of biocatalysts. Indeed, hydrophilic vinyl monomers were utilized in most previous studies using HRP as an initiator. [120-123, 125] Cosolvents have also been utilized to allow polymerization of hydrophobic monomers. [118] However, the yields of polymer were relatively low under these conditions, i.e. 21.2% in THF-H_2O and only 3.8% in methanol-H_2O cosolvent after 24 h. [118]

Here we demonstrate a simple way to realize the enzyme-initiated polymerization of hydrophobic vinyl monomers in an aqueous system by the use of miniemulsion polymerization. The methodology demonstrated here can also achieve enzyme-initiated polymerization of various hydrophobic vinyl monomers other than styrene, taking advantage over conventional polymerizations in mild and "greener" conditions, especially suitable for those thermosensitive monomers or chemoselective polymerization.[126]

2.2 Experimental Section

2.2.1 Materials

Styrene (J.T. Baker) was purified by removing the inhibitor tert-butylactechol by passing the monomer through a column packed with inhibitor remover (Aldrich), followed by distillation under vacuum. Hexadecane (Aldrich, 99%), and sodium dodecyl sulfate (SDS) (J.T. Baker. 99.8%) were used as received. Deionized water was generated with a U.S. Filter Systems Deionizer and was used without further purification. Horseradish peroxidase (HRP) (TCI America), hydrogen peroxide (Aldrich, 30% w/w) and 2, 4-pentanedione (ACAC) (Alfa Aesar, 99%) were used as received.

2.2.2 Polymerization

The miniemulsion was prepared by adding a solution of degassed styrene and hexadecane to a solution of sodium dodecyl sulfate in deionized water. The mixture was stirred under nitrogen in an ice bath for 10 min, and then sonicated with a Fischer Model 30 sonic dismembrator operated at 70% power output for approximately 10 min, while being stirred under nitrogen and cooled in an ice bath. HRP was dissolved in a small

amount of deionized water and purged with nitrogen for 10 min. A portion of the HRP solution was injected in the styrene miniemulsion and stirred for 5 min, followed by adding ACAC and H_2O_2 simultaneously. The miniemulsion was stirred under nitrogen and samples were drawn at intervals. The samples were poured into a large excess of cold methanol. The polymer was precipitated and filtered, washed with cold methanol and dried under vacuum at 30°C.

2.2.3 Characterization

The dried polymer was dissolved in chloroform (J.T. Baker, HPLC) and filtered through a 0.2 μm syringe filter. GPC analyses were carried out using three columns (American Polymer Standards styrene-divinylbenzene 100, 1000, and 10^5 Å) at 30 °C. The columns were connected to a Viscotek GPCMax pump and autoinjector, a Waters 410 refractive index detector, and calibrated with narrow poly(styrene) standards (Polymer Laboratories). Chloroform was used as the eluent at a flow rate of 1.0 mL/min, and the injection volume was 100 μL.

Latex particle radius were analyzed using quasi-elastic light scattering (QELS, Protein Solutions DynaPro). The conversion of styrene monomer conversion was determined gravimetrically.

2.3 Results and Discussion

2.3.1 Kinetic study of HRP catalyzed miniemulsion polymerization

Assuming the polymerization follows the mechanism outlined in the introduction[118], it is believed that H_2O_2 oxidizes HRP and the oxidized metal center is reduced by ACAC, yielding ACAC-derived radicals in the aqueous phase. These radicals presumably can do two things to initiate the polymerization, either (i) enter the monomer droplets and start the polymerization directly in the droplet, or (ii) oligomerize the small fraction of styrene that is present in the aqueous phase, with these active styryl chains entering the droplets as they get more hydrophobic with increasing chain length.

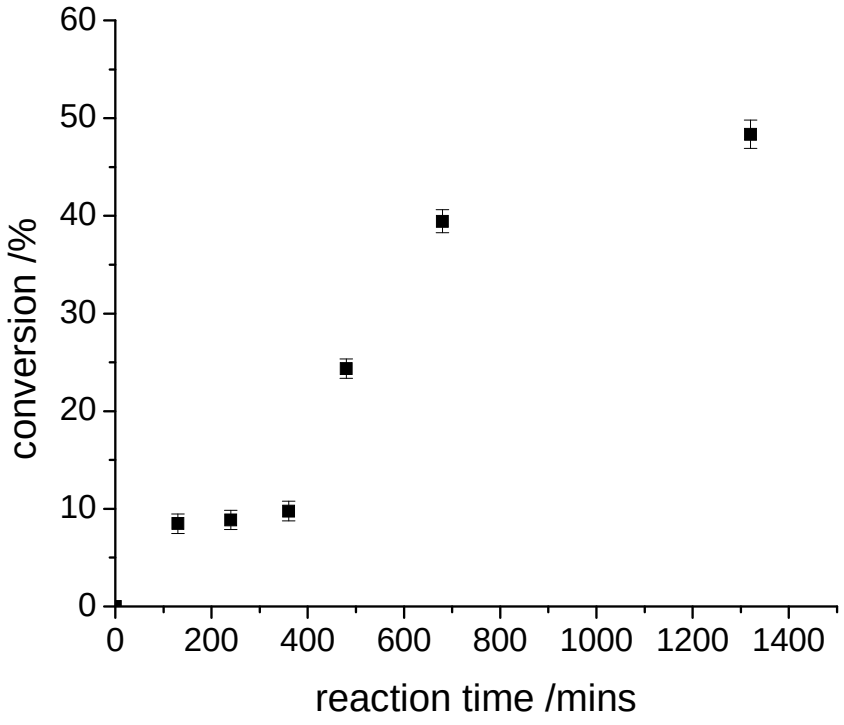

Figure 2.1 Relationship between of conversion and reaction time of the HRP mediated miniemulsion using the recipe in Table 2.1.

The main recipe used for HRP-initiated miniemulsion polymerization is shown in Table 2.1. It is interesting to note that the conversion of styrene proceeded slowly until 360 min, as shown in Figure 2.1. After 360 min, the conversion of styrene increased significantly, followed by a gradual decrease in polymerization rate after around 800 min. There are many possible causes of these observations. The consumption of ACAC and H_2O_2 with time, which decreases the radical initiation rate, could cause the decreased polymerization rate observed at long times. A loss of enzyme activity or degradation of HRP with increasing reaction time could also contribute to this phenomenon. Concerning the induction time, one potential cause is an imbalanced ratio of ACAC:H_2O_2 in the aqueous phase. Although the molar ratio of ACAC:H_2O_2 was chosen to be close to an optimal ratio reported previously for another polymerization system (set at 1.3:1, (Table 2.1)) [59], the actual ratio of ACAC:H_2O_2 in the aqueous phase, where the enzyme is presumed to reside, could be much lower due to the preferential partitioning of ACAC into the monomer droplets. Additionally, it is possible that a different initiation

mechanism operates under these conditions. Derango et al. suggested a different mechanism could operate under some conditions, and found that with a low ratio of vinyl monomer:H_2O_2, polymerization could take place even without ACAC (vide supra). [120, 126] In the present work, the concentration ratio of styrene to H_2O_2 in the aqueous phase may be quite low. Assuming that all the H_2O_2 was dissolved in the aqueous phase that was saturated with styrene, the molar ratio of styrene to H_2O_2 was around 0.04 at the start of the polymerization. [127] These conditions may favor the alternate mechanism of Derango et al. Furthermore, the drastic changes in polymerization rate at certain times throughout the process may be indicative of the system operating via different mechanisms at different times.

Table 2.1 Recipe for HRP-catalyzed miniemulsion polymerization

Miniemulsion		Enzyme and substrates	
H_2O	2.88g	HRP	2.4mg
Styrene	0.689g	H_2O_2(30W$_t$%)	7μL
SDS	0.0155g	ACAC	9μL
Hexadecane	0.0162g		

Although a much smaller amount of HRP and H_2O_2 were used than the previous report, [118] the conversion after 24 h, around 48%, was still much higher than previously reported using co-solvent solutions. Moreover, a stable poly(styrene) latex with a narrowly distributed particle radius distribution around 50nm was achieved, as shown in Figure 2.2. The ^{1}H-NMR spectrum of the poly(styrene) is shown in Figure2.3.

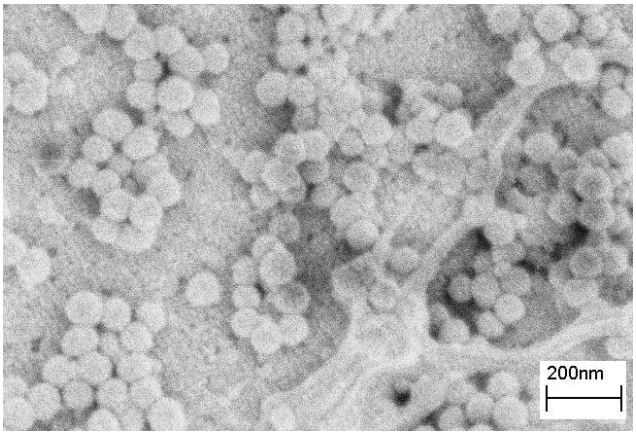

Figure 2.2 SEM photograph of poly(styrene) latex nanospheres obtained from HRP-initiated miniemulsion with the recipe in Table 2.1 after 24 h.

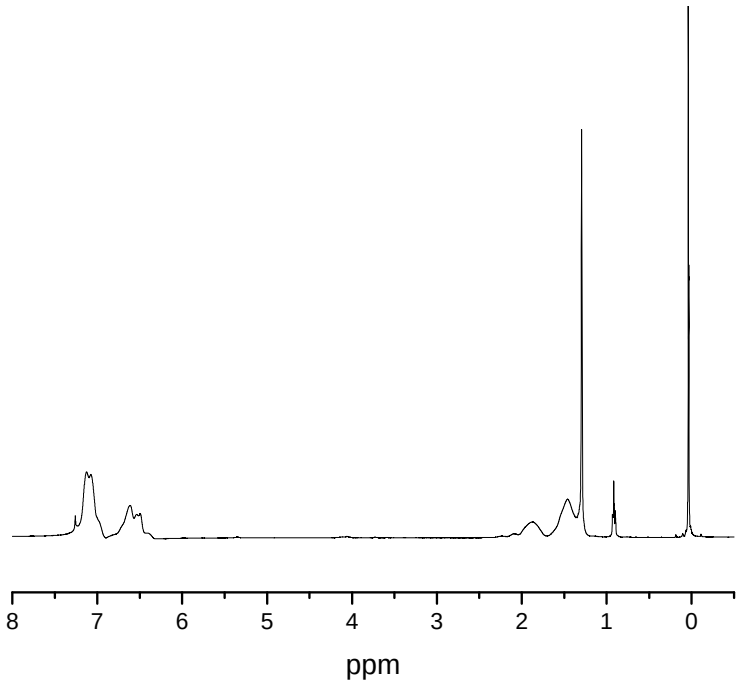

Figure 2.3 ^{1}H-NMR spectrum of HRP catalyzed poly(styrene) with the recipe in Table 2.1 after 24 h using $CDCl_3$ as solvent.

There was a discontinuity in the number average molecular (M_n) weight of poly(styrene) in this HRP-initiated miniemulsion polymerization, similar to the trend observed in conversion. The M_n was almost constant at the beginning of the polymerization, and then sharply increased afterwards, as shown in Figure 2.4. It is worth pointing out the relatively high molecular weight of the poly(styrene), as high as to 406K, compared to the previous enzyme mediated work using a cosolvent, which gave molecular weights of ~30K. [118] A low concentration of ACAC in aqueous phase may lead to a low total radical concentration, accounting for the high molecular weight of the poly(styrene). The radical segregation effect in miniemulsion also favors high molecular weights by inhibiting termination of propagating radicals.

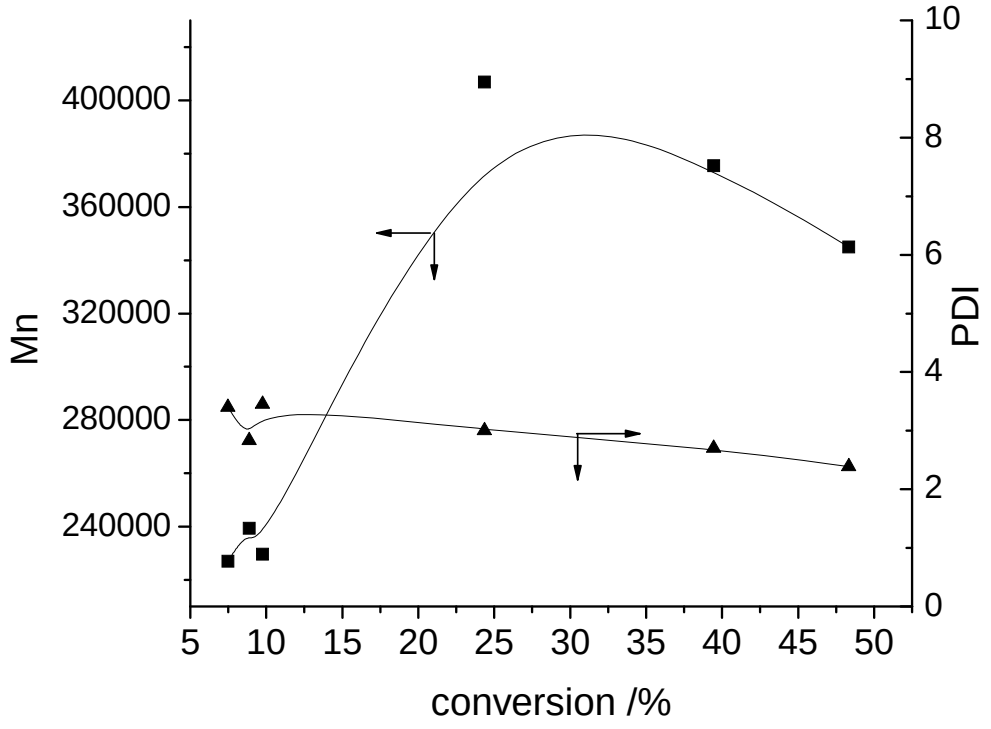

Figure 2.4 Relationship of Mn, PDI and the conversion using the recipe in Table 2.1.

2.3.2 Effect of reaction temperature

It is well known that temperature has significant effects on the reactivity of enzymes. Therefore the conversion of styrene at different temperature was measured after about 24 h. As shown in Table 2.2, temperature has dramatic influence on the miniemulsion polymerization and the conversion was lower at high temperatures. At 305K, only 9.8% conversion was achieved after 24 h, while a much higher conversion could be achieved at a lower temperature at 279-296K. The result is reasonable given that a previous study showed that HRP has its highest activity at 5°C and gradually loses its activity at higher temperatures. [128]

Table 2.2 Effects of reaction temperature on the HRP-catalyzed miniemulsion polymerization

Exp	Temperature (K)	Reaction time (mins)	Conversion (%)	Average particle radius (nm)
1	279	1355	50.2	50.63
2	296	1320	48.3	54.09
3	305	1375	9.8	47.42

2.3.3 Effect of enzyme amount

The effect of the amount of enzyme used in the miniemulsion polymerization was investigated. The conversion of three experiments with increasing HRP concentration was measured after 24 h. With a doubling of HRP in experiment 4, the conversion in experiment 5 was greatly improved from 48.3% to almost a full conversion (Table 2.3).

Table 2.3 Effects of the amount of enzyme on the HRP-catalyzed miniemulsion polymerization

Exp	HRP (mg)	ACAC (μL)	H_2O_2 (μL)	Conversion (%)	Average particle radius (nm)
4	2.4	9	7	48.3	54.09
5	5.0	9	7	98.3	62.76
6	9.0	9	7	100.0	65.16

2.3.4 Effect of H_2O_2/ACAC ratio

Previous studies have indicated the ratio of ACAC:H_2O_2 has a major influence on HRP-mediated polymerizations.[118, 119, 121, 122, 125] At low concentrations, hydrogen peroxide functions as an electron acceptor and initiator, while at higher concentrations it can inhibit enzyme activity. Therefore, a study was carried out for 24 h at 296K to determine how the concentrations of hydrogen peroxide and 2,4-pentanedione affected the outcome of styrene miniemulsion polymerizations. Four control experiments were carried out first. In these control experiments, one component in the reaction (HRP, ACAC, H_2O_2) was removed from the recipe to see the impact of each individual component on the polymerization. No poly(styrene) was formed in the control experiments except for a trace of polymer in the case where ACAC was not used (Table 2.4). These results agreed with the results reported before. [118]

Table 2.4 Effects of H_2O_2 and ACAC on the HRP-catalyzed miniemulsion polymerization

Exp	HRP (mg)	ACAC (μL)	H_2O_2 (μL)	Conversion (%)
Control 1	2.4	0	0	0
Control 2	2.4	0	7	trace
Control 3	2.4	9	0	0
Control 4	0	9	7	0
7	2.4	40	7	32.7
8	2.4	20	7	51.2
9	2.4	9	7	48.3
10	2.4	9	15	52.6
11	2.4	9	40	33.4

As shown in Table 2.4, with an increase of ACAC concentration from 9 μL to 20 μL, the conversion only slightly increased from 48.3% to 51.2%. Further increasing the concentration of ACAC, however, lead a slight decrease in the conversion. A similar phenomenon was observed by altering the concentration of H_2O_2. Increasing the amount of from 7uL to 15uL contributed an increase in conversion from 48.3% to 52.6%, while further increasing H_2O_2 resulted in a decrease in the final yield. Thus it is reasonable to assume that there should be an optimal ratio range of ACAC:H_2O_2 in the HRP catalyzed miniemulsion polymerization, although such conditions were not identified here.

2.4 Conclusion

Enzymatic miniemulsion polymerization was demonstrated in this work for the first time to be a way to use enzymes to polymerize hydrophobic vinyl monomers. Stable poly(styrene) latexes were synthesized by HRP initiated miniemulsion polymerization. A very small amount of HRP, H_2O_2 and ACAC was required to facilitate the miniemulsion polymerization while a relatively high conversion was achieved.

CHAPTER 3

CONTINUOUS RAFT MINIEMULSION POLYMERIZATION -TRANSIENTS IN CSTR TRAINS*

3.1 Introduction

As mentioned in the first chapter, RAFT polymerization has been demonstrated to be a powerful and important new approach to produce polymers with well-defined or special architectures.[71, 72] Combining RAFT chemistry with miniemulsion polymerization leads to one kind of unconventional miniemulsion polymerization: RAFT miniemulsion polymerization.

From an industrial standpoint, continuous miniemulsion polymerization is very attractive because it is robust to contamination and operating errors, and is generally considered to be a ‘‘green’’ process since it is based on an aqueous system. In addition, miniemulsions can produce polymers of uniform composition and final latexes with excellent shear stability exceeding those of conventional emulsion polymerizations. Therefore, performing RAFT miniemulsion polymerization in continuous reactors offers a promising solution to economically synthesize unique polymers on a large scale. However, most RAFT polymerization studies have been performed in batch conditions. There is only very limited work focused on controlled radical polymerization in continuous systems up to now. Cunningham et al. reported nitroxide mediated miniemulsion polymerization in a continuous tubular reactor recently.[129] Zhu, et al. also successfully employed continuous ATRP of methyl methacrylate in a tubular reactor.[130, 131] Our group has performed continuous RAFT miniemulsion polymerizations in tubular reactors[97-99] and CSTR trains.[1, 2, 83, 132]

Stability of CSTRs is a key issue for industrial processing to insure a uniform quality of product. It is well known that the kinetics of batch RAFT miniemulsion polymerizations are significantly different from conventional free-radical miniemulsion polymerizations. Therefore, it is important to understand the stability of CSTRs when

* Portions of this chapter have been published in *Ind. Eng. Chem. Res.* 2006, 45, 7084-7089.

they are used with RAFT miniemulsion systems. During our initial study of continuous RAFT miniemulsion polymerization in a CSTR train, some interesting phenomena were observed that warranted further investigation:[1, 2] (i) the conversion in each reactor in the CSTR train slowly increased with time, and (ii) there was a discontinuity in measured conversion values with time, as shown in Figure 3.1. The second effect seemed to suggest oscillations in the reactors. Both the conversion variations were of the order of 6-10%, which seems beyond the error range of gravimetry, the method used to measure conversions in our initial study. These results suggested the questions: is it possible for CSTRs carrying out RAFT miniemulsion polymerizations to achieve a steady state? What are the possible reasons for the previously observed instability? Here we revisit the RAFT miniemulsion polymerization of styrene in a CSTR train to investigate these transient phenomena and further explore the above questions.

3.2 Experimental Section

3.2.1 Materials

Styrene (J.T. Baker) was purified by a column packed with inhibitor remover (Aldrich) specific for tert-butylactechol. Hexadecane (Aldrich, 99%), sodium persulfate (Aldrich, 98%), and sodium dodecyl sulfate (SDS) (J.T. Baker, 99.8%) were used as received. Deionized water was generated with a U.S. Filter Systems Deionizer and was used without further purification. The RAFT agent 1-phenylethyl phenyldithioacetate (PEPDTA), as shown in Figure 3.2, was synthesized according to literature procedures, [133] using the following materials: carbon tetrachloride (Aldrich, 99.9%), benzyl chloride (J.T. Baker, 99.9%), carbon disulfide (J.T. Baker, 99.9%), magnesium turnings (Lancaster, 99+%), methanol (J.T. Baker, 100.0%), ethyl ether (Fischer, certified A.C.S., anhydrous), and p-toluenesulfonic acid monohydrate (Aldrich, 98%).

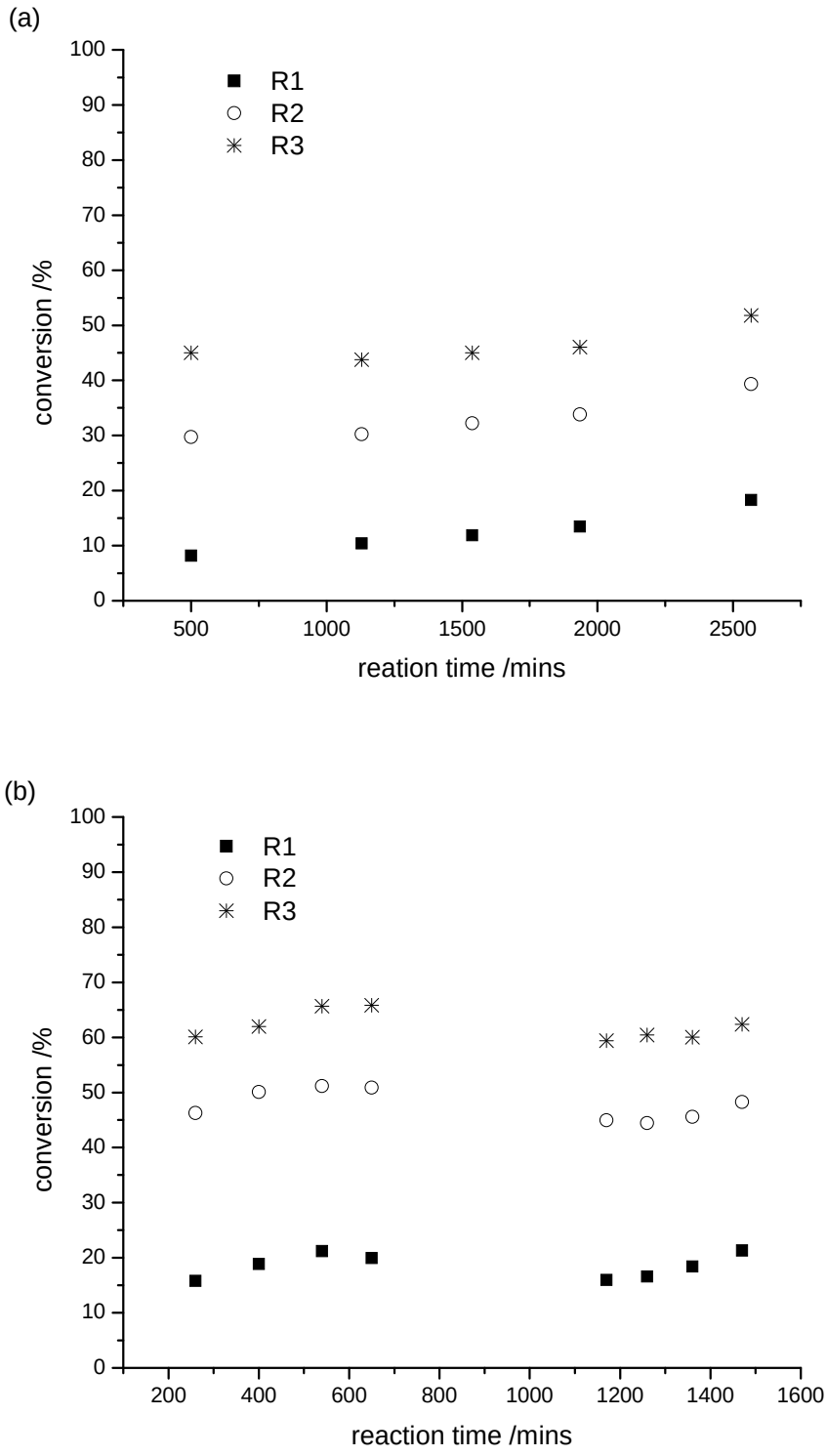

Figure 3.1 Unexpected transients in CSTR trains in our previous study.[1, 2] (a) The conversion in each reactor slowly increased with time; (b) The discontinuity in measured conversion values with reaction time.

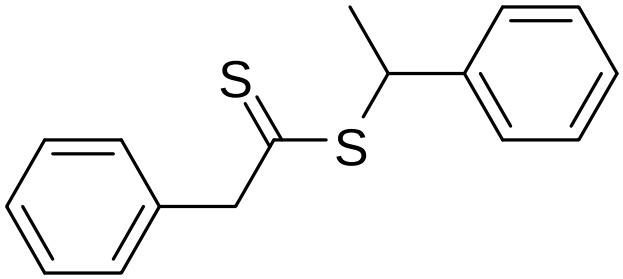

Figure 3.2 Structure of RAFT agent used in this study. 1-phenylethyl phenyldithioacetate (PEPDTA).

3.2.2 CSTR trains

A schematic of the CSTR train is shown in Figure 3.3. The train was kept under a slight nitrogen pressure. The miniemulsion was fed from a stirred and cooled (using a Fischer Scientific Isotemp 3016 cooler) flask into reactor 1 (R1) using a FMI valveless piston pump (P1). The sodium persulfate initiator solution was fed separately using a kdScientific syringe pump (P2). The CSTRs were 50 mL three-neck round-bottom flasks with an overflow weir that maintained each CSTR volume at approximately 40 mL. All CSTRs were equipped with a condenser and kept under nitrogen. The temperature in the oil baths was set to 71 °C to maintain a temperature of 70 °C inside the CSTRs throughout an experiment.[2] Experiments were started after the CSTRs and styrene miniemulsion feed were purged with nitrogen for about 1 h. The first two CSTRs were filled with miniemulsion and initiator solution in the same mass ratio as the mass flow ratio of pumps P1 and P2 during the experiment, and R3 was filled with one-third of its volume of miniemulsion. Before the first samples were taken, the system was allowed to stabilize for 20 h. Samples were withdrawn and put in hydroquinone-coated pans and dried under vacuum at room temperature. The conversion of the samples was analyzed gravimetrically. Potential changes in the miniemulsion feed associated with oligomerization were checked by monitoring the normalized UV absorbance of the GPC at 311nm,[2, 98] which will be discussed in detail below.

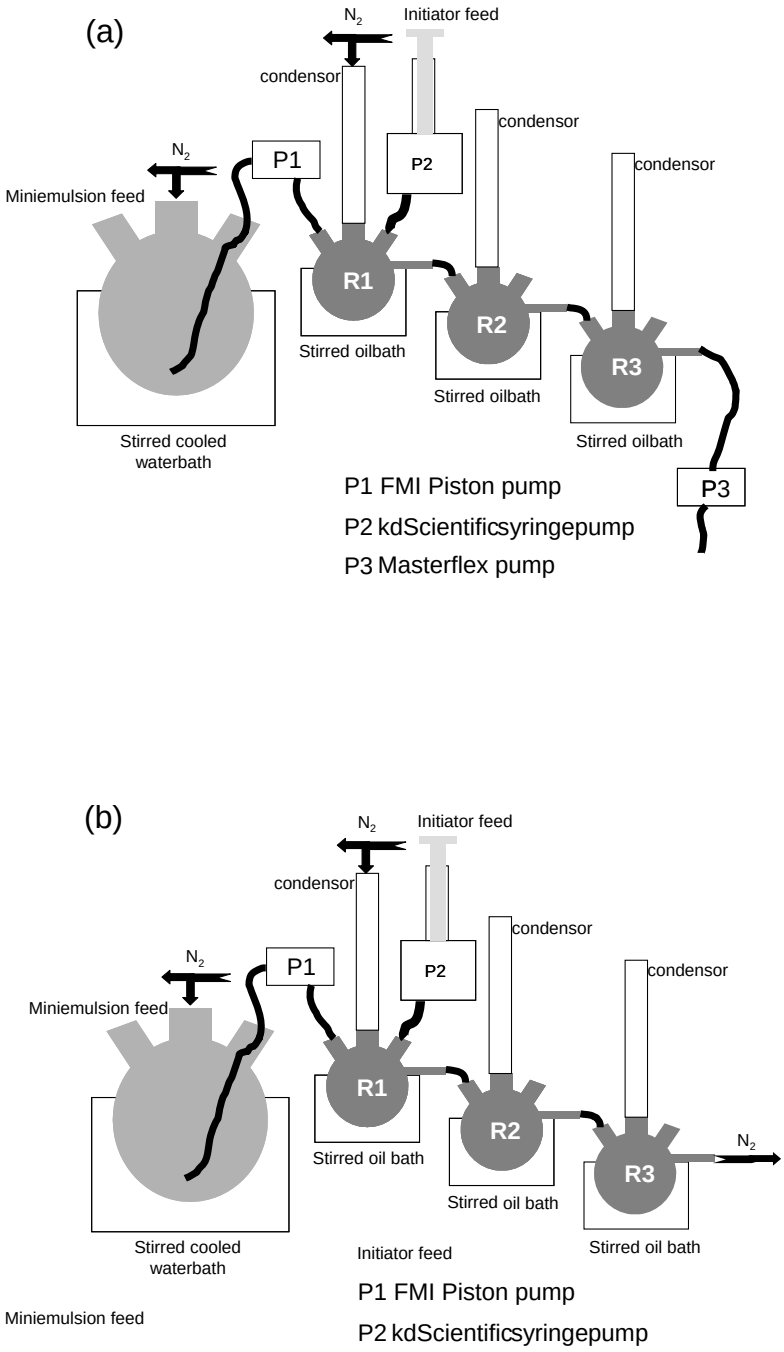

Figure 3.3 RAFT miniemulsion CSTR train setup. (a) The setup in the previous study[1, 2]; (b) The modified setup in this study (P3 was removed).

3.2.3 Miniemulsion preparation and recipe

The miniemulsion was prepared by adding a solution of styrene, hexadecane, and RAFT agent to an aqueous solution of sodium dodecyl sulfate. The mixture was first homogenized for 10 min using a Virtis Cyclone I.Q.2 at 10,000 rpm in an ice bath and then sonicated via a Fischer Model 30 sonic dismembrator operated at 70% power output for approximately 2 h, while being stirred and cooled in an ice bath. The initiator solution was an aqueous solution of sodium persulfate, purged with nitrogen for 30 min. A typical recipe and the corresponding flow rates in the previous study are shown in Table 3.1.

Table 3.1 A typical recipe and corresponding flow rates of continuous RAFT miniemulsion polymerization in the previous work.

Miniemulsion feed (g)		Initiator feed (g)	
Water	1176	Water	200
SDS	6.36	SPS	2.45
Styrene	283		
Hexadecane	6.61		
PEPDTA	2.44		
Flow rate=0.350 mL/min		Flow rate=0.888 mL/h	

3.2.4 Analysis

GPC.

The dried polymer was dissolved in tetrahydrofuran (THF, Baker) and filtered through a 0.2 μm syringe filter. GPC analyses were carried out using three columns (American Polymer Standards styrene-divinylbenzene 100, 1000, and 10^5 Å) at 30 °C. The columns were connected to a Viscotek GPCMax pump and autoinjector, a Waters 410 refractive index detector, and a LDC Milton Roy 3000 UV spectromonitor (analyzing at 311 nm) and calibrated with narrow poly(styrene) standards (Polymer Laboratories; M_n: 580-200K, M_w/M_n: 1.02-1.16). THF was used as the eluent at a flow rate of 1 mL/min, and the injection volume was 100 μL.

NMR.

The structure of RAFT agent was verified by ^{1}H NMR using a 300 MHz Varian Gemini at room temperature, using $CDCl_3$ as the solvent. ^{1}H NMR (ppm): δ 1.7d (3H, =CH-C**H**$_3$), 4.2s (2H, S=C-C**H**$_2$-), 5.1q (1H, =C**H**-CH3), 7.3m (10H, -C_6**H**$_5$).

3.3 Results and Discussion

As noted above, there were two types of transients observed in our initial experiments using a train of CSTRs. The first one, as shown in Figure 3.1a, is the continuous slow increase in conversion over time. The second is the discontinuity of conversion observed when taking samples on different days, as shown in Figure 3.1b.

There are many factors that could contribute to these transient states in our CSTR train. Here we classify them into two categories: (i) factors associated with equipment design and operation; (ii) factors derived from the polymerization mechanism. These possible causes are discussed below.

3.3.1 Equipment design and operation

As shown in Figure 3.3, the miniemulsion feed was continuously pumped into the first CSTR reactor R1 and at the same time, the initiator was fed to R1 by the syringe pump P2. The syringe is of 30ml volume, so typically it is necessary to refill it with initiator feed every few days using the flow rate denoted in Table 3.1. It is possible that newly-filled syringes may have a slightly different concentration of initiator and this could be a cause of the discontinuity observed in Figure 3.1b, where a "gap" of conversion was observed. There is another important possible equipment design issue that could also lead to the poor performance of the CSTR train. The overflow weir of each reactor was relatively small (around 5mm in diameter). Consequently, when gravity was used as the only driving force for flow (Figure 3.3a), it was sometimes observed that the latex in the reactors did not flow smoothly and even clogged the weirs, likely due to the high surface tension of latex in the narrow overflow weir. If latex continued to accumulate in the reactor, it would cause an increased residence time in the reactor, thus increasing the conversion in the CSTRs. Eventually, once the volume of the latex accumulated beyond a threshold, flow would resume and the residence time would return to the normal state. This could result in a discontinuity of the type shown in Figure 3.1b.

To remove the potential for these effects, the original CSTR train shown in Figure 3.3a was modified as shown in Figure 3.3b. The latex overflow was kept flowing smoothly under a pressure of nitrogen and pump 3 was removed from the final reactor outlet. To probe the stability of the modified reactor train, both one free-radical miniemulsion polymerization (Table 3.2) and one RAFT miniemulsion polymerization experiment (Table 3.3) were conducted, where the initiator feed concentration was doubled and the initiator flow rate was halved relative to the typical recipe used the previous study.

Table 3.2 Recipe and corresponding flow rates for the continuous conventional free-radical miniemulsion polymerization in this work.

Miniemulsion feed (g)		Initiator feed (g)	
Water	1170	Water	100
SDS	6.37	SPS	2.44
Styrene	284		
Hexadecane	6.62		
Flow rate = 0.300 mL/min		Flow rate = 0.444 mL/h	

Table 3.3 Recipe and corresponding flow rates for continuous RAFT miniemulsion polymerization in this work.

Miniemulsion feed (g0		Initiator feed (g)	
Water	1173	Water	100
SDS	6.35	SPS	2.45
Styrene	281		
Hexadecane	6.62		
PEPDTA	2.44		
Flow rate = 0.300 mL/min		Flow rate = 0.444 mL/h	

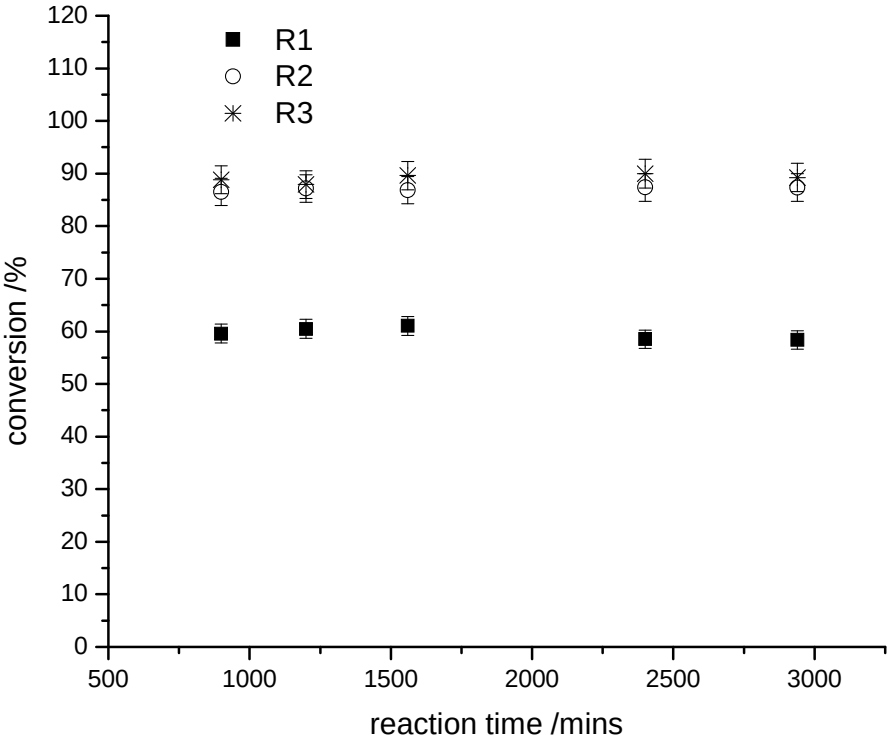

Figure 3.4 The conventional free-radical miniemulsion polymerization of styrene in modified CSTR trains.

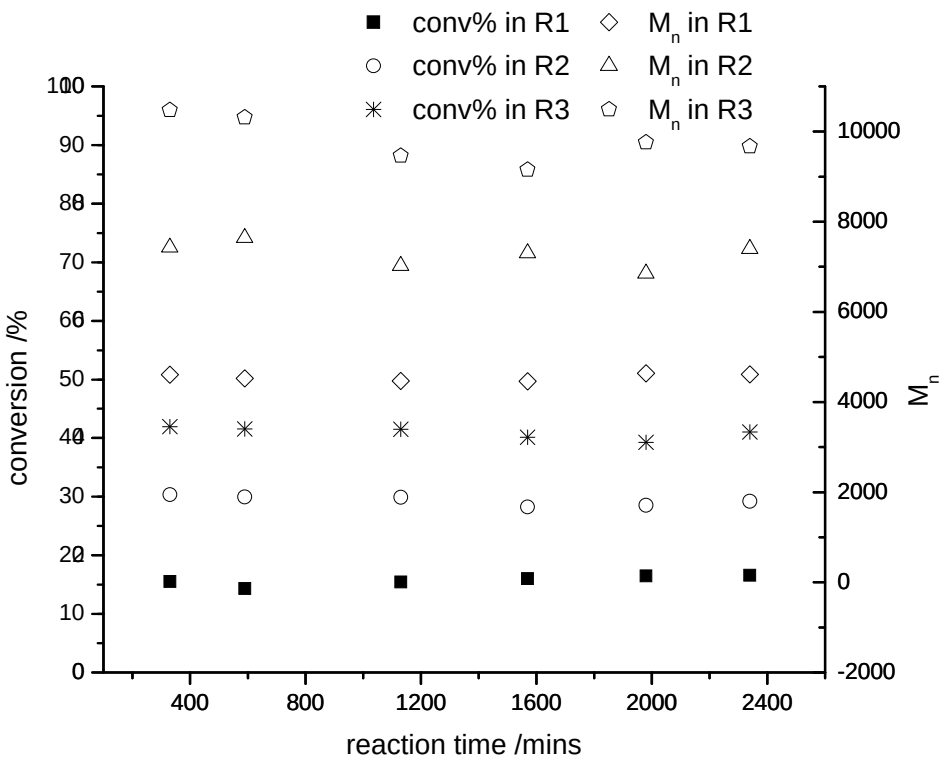

Figure 3.5 RAFT miniemulsion polymerization of styrene with double initiator concentration and half initiator feed flow rate in modified CSTR trains.

As shown in Figure 3.4 and Figure 3.5, there was no evidence of the transient behavior found in the previous study. The experiments were repeated several times with the new equipment setup and no transient behavior was ever observed. Figure 3.6 shows the relationship between Mn, PDI and the conversion in the reactors. With an increasing number of reactors, the Mn increased linearly with the conversion and the PDI decreased slowly. Clearly, the modified CSTR train exhibited good stability. Compared with the conventional free-radical miniemulsion polymerization, the RAFT miniemulsion polymerization in Figure 3.7 experienced a slower polymerization rate due to the retardation effect of RAFT agent.[134] However, the conventional miniemulsion free-radical polymerization seemed to suffer a limited conversion in the third reactor though it had a much faster polymerization rate, which could be due to the glass effect at high conversion.

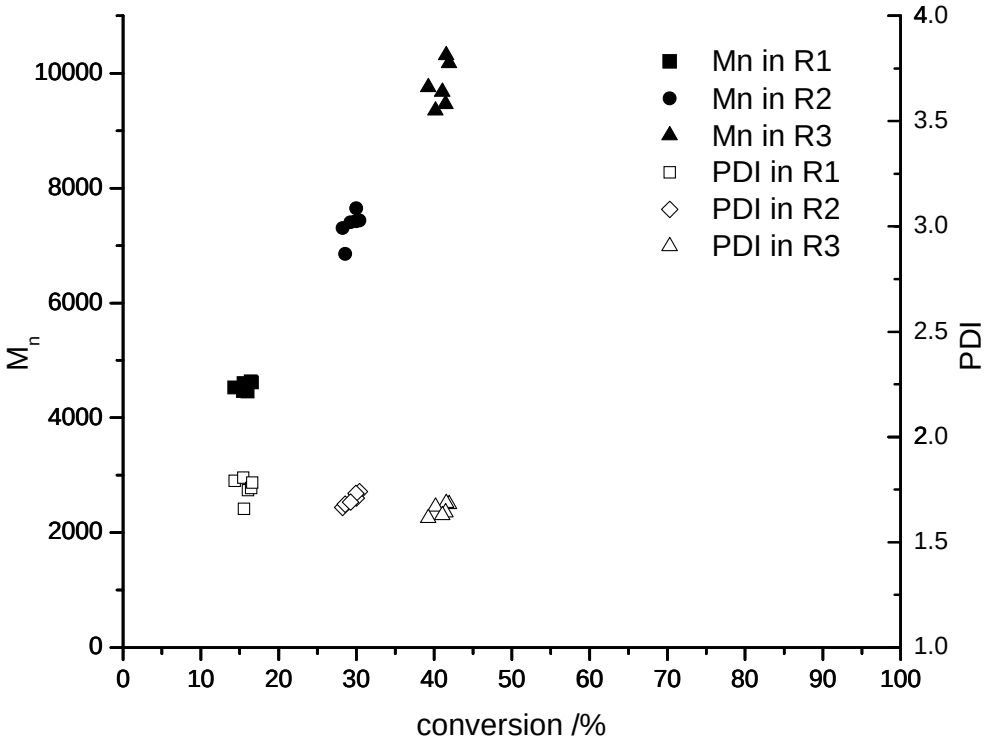

Figure 3.6 Relationship between Mn, PDI and conversion of RAFT miniemulsion polymerization of styrene in the reactors. The recipe is shown in Table 3.3.

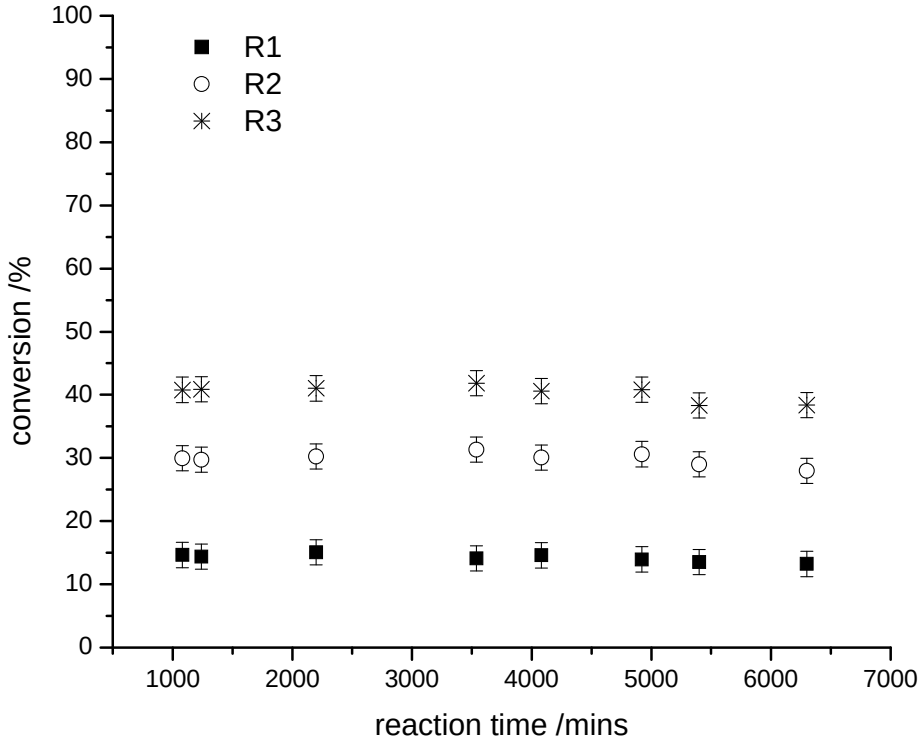

Figure 3.7 RAFT miniemulsion polymerization of styrene in the CSTR trains over five days.

3.3.2 Polymerization mechanism

3.3.2.1 Micellar nucleation

Oscillatory transients in conventional emulsion polymerization in a CSTR are well known.[135-137] Thus, it was necessary to evaluate whether the discontinuity in conversion in Figure 3.1b might be a similar oscillatory transient.

Oscillation in continuous emulsion polymerization results from the competing processes of particle growth and particle nucleation. It results in periods of more particle nucleation followed by periods where less nucleation takes place, which generate oscillations in particle number and monomer conversion. Miniemulsion polymerizations, however, should not be subject to the oscillatory behavior of conventional emulsion polymerizations in a CSTR. The locus of nucleation in miniemulsions is typically in the

monomer droplets instead of in micelles. In addition, the surfactant concentration in miniemulsions is much less than in emulsion polymerization. There should be no micelles to cause oscillation, so theoretically continuous RAFT miniemulsion should not have oscillations.

However, to verify this reasoning, one experiment was run that lasted for one week, as shown in Figure 3.7. Typically, the frequency of oscillation is approximately four times the residence time. For this reactor train, the residence time in each reactor is about 2 h; however, as shown in Figure 3.7, the conversion stayed quite steady over one week. Thus, oscillation can be safely ruled out.

3.3.2.2 Possible Feed Changes in the Storage Tank

Given the above results, changes in the quality of the feed are the most likely reasons for the observed steady state drift in Figure 3.1. Several potential changes should be considered:

1. Hydrolysis of the RAFT agent

Dithioesters have been reported to hydrolyze under certain temperature and pH conditions.[138-140] Temperature and pH both play a significant role in the hydrolysis process. Higher temperatures and higher pH (above 7) tend to favor hydrolysis.[141, 142] It is also well known that PEPDTA shows inhibition and retardation phenomena.[134, 143-146] Thus it is reasonable to consider the gradual hydrolysis of PEPDTA in the feed tank as one cause of the increasing conversion observed in the CSTRs. However, in our CSTR train, both the low temperature and the use of anionic surfactants such as SDS generate a low PH environment that should suppress the hydrolysis process. In addition, PEPDTA is hydrophobic, and most of the RAFT agent will partition into the styrene droplets, making hydrolysis much less likely. Even so, to examine the above argument, the RI and UV detectors of the GPC were used to monitor possible changes in the miniemulsion feed. The onset of the possible RAFT degradation can be sensitively detected by the evolution of the absorbance via the RI and UV detectors. If there is indeed a hydrolysis, the small hydrolysis product molecules would cause the peak to slowly move towards lower molecular weight in the RI chromatograms and at the same time, the C=S UV absorption of the RAFT agent at 311 nm would decrease if there is a loss of C=S functionality. To

assess whether a degradation of C=S of PEPDTA might occur, the areas under the UV and RI curves of the chromatograms were compared. A relationship between the total mass of reactants and the total number of C=S bonds remaining using normalized UV/RI curves can be established by taking the ratio of the areas under the UV and RI peaks. Since the area under the RI peak is proportional to the total mass of the sample, which would not change over time, and that of the UV signal is proportional to the amount of C=S moiety or concentration of PEPDTA in the sample, a decrease in the UV/RI area ratio would indicate loss of the C=S bond. Figure 3.8 shows the normalized UV/RI area ratios plotted against the hydrolysis time for the miniemulsion feed in Table 3.3. It shows only marginal evidence of hydrolysis in the miniemulsion feed, even after 2 days.

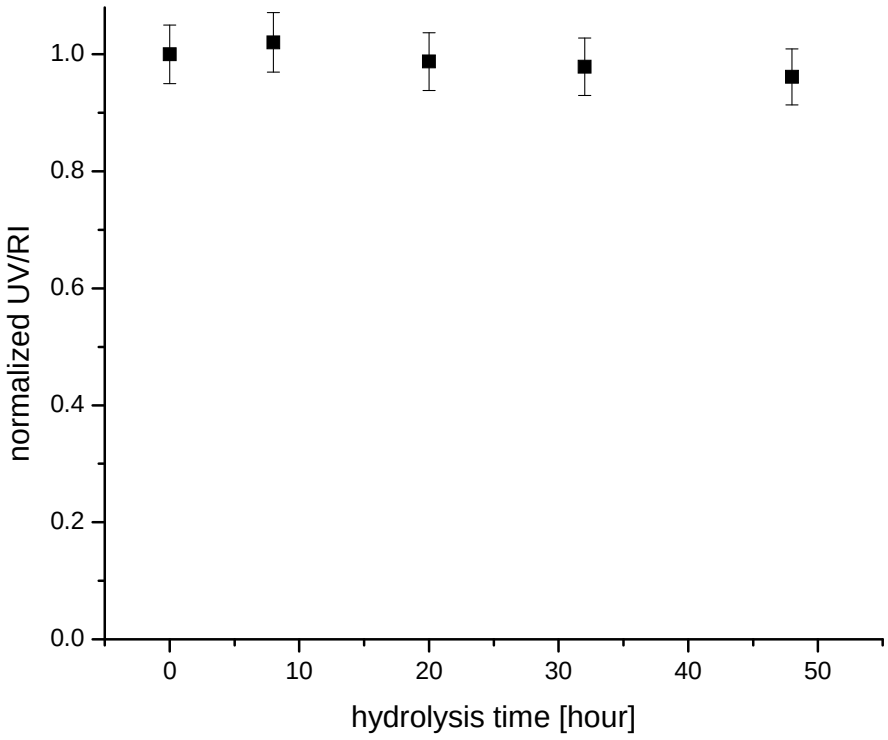

Figure 3.8 Hydrolysis test of PEPDTA in the miniemulsion feed. The UV absorbance at 311 nm was normalized by the area under the RI curve.

2. Oligomerization

For controlled emulsion or miniemulsion polymerization, it is interesting to note that there is often some phase separated oil phase at the vortex. This is not just a special characteristic of RAFT miniemulsion polymerization,[83, 86] but occurs often in CSTR miniemulsion polymerization. In our previous experiments, there was also a thin layer of separated oil phase at the vortex of the miniemulsion feed.[2]

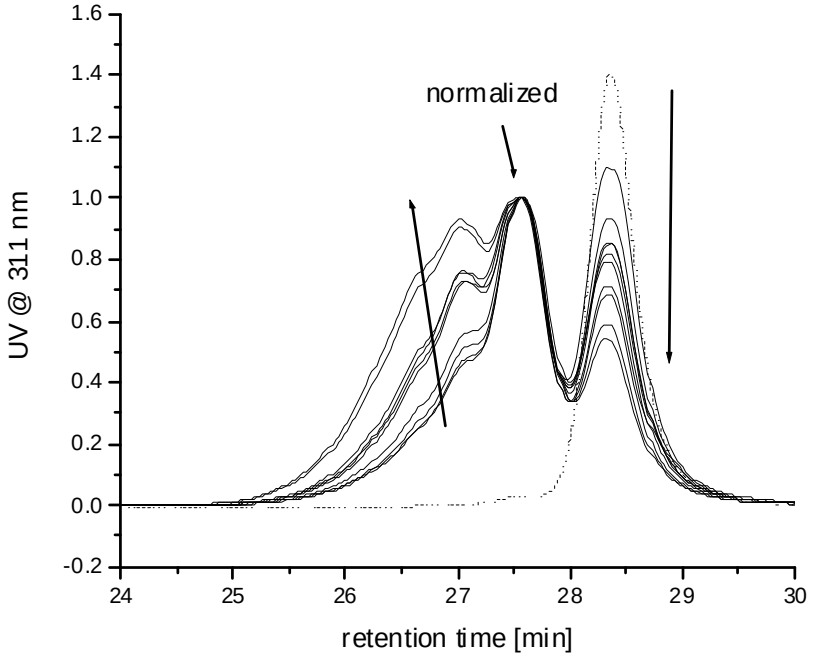

Figure 3.9 Evidence of oligomerization in the previous work.[2] The UV absorbance peak with higher molecular weight at 311nm increased with time as a sign of oligomerization.

In the previous work, it was found that the miniemulsion feed in the storage tank was slightly oligomerized, as shown in Figure 3.9 and that the oligomerization rate was surprisingly fast.[2] Oligomerization in the feed should have two effects on the total polymerization rate. First, it generates RAFT-mediated oligomeric radicals or oligomers. If oligomerization occurs in the storage tank, this would eliminate the preequilibrium step

or initiation step of RAFT polymerization in which RAFT agent reacts with the monomer.[80, 134, 147] This helps to increase the polymerization rate over time. At the same time, these oligomeric radicals are less likely to desorb from the miniemulsion droplets. With a longer lifetime and the segregation effects in the miniemulsion droplets, these radicals have more opportunity to propagate, thus increasing the overall conversion. Second, oligomerization may contribute to superswelling of droplets.[86] Due to an uneven polymerization in the miniemulsion droplets at the initial stage of an experiment, the oligomerized droplets may draw monomer from the unreacted monomer droplets until the unoligomerized ones are completely consumed. Thus the total droplet number may decrease and this would slow the polymerization rate. These two effects are competitive. Whether the conversion increases or not depends on which the two effects dominates the process.

We now consider the assumption of oligomerization in the miniemulsion feed tank.[2] Notice that, in Figure 3.1b, the conversion curve for the second day looks like a duplicate of that in the first day, and the conversion at 1200 min was even lower than at 600 min, so the unsteady state was likely not caused just by oligomerization. Furthermore, there was no initiator added in the miniemulsion feed and the feed tank was cooled with an ice bath. So the question becomes: does oligomerization really happen in the miniemulsion feed under all conditions? Figure 3.10 shows that the UV adsorption of miniemulsion feed samples (at 311 nm) taken every 12 h. These correspond to the C=S content in the polymer chains. If oligomers were formed, the UV adsorption would move toward a lower retention time. However, Figure 3.10 shows no change of UV adsorption even after 36 h, indicating no oligomerization in the miniemulsion feed using the revised reactor setup.

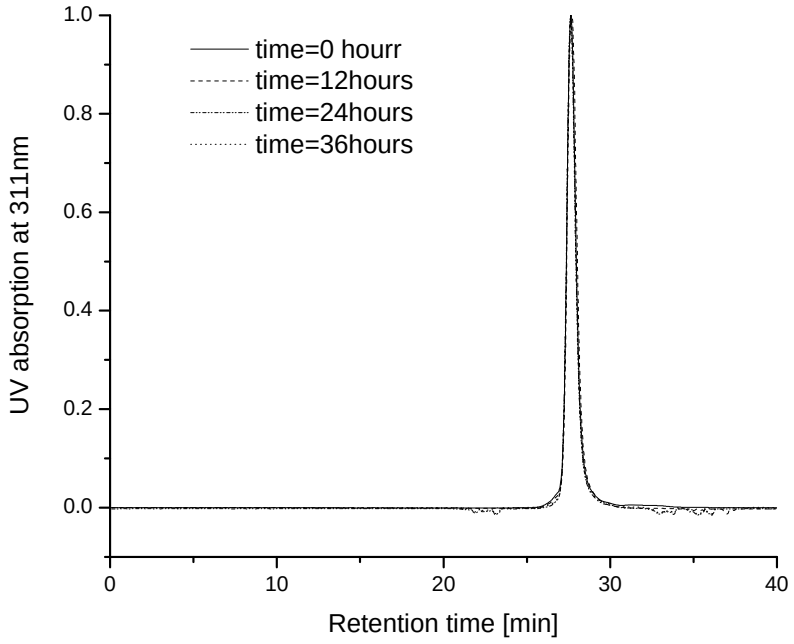

Figure 3.10 Normalized UV absorbance at 311 nm of the miniemulsion feed.

To further investigate the assumption of oligomerization in the miniemulsion feed, the top orange oil phase at the vortex, which should contain RAFT-mediated oligomers if there is oligomerization in the miniemulsion feed, was separated and analyzed by GPC. The results are shown in Figure 3.11. Again, there is no evolution of the curves, indicating no oligomerization in the separated oil phase. This again suggests that oligomerization in the miniemulsion feed is not significant.

In the previous study, [1, 2] there was an oligomerization in the miniemulsion feed and it was suggested that the oligomerization process could contribute to the transient phenomena in the CSTR. This may be due to small amounts of impurities in the RAFT agent and the surfactant SDS. [148, 149] These effects of the impurities are very difficult to reproduce because of the different batch of the chemicals used. However, in this work there was no oligomerization observed in the miniemulsion feed.

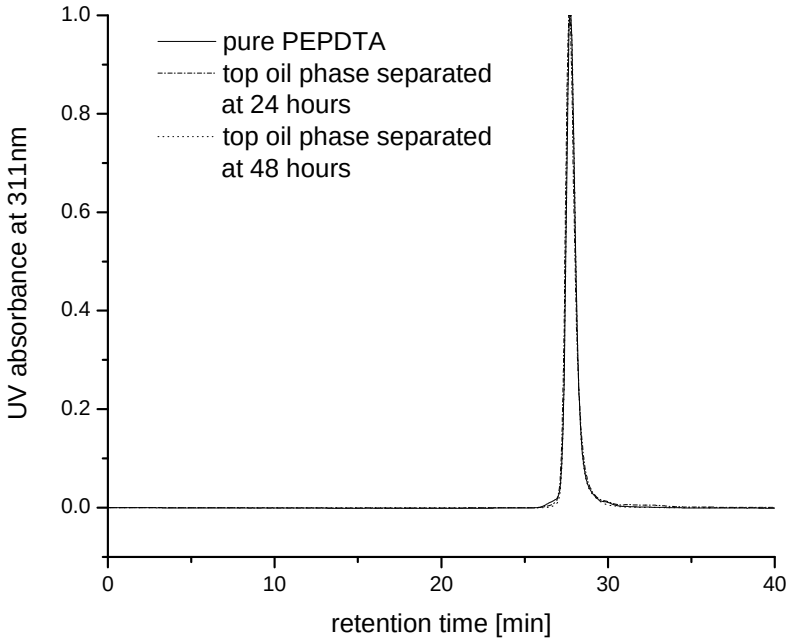

Figure 3.11 Normalized UV absorbance of the oil phase separated at vortex of the miniemulsion feed tank.

3. Redistribution of RAFT agent.

It is well known that there is a loss of stability for miniemulsions that include a RAFT agent compared with conventional miniemulsions.[86] A common observation is the presence of a tiny oil phase separated at the vortex. This was also found in our experiments after long periods of time. Thus, concern should be given to the stability of the miniemulsion feed since it would directly affect the stability of the following CSTR train.

Up to now there have been very few papers dealing with the stability of controlled radical miniemulsions. A superswelling theory was recently proposed to explain the loss of stability that is sometimes observed.[86] However for the miniemulsion feed, the superswelling theory can not be applied since the superswelling theory requires oligomers to form unevenly in different droplets in the miniemulsions, and therefore does not account for colloidal instability of the miniemulsion feed prior to the onset of polymerization. From a colloidal stability standpoint, RAFT agent can be considered to

be a special costabilizer, but not of the same stabilizing effectiveness as costabilizers such as hexadecane. RAFT agent improves the stability of miniemulsions as when its solubility is comparable to hexadecane; when the RAFT agent is more hydrophilic than the costabilizer, it dilutes the costabilizer, making the miniemulsion less stable and contributing to oil phase separation. A simple model on the stability of RAFT miniemulsion is included in the Appendix A.

Given the hydrophobicity of the RAFT agent used in this work, the RAFT agent is thought to have little effect on colloidal stability. Besides, the experiments showed indicate that the miniemulsion feed was stable for one week or more without obviously phase separation or creaming. Therefore, the possibility of an unstable miniemulsion feed being a key cause for the previously observed transients is ruled out.

3.4 Conclusion

Two categories of factors potentially contributing to unstable transients in RAFT miniemulsion polymerization in CSTR trains were examined in this work. Possibilities from equipment design and operation were first checked. When keeping the CSTR train under nitrogen pressure and constant concentration of initiator feed, no significant transient state was observed. Possibilities related to the polymerization mechanism were then evaluated. However, such possibilities were ruled out after careful analysis. Therefore, the transient states in the previous work appear to be a result of the previous equipment design and operation (and/or impurities) rater than mechanistic issues associated with RAFT miniemulsion polymerizations. A steady state in RAFT miniemulsion polymerization in a CSTR train can be achieved.

CHAPTER 4

RAFT MINIEMULSION POLYMERIZATION OF PARTIALLY WATER SOLUBLE MONOMER*

4.1 Introduction

As mentioned in the first chapter, RAFT polymerization has been demonstrated to be a powerful tool to produce polymers with well-defined or special architectures. Besides the common homogeneous systems,[72, 150] the application of controlled radical polymerization to heterogeneous media such as miniemulsion has gained increasing interest in the last few years.[1, 2, 83, 97, 151-159]

In the previous chapter, we discussed RAFT miniemulsion polymerizations in a CSTR. The monomer in the study was styrene, a typical hydrophobic monomer widely used in different applications. In this chapter, we will explore RAFT miniemulsion polymerization of partially water soluble monomers. Here we take γ-methyl-α-methylene-γ-butyrolactone (MeMBL) as a representative partially water soluble monomer.

One of the reasons why we selected MeMBL as our target monomer is that α-methylene lactones have numerous unique physical, biological and chemical properties.[160-162] α-Methylene lactones are typically colorless low viscosity liquids but with a very high boiling point due to their polar, cyclic structure. As a result, α-methylene lactones can serve as excellent high boiling solvents for oligomers and polymers.[163] α-Methylene lactones are integral building blocks of many known natural products, such as the sesquiterpene lactones. [164] They exhibit various important biological activity responses, including cytotoxic, antitumoral and bactericidal properties. [160] Some α-methylene lactones are also highly reactive monomers for polymerizations. Free-radical and anionic homopolymerization of α-methylene lactones have been

* Portions of this chapter have been published in J. Polym. Sci., Poly. Chem., 2008, 46, 5929-5944.

reported. [165, 166] α-Methylene lactones have also been copolymerized with different monomers such as styrene, methyl methacrylate and methoxystyrene.[166-170]

The unique structure of α-methylene lactones endows their polymers with useful properties and potential applications in a wide range of fields. Poly(α-methylene lactone)s can be used as precursors of a class of polymers with multiple pendent functional groups on the backbone. Due to the incorporation of the lactone structure into the polymeric chain, poly(α-methylene lactone)s usually have high glass transition temperatures (Tg) and excellent resistance to common organic solvents.[165] Therefore they can be used for thermoplastic tougheners, heat resist resins and dental resins.[163, 171-173] In addition to these favorable properties, poly(α-methylene lactone)s exhibit superior optical clarity and brilliance to poly(styrene), which makes poly(α-methylene lactone)s excellent candidates for optical fibers, moldings and organic glasses. [174-176]

Among the α-methylene lactone family, γ-methyl-α-methylene-γ-butyrolactone (MeMBL) is of a particular importance. MeMBL is a cyclic analogue of methyl methacrylate (MMA) containing an exomethylene functional group and thus it is potentially a good substitute for MMA in various applications. Moreover, it has potential to be manufactured on an industrial scale from renewable sources. DuPont has developed a process for MeMBL synthesis from levulinic acid, a chemical intermediate derived from biomass. [162]

Despite the interesting properties and applications of MeMBL and its polymers, only very limited investigations have been reported in the open literature on MeMBL, with most studies focused on the synthesis of MeMBL. [162, 177] The polymerizations of MeMBL remain barely explored. To date, free-radical and anionic solution polymerizations of MeMBL have been reported in only one paper.[178]

Many radical polymers are made in aqueous dispersed processes that allow production of polymer latexes with tailored properties. Poly(MeMBL) copolymers and blends by emulsion polymerization have been reported in several patents.[171, 172, 179] However, no detailed emulsion polymerization kinetics of MeMBL have been reported. Therefore, it is of significant importance to explore the polymerization properties and kinetics of MeMBL in aqueous dispersed systems such as emulsion (micellar nucleation dominant) and miniemulsion (droplet nucleation dominant).[180] As an added benefit, the

ability to control the course of the polymerization of MeMBL would be a significant advantage.

Past work has shown that the miniemulsion polymerization of monomers with significant water solubility, such as acrylonitrile (~7wt%), can lead to different reaction behavior.[13] [181] In particular, use of monomers with significant water solubility can lead to severe latex stability issues. In this chapter, we take MeMBL as a representative partially water soluble monomer and present a free-radical and RAFT kinetic study of emulsion/miniemulsion homopolymerization of MeMBL and copolymerization with styrene.[182] In doing so, we push the limits of the miniemulsion technique, as MeMBL is a monomer with significant water solubility (~9wt% based on water).

4.2 Experimental Section

4.2.1 Materials

Styrene (ST) (Aldrich, >99%) and MeMBL (Dupont, >97%; major impurity is γ–methyl–γ-butyrolactone) were purified by a column packed with inhibitor remover (Aldrich) specific for hydroquinone. Hexadecane (HD) (Aldrich, 99%), sodium persulfate (SPS) (Aldrich, 98%), and sodium dodecyl sulfate (SDS) (J.T. Baker, 99.8%) were used as received. Deionized water was generated with a U.S. Filter Systems Deionizer and was used without further purification. The RAFT agent, 1-phenylethyl phenyldithioacetate (PEPDTA), was synthesized according to a literature procedure, [133] using the following materials: carbon tetrachloride (Aldrich, 99.9%), benzyl chloride (J.T. Baker, 99.9%), carbon disulfide (J.T. Baker, 99.9%), magnesium turnings (Lancaster, 99+%), methanol (J.T. Baker, 100.0%), ethyl ether (Fischer, certified A.C.S., anhydrous), and *p*-toluenesulfonic acid monohydrate (Aldrich, 98%). The structures of MeMBL and PEPDTA are shown in Figure 4.1.

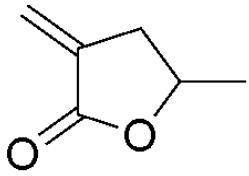

γ-Methyl-α-methylene γ-butyrolactone (MeMBL)

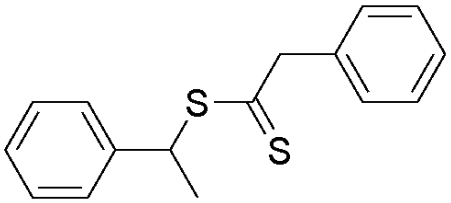

1-phenylethyl phenyldithioacetate (PEPDTA)

Figure 4.1 The monomer, MeMBL, and the RAFT agent, PEPDTA, used in the study

4.2.2 Polymerization

4.2.2.1 Free-radical "miniemulsion" homopolymerizations of MeMBL [183]

Table 4.1 shows a representative recipe for free-radical "miniemulsion" homopolymerizations (Exp.1-9). The continuous phase of the miniemulsion was made by adding 0.28g surfactant, SDS, to 49g water and mixing for 15 min. The dispersed phase was a solution of 11.2g MeMBL and 0.22g costabilizer, HD. The coarse emulsions were prepared by adding the dispersed phase to the continuous phase and homogenizing for 5 min in an ice bath (Virtis Cyclone I.Q.2 at 10000 rpm). The miniemulsions were made by sonication of the coarse emulsions for about 5 min (Fischer Model 30 sonic dismembrator operated at 70% power output), with stirring in an ice bath. The initiator, SPS (0.036g), was dissolved in 1 ml water. After the miniemulsion was heated to the reaction temperature, the initiator solution was injected to initiate the polymerization. Samples were taken with syringe every certain interval for characterizations.

Table 4.1 Recipe for free-radical miniemulsion homopolymerization of MeMBL.

Component		Mass (g)	Notes
	water	50.0	
Surfactant	SDS	0.28	0.018mol/L
Initiator	SPS	0.036	
Monomer	MeMBL	11.2	22 wt% of water
Costabilizer	Hexadecane	0.22	2 wt% of monomer

4.2.2.2 Emulsifier free free-radical emulsion homopolymerizations of MeMBL

11.2g of MeMBL was dispersed into 49g water under magnetic stirring at 80 rpm and purged with N_2 for 15 min. SPS (0.036g) was dissolved in 1 ml water and injected to the dispersion when the dispersion was heated to 60^{o}C to initiate the polymerization. The stirring rate was kept at 80 rpm throughout the polymerization. The translucent dispersion became milky within 5 min. At a conversion of 15%, the shelf life of resulting latex was more than 2 h. However, the latex became less stable with time and aggregation was observed during polymerization.

4.2.2.3 Free-radical miniemulsion copolymerizations and RAFT miniemulsion polymerizations of MeMBL and styrene

A representative recipe for free-radical miniemulsion copolymerizations (Exp. 12-14) and RAFT miniemulsion polymerizations (Exp. 17 and Exp.18) is shown in Table 4.2. The continuous phase of the miniemulsions was made by adding 0.17g SDS to 30g water and mixing for 15 min. For free-radical miniemulsion copolymerizations of MeMBL and styrene, the dispersed phase was a solution of 3.5g MeMBL, 3.25g styrene and 0.22g HD. The oil soluble initiator, AIBN, was dissolved in the dispersed phase. For RAFT miniemulsion polymerizations, the RAFT agent, PEPDTA, was added to the dispersed phase. The coarse emulsions and the miniemulsions were prepared in the same procedure as for the free-radical "miniemulsion" homopolymerizations of MeMBL.

Table 4.2 Recipes for free-radical and controlled miniemulsion copolymerizations of MeMBL and styrene.

	Component		Mass	Notes
	Free-radical mini	RAFT mini	(g)	
	Water	water	30.0	
Surfactant	SDS	SDS	0.17	0.018mol/L
Monomer	MeMBL	MeMBL	3.50	22 wt% of water
	ST	ST	3.25	[MeMBL]:[ST]=1:1
Initiator	AIBN	AIBN	0.010	[ST]:[Initiator]=500:1
Costabilizer	Hexadecane	Hexadecane	0.30	3 wt% of monomer
RAFT	-	PEPDTA	0.068	[ST]:[RAFT]=125:1

Table 4.3 Experimental parameters for the polymerizations of MeMBL.

Expt.	Temp. (°C)	MeMBL (g)	ST (g)	[MeMBL]/[ST]	SDS (g)	PEPDTA (g)	HD (g)	SPS (g)	AIBN (g)
1	60	11.2	-	-	0.28	-	0.22	0.036	-
2	55	11.2	-	-	0.28	-	0.22	0.036	-
3	65	11.2	-	-	0.28	-	0.22	0.036	-
4	60	11.2	-	-	0.28	-	0.22	0.024	-
5	60	11.2	-	-	0.28	-	0.22	0.048	-
6	60	11.2	-	-	0.18	-	0.22	0.036	-
7	60	11.2	-	-	0.42	-	0.22	0.036	-
8	60	11.2	-	-	0.28	-	0.14	0.036	-
9	60	11.2	-	-	0.28	-	0.34	0.036	-
10	60	11.2	-	-	-	-	-	0.036	-
11	70	5.61	-	-	-	-	-	-	0.008
12	70	1.40	5.21	1:4	0.17	-	0.30	-	0.01
13	70	3.50	3.25	1:1	0.17	-	0.30	-	0.01
14	70	5.61	1.30	4:1	0.17	-	0.30	-	0.01
15	70	1.40	5.21	1:4	-	0.068	-	-	0.01
16	70	3.50	3.25	1:1	-	0.068	-	-	0.01
17	70	1.40	5.21	1:4	0.17	0.068	0.30	-	0.01
18	70	3.50	3.25	1:1	0.17	0.068	0.30	-	0.01

4.2.3 Characterization

The monomer conversions were measured gravimetrically after the polymers were precipitated in chilled methanol and dried under vacuum at 50^{o}C.

The molecular weight and polydispersity of the polymers were measured by gel permeation chromatography (GPC). The dried polymer samples were dissolved in chloroform and filtered through a 0.2μm syringe filter. GPC analyses were carried out using three columns (American Polymer Standards styrene-divinylbenzene 100, 1000, and 10^5 Å) at 30°C. The columns were connected to a Viscotek GPCMax pump and autoinjector, a Waters 410 refractive index detector, calibrated with narrow poly(styrene) standards (Polymer Laboratories; Mn: 580-200K, Mw/Mn: 1.02-1.16). Chloroform was used as the eluent at a flow rate of 1 mL/min, and the injection volume was 100 μL.

The ^{1}H NMR spectra of MeMBL-styrene copolymers were recorded at 24°C with a Bruker AMX 400 system. $CDCl_3$ was used as solvent with tetramethylsilane (TMS) as a reference.

The stability of the emulsions and latexes was evaluated by their shelf lives which were measured by the time before significant phase separation of the stored emulsions or latexes was visually observed at room temperature.

Latex particle radius and polydispersities were analyzed using quasi-elastic light scattering (QELS, Protein Solutions DynaPro with DynaPro DCS v 5.26 software). The particle number N_p was estimated with the following equation:

$$N_p = \frac{m_0 x}{\frac{4}{3}\pi r^3 \rho_p} \tag{4.1}$$

where m_0 is the initial weight concentration of the monomer (g/mL H_2O), x is the conversion of the monomer, r is the average radius of particles and ρ_p is the density of poly(MeMBL). Here the density of poly(MeMBL) was estimated as 1.4g/cm^3. For the homopoly(MeMBL) latex, the samples were diluted in pure water, while the copolymers of MeMBL were diluted in styrene saturated water**.**

4.3 Results and Discussion

To explore the polymerization of MeMBL in aqueous dispersed systems, we used the following approach. First, the free-radical miniemulsion homopolymerization was explored to elucidate general reactivity patterns of the monomer and to elucidate basic features of dispersed polymerization with this new monomer. With this information in hand, we then developed a strategy to realize the controlled radical polymerization using RAFT in a dispersed system.

4.3.1 Free-radical "miniemulsion" homopolymerization

Poly(MeMBL) has a high Tg and good solvent resistance that can lead numerous process difficulties in industrial production. Miniemulsion polymerizations provide a solution to overcome these problems and can be used to produce a poly(MeMBL) latex in a "green" environment since it is based on an aqueous system. Since there is no report on the kinetics of miniemulsion polymerization of MeMBL so far, a kinetic study was first performed to build our knowledge of the properties of the polymerization.

In the study of miniemulsion homopolymerization of MeMBL, there is significant concern about the colloidal stability of the miniemulsion droplets since the solubility of MeMBL in water is as high as 9wt% (based on water) at room temperature. Several widely used anionic or cationic surfactants, (i.e. SDS, cetyltrimethylammoniumbromide (CTAB)) were tried here with HD as costabilizer to prepare a relatively stable miniemulsion of MeMBL. Even after optimization of the recipe, the miniemulsions had poor shelf lives of <1 h due to the extremely high solubility of MeMBL in water. Combinations of anionic or cationic surfactants with nonionic surfactants such as Triton X-405, Tween 80 and polyvinyl alcohol did not achieve a stable miniemulsion of MeMBL as well, although similar combinations improved the miniemulsion stability of some partially water soluble monomers such as vinyl acetate.[97] In spite of the above difficulties, appropriate formulation of the recipe allowed fairly stable poly(MeMBL) latexes with particle radius from 60 to 200 nm to be produced (shelf life more than 4 months) if the completion of the nucleation process was fast enough to create particles before the miniemulsion lost its stability. To simplify the kinetic study of the miniemulsion polymerization of MeMBL, a relatively standard recipe for miniemulsions (similar to that reported by Landfester for miniemulsion polymerization of acrylonitrile) was used here, as shown in Table 4.1.[1, 157, 181]

The conversion-time plot of free-radical "miniemulsion" polymerization of MeMBL (Exp.1) is shown in Figure 4.2. The evolution of the particle radius and particle number of Exp.1 is shown in Table 4.4 and Figure 4.3. The polymerization rate increased until the conversion reached around 40%. The evolution of particle radius and particle number in Exp.1 showed a significant deviation from that of conventional miniemulsion polymerizations, even miniemulsions of partially water soluble monomers such as vinyl acetate and methyl methacrylate.[9, 184] There was a bimodal distribution of particle radius at a low conversion. The small portion of large particles was centered at about 100nm while most of the particles were small ones centered at around 35nm, with these smaller particles growing with time to about 80nm (Table 4.4). As for the particle number, there was a sharp jump at the start of the polymerization and a steady increase until about 15% conversion, followed by a slight decrease to almost a constant value. Similar trends in particle number for Exps. 2-9 are shown in Figure 4.4. For an ideal miniemulsion

polymerization, droplets nucleate to particles in a one to one transformation.[180] Therefore, a constant value of particle number and a uniform distribution of particle radius should be obtained during the polymerization. The significant deviation in the particle number and the particle size distribution in the "miniemulsion" polymerization of MeMBL [183] implies there may be mechanisms other than the droplet nucleation that generate the particles. That is why quotations are added to the term "miniemulsion" polymerization here.

Table 4.4 Particle radius distribution of free-radical "miniemulsion" homopolymerization of MeMBL in experiment 1 at 60ºC.

Conversion (%)	Small particles <70nm		Large particles >70nm	
	Particle radius (nm)	Weight* percentage (%)	Particle radius (nm)	Weight* percentage (%)
0.26	35	76	110	19
			161	5
5.6	35	80	110	9
	50	6	162	4
			238	1
13.8	24	40	75	2
	35	53	110	4
			162	1
23.4	35	34	111	1
	51	63	163	2
41.5	35	35	76	15
	52	46	111	3
			164	1
58.5	52	61	76	32
			112	8
68.8	52	28	77	71
			113	1
73.6	52	27	77	72
78.0			77	99
			113	1

* The weight percentage of particles is given by DynaPro DCS v 5.26 software.

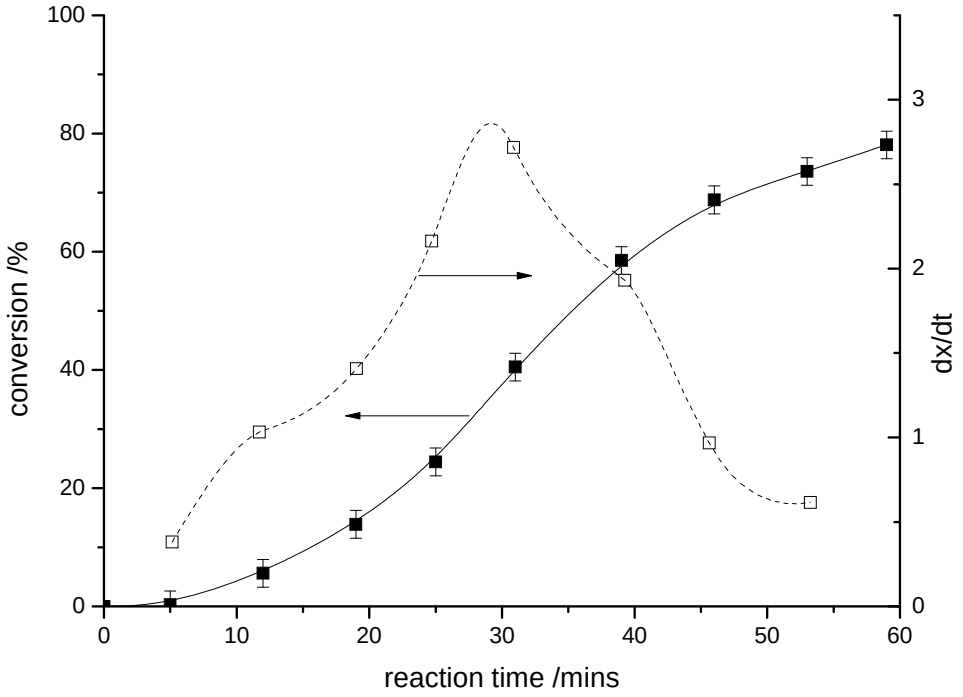

Figure 4.2 Conversion-time plot of free-radical "miniemulsion" polymerization of MeMBL in experiment 1 at 60 ^{o}C.

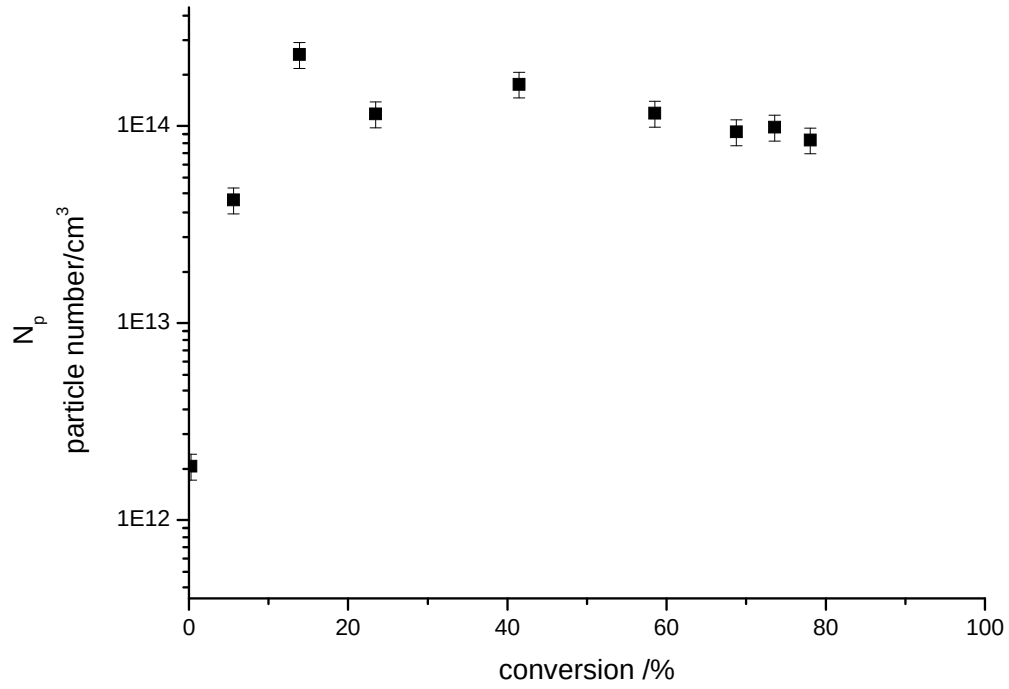

Figure 4.3 Particle number evolution in free-radical "miniemulsion" polymerization of MeMBL in experiment 1 at 60ºC.

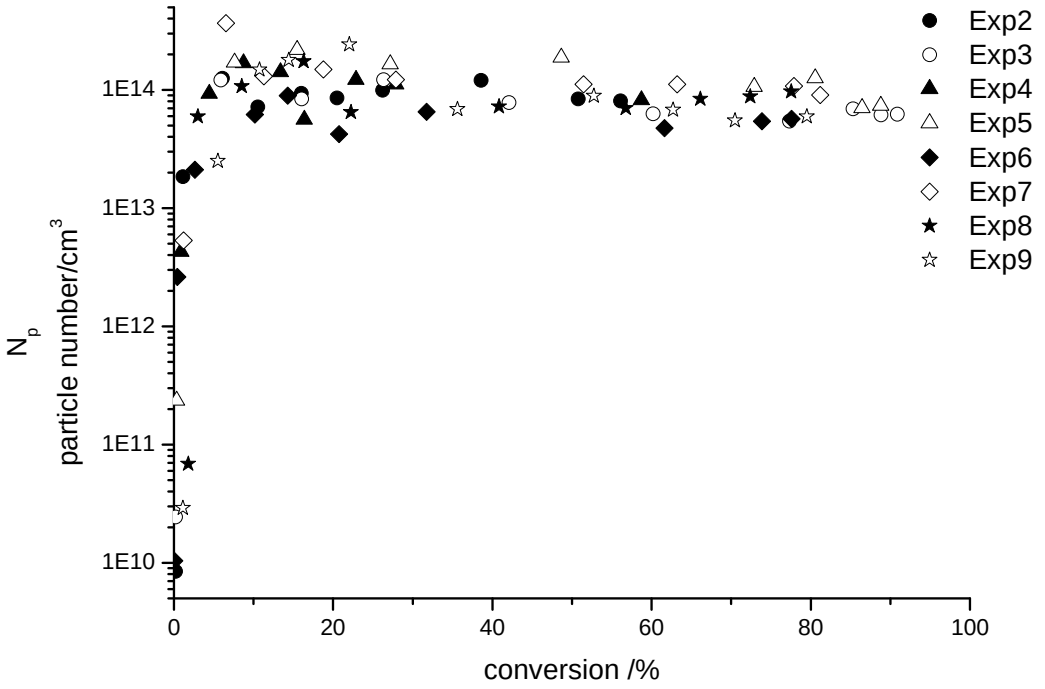

Figure 4.4 Particle number evolutions in free-radical "miniemulsion" polymerizations of MeMBL.

An emulsifier-free emulsion polymerization was carried out in Exp. 10 to validate the homogeneous nucleation assumption in the "miniemulsion" polymerization of MeMBL. Different mechanisms have been proposed to explain the nucleation process of emulsifier-free emulsion polymerizations: homogeneous nucleation,[14, 185] coagulation nucleation,[186] and micellar nucleation.[187-190] None of the three mechanisms alone can predict nucleation behavior for all the monomers studied.[191] However, when a monomer with high water solubility and little or no surfactant was used (e.g. the conditions in Exp.10), the homogeneous nucleation mechanism is highly favored and dominates in emulsifier free emulsion polymerizations.[14, 185, 191] As shown in Figure 4.5, the conversion in emulsifier-free Exp.10 increased with reaction time but at a much slower rate than in Exp.1. The evolution of particle number in Exp.10 had a similar trend as Exp.1 - a burst of particle number at the start of the polymerization and then a decrease to

a constant value (Figure 4.5). The number of particles in Exp.10 was significantly lower than in Exp.1, mainly due to the absence of surfactant to stabilize the primary particles. It is interesting to note that the particle radius at the start of emulsifier free emulsion polymerization, as shown in Table 4.5, was around 35nm, almost the same size as that of the smaller particles in the bimodal distribution of Exps.1-9. These results show significant, although not conclusive, signs of dominant homogeneous nucleation in the Exps.1-9.

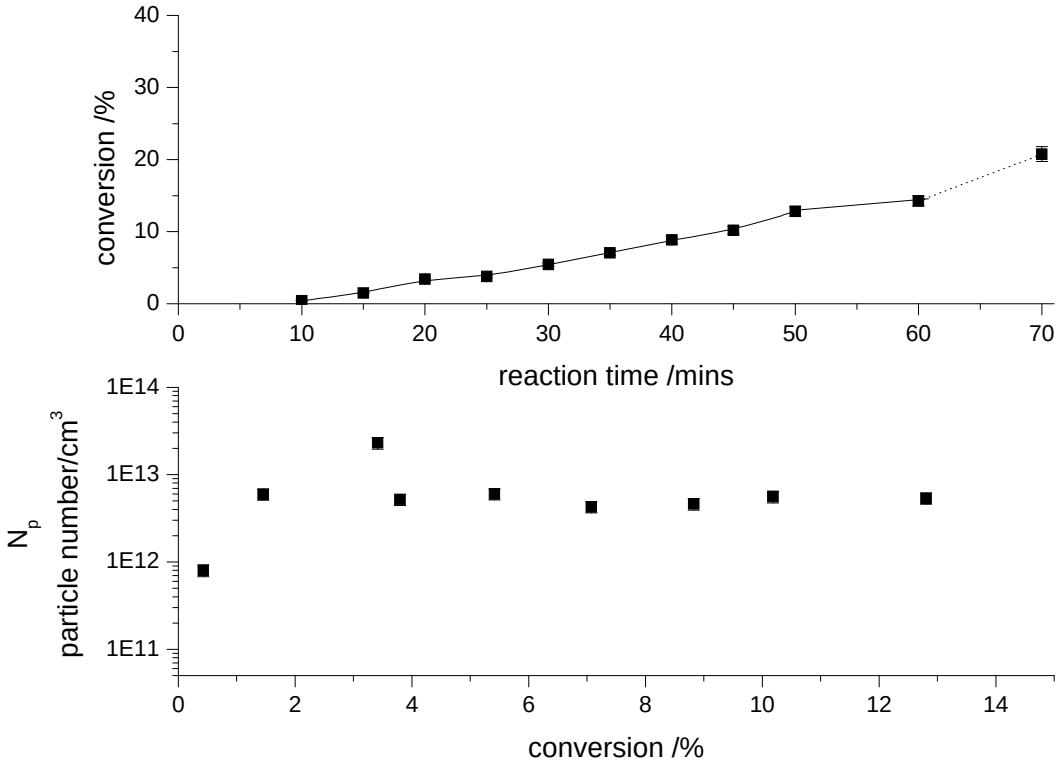

Figure 4.5 Emulsifier free emulsion polymerization of MeMBL at 60ºC. The latex became unstable when the conversion was above ~15% (shown as the dotted curve).

Table 4.5 Particle radius distribution of emulsifier free emulsion polymerization of MeMBL at 60ºC.

Reaction time (min)	Particle radius (nm)	Weight percentage (%)
5	39	70
	58	26
7.5	39	50
	58	49
10	56	85
	83	14
15	57	37
	84	62
25	59	59
	86	41
35	86	100
45	85	84
	125	15

4.3.2 Effect of reaction parameters

Experiments 1-9 were carried out to explore the effects of different reaction parameters on the kinetics of free-radical "miniemulsion" polymerization.

Figure 4.6 shows the conversion-time curves at various reaction temperatures. The effect of temperature on the rate of free-radical miniemulsion polymerization of MeMBL was evaluated at 55, 60 and 65°C. As expected, the rate of polymerization increased with increasing temperature. This is likely due to both a lower propagation rate constant and a smaller population of free-radicals generated from initiator at lower temperatures.

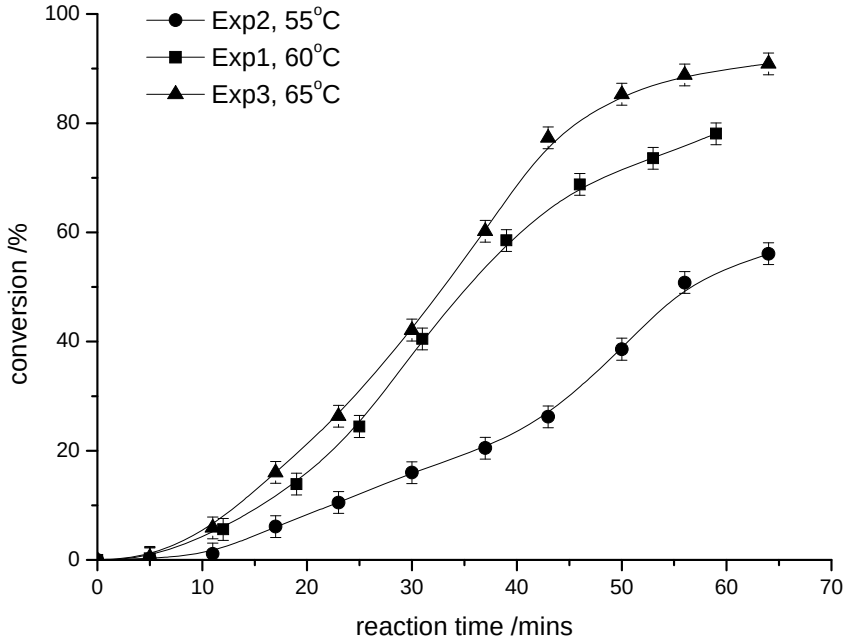

Figure 4.6 Free-radical "miniemulsion" polymerization of MeMBL at different temperatures.

Figure 4.7 shows the conversion-time curves at various initiator concentrations. Like the effect of temperature, the polymerization rate increased with increasing amount of initiator since more radicals can be generated. The amount of initiator seems have no effect on the final particle number, as shown in Figure 4.4. All the particle numbers in Exp.1, Exp.4 and Exp.5 were close to 10^{14}/L after the conversion passed 40%.

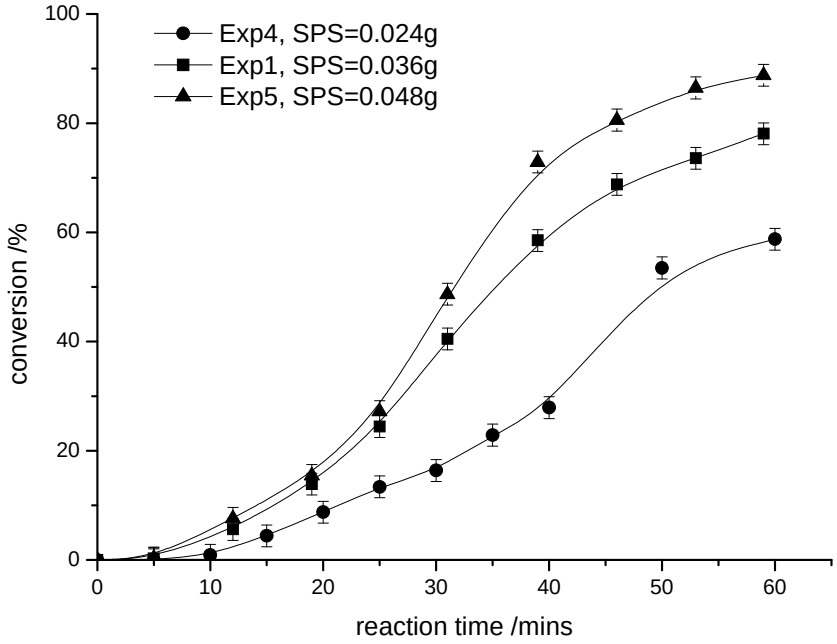

Figure 4.7 Free-radical "miniemulsion" polymerization of MeMBL at different initiator concentrations.

Figure 4.8 shows the effect of surfactant concentration on the free-radical "miniemulsion" polymerization of MeMBL. Higher conversion was achieved at a higher concentration of surfactant for the same reaction time. A larger number of particles can be obtained with a higher concentration of surfactant, since more primary particles can form and survive with the help of surfactant. The higher number of particles can contribute to the higher polymerization rate in the Exp.7, compared with Exp.6.

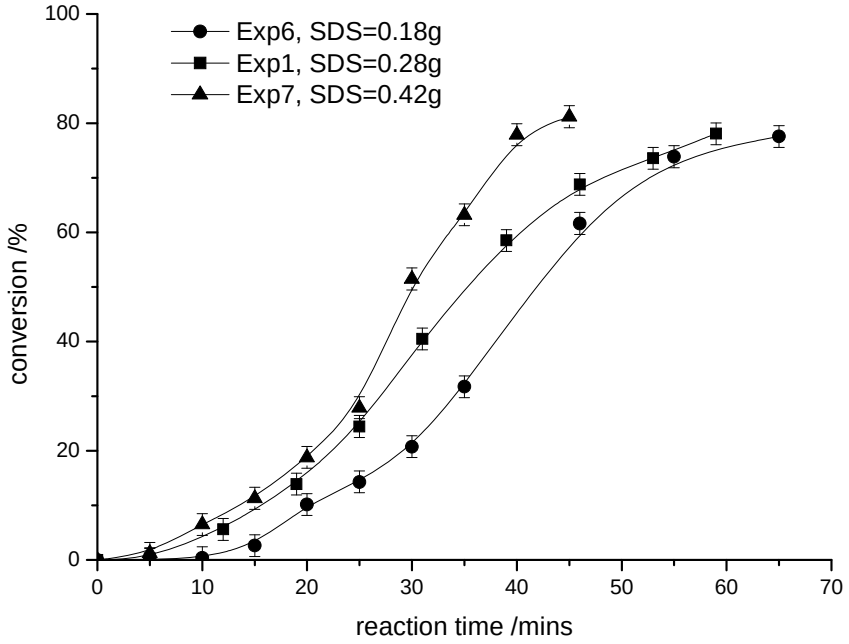

Figure 4.8 Free-radical "miniemulsion" polymerization of MeMBL with different concentrations of surfactant.

Figure 4.9 shows the effect of costabilizer concentration on the free-radical "miniemulsion" polymerization of MeMBL. An increase in the amount of costabilizer from 1% to 3% (based on monomer) had no significant effect on the kinetics of miniemulsion polymerization. Even with a relatively high concentration of HD, the evolution of particle number in Exp.9 still showed a similar trend to Exp.1 (Figure 4.4), indicating that an increase of HD might not effectively suppress the non-droplet nucleation mechanisms.

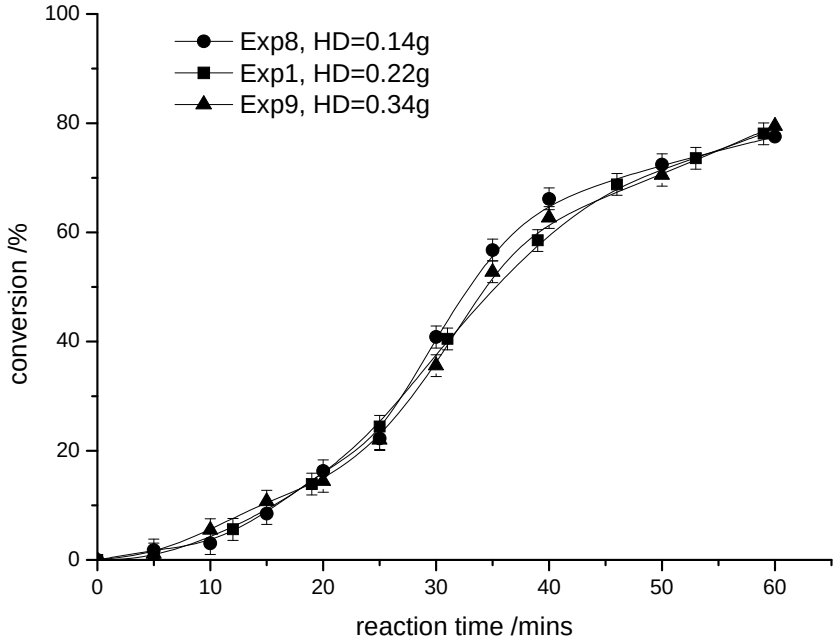

Figure 4.9 Free-radical "miniemulsion" polymerization of MeMBL at 60 ºC with different concentrations of costabilizer.

4.3.3 Controlled miniemulsion polymerization of MeMBL

4.3.3.1 Strategy for control of the miniemulsion polymerization of MeMBL

Based on the study of free-radical miniemulsion homopolymerization, several problems have to be overcome to achieve a well-controlled miniemulsion polymerization of MeMBL.

1. *Stability of the RAFT miniemulsion.* Although the RAFT agent itself has limited influence on the stability of miniemulsions,[192] RAFT miniemulsions, as compared with conventional miniemulsions, can lose their colloidal stability at the onset of the polymerization.[83, 90, 193, 194] Luo has pointed out that this could be caused by an uneven nucleation in the controlled polymerizations.[86]
2. *Homogeneous nucleation for the miniemulsion polymerization of MeMBL reported above.* As discussed above, homogeneous nucleation may dominate the nucleation process of the free-radical miniemulsion polymerization of MeMBL.

As a result, the solubility difference of the RAFT agent and MeMBL in the aqueous phase where initiation occurs can lead to poor control of the polymerization.

3. *Identification of a suitable RAFT agent for controlled polymerization of MeMBL.* The choice of a suitable RAFT agent for MeMBL is complicated by the fact that the growing polymeric chains are tertiary radicals. MeMBL has a structure similar to MMA, and so RAFT agents that are known to work well with MMA would be good candidates. To achieve a good control over the polymerization of MeMBL, the R group of the RAFT agent (R-S-(C=S)-Z) should be a very good leaving group and also a good reinitiating radical. [80] At the same time, the Z group is required to increase the reactivity of propagating radicals towards the S=C bond. [79] Moreover, the RAFT miniemulsion polymerization of MeMBL must have a reasonable polymerization rate before the miniemulsion droplets lose their stability. A widely used RAFT agent effective for MMA, cumyl dithiobenzoate, showed some level of control over MeMBL in bulk polymerization. However, severe aggregation of the latex was observed during the RAFT miniemulsion homopolymerization of MeMBL, along with significant rate retardation (data not shown). On the other hand, cumyl phenyldithioacetate, which led to less rate retardation than cumyl dithiobenzoate, gave only limited control over the polymerization of MeMBL.

To overcome the above difficulties, styrene was used as a comonomer. The introduction of styrene enabled controlled miniemulsion copolymerization of MeMBL due to several factors. First, the use of styrene can enhance the stability of MeMBL miniemulsions. Styrene has a much lower solubility in water compared with MeMBL and MeMBL dissolves well in styrene. The addition of styrene thus can shift the partitioning of MeMBL between water and the droplets. Both styrene and HD can help lower the degradation rate of the droplets by Otswald ripening, thus making MeMBL miniemulsions more stable.[192] Second, styrene is an easily controlled monomer using various common RAFT agents. Here we chose to use PEPDTA. [1] Thus, we use styrene as a comonomer to realize controlled miniemulsion polymerization of MeMBL, bypassing for now the difficulty of finding an ideal RAFT agent specific for MeMBL. An

added benefit is that the introduction of styrene will improve the solubility and tune the toughness of poly(MeMBL), although one may argue that at higher styrene loadings, enhanced polymer properties and the unique, "green" attributes of having a renewable monomer are lessened.

Based on the well known RAFT polymerization mechanism,[71] there are two possible types of propagating radicals, three possible intermediate radicals, and two possible types of macro-RAFT agents in the RAFT copolymerization of MeMBL and styrene (see Figure 4.10). With PEPDTA as a RAFT agent, the styrene-terminated radical (b) is a better addition group and a poorer leaving group compared with a MeMBL-terminated radical (a). Therefore, (g) is the dominant form of the RAFT agent we expect in the copolymerization of MeMBL/styrene. Thus, the RAFT process would be similar to that of RAFT homopolymerization of styrene; MeMBL should be incorporated in the copolymer but the polymerization will be under control similar to a homopolymerization of styrene.

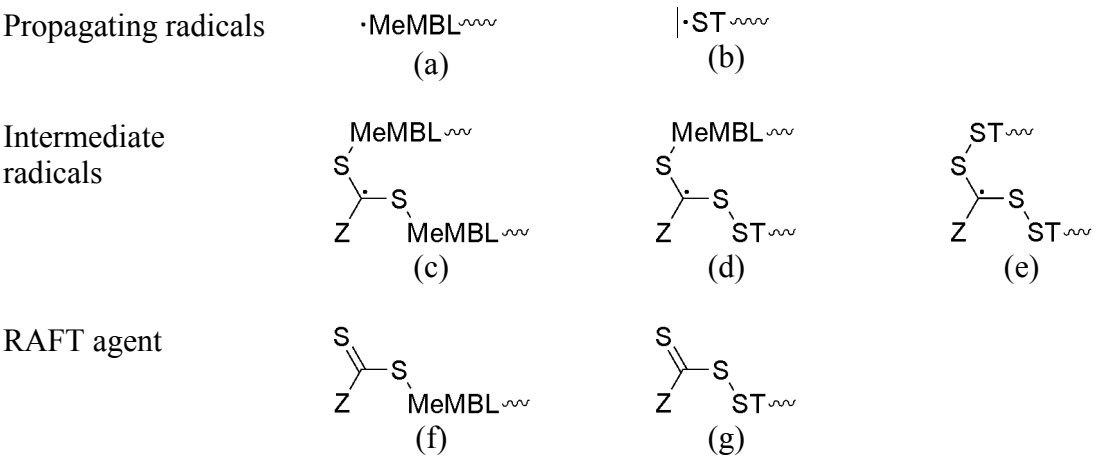

Figure 4.10 Structures of radicals and macro-RAFT agents in the RAFT copolymerization of MeMBL and styrene.

4.3.3.2 Kinetic study of miniemulsion copolymerizations of MeMBL and styrene

Controlled miniemulsion copolymerizations of MeMBL were performed at 70°C with different molar ratios of MeMBL and styrene in Exp. 17 and 18. As a comparison, free-radical miniemulsion copolymerizations of MeMBL were also run in Exp. 12-14,

and bulk copolymerizations in Exp. 15 and 16 (control experiments). AIBN was used as an organophilic initiator to suppress potential homogeneous nucleation. It should be noted that when the molar ratio, [MeMBL]:[styrene]= 4:1, the controlled miniemulsion copolymerization was unstable, so limited data for these experiments are presented.

The conversion-time curves for free-radical miniemulsion copolymerization of MeMBL and styrene are shown in Figure 4.11. When the molar ratio of MeMBL to styrene was less than 1, the polymerization rate increased as the concentration of MeMBL increased. A lower polymerization rate, however, was observed in Exp. 14 when the molar ratio of MeMBL to styrene was at 4.

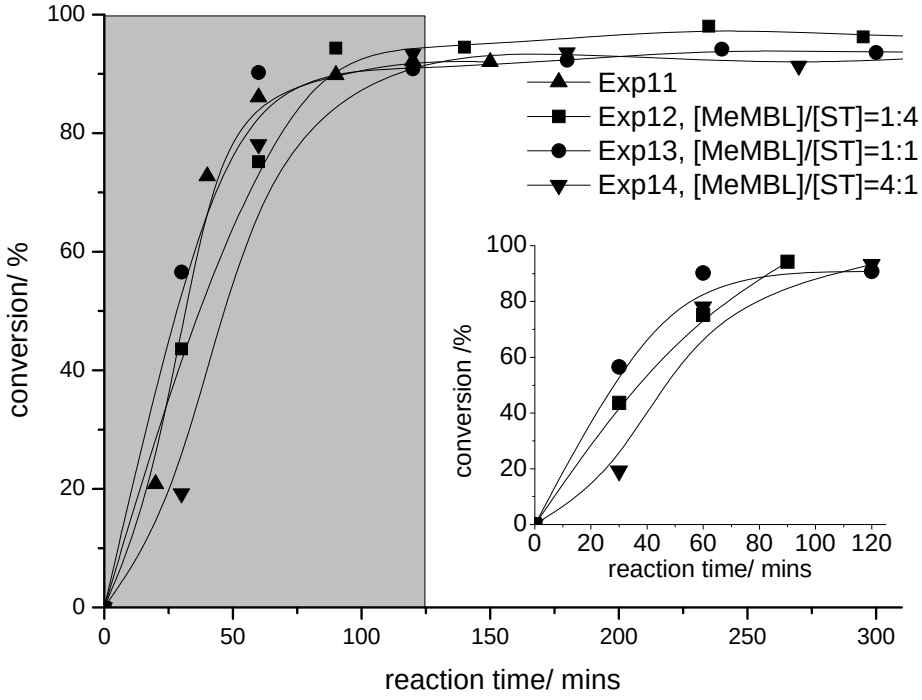

Figure 4.11 Free-radical miniemulsion copolymerization at 70ºC with different ratios of MeMBL and styrene. The conversion curve before 120 min was magnified as the inset.

The polymerization rate of the free-radical miniemulsion copolymerization of MeMBL depends on several factors, such as the propagation rate constant of the monomer and the number of particles in the latex. Figure 4.12 shows the evolution of the particle radius and polydispersity as functions of time. As shown in Figure 4.12, the particle radius in Exp. 13 (1:1 MeMBL: Styrene) was essentially the same as in Exp. 12

(1:4 MeMBL: Styrene); therefore, the number of particles in the two experiments is quite similar. Since the bulk homopolymerization rate of MeMBL is much higher than that of styrene, the overall copolymerization rate is likely to increase with higher concentrations of MeMBL. This may explain why Exp. 13 ([MeMBL]/[ST]=1:1) had a higher polymerization rate than Exp. 12 ([MeMBL]/[ST]=1:4). However, it should be noted that the average particle radius in Exp. 14 ([MeMBL]/[ST]=4:1) was much larger than in Exp. 12 and Exp. 13. Landfester et al. also observed a similar phenomenon in the miniemulsion copolymerization of styrene and acrylonitrile, a more hydrophilic monomer than styrene. The droplet radius for their recipe with 50 wt% styrene was 84 nm vs. 163nm for the 10 wt% styrene system.[181] They postulated that the reason for the size difference was that SDS is not an optimal surfactant for the very hydrophilic monomer acrylonitrile, i.e. the binding between the C_{12} tail of SDS and acrylonitrile was weak. The significantly lower particle number in Exp. 14 ($N_p \sim 8.7\times10^{13}/cm^3$) likely caused the slower polymerization rate compared to Exp. 12 ($N_p \sim 1.0\times10^{15}/cm^3$) and Exp. 13 ($N_p \sim 8.0\times10^{14}/cm^3$), even though the concentration of MeMBL was highest in this latter case. The nearly constant particle size and the narrow particle size polydispersity throughout each of the experiments 12-14 suggest that the addition of styrene and the use of AIBN as initiator limited the homogeneous nucleation process seen in the "miniemulsion" homopolymerization of MeMBL.

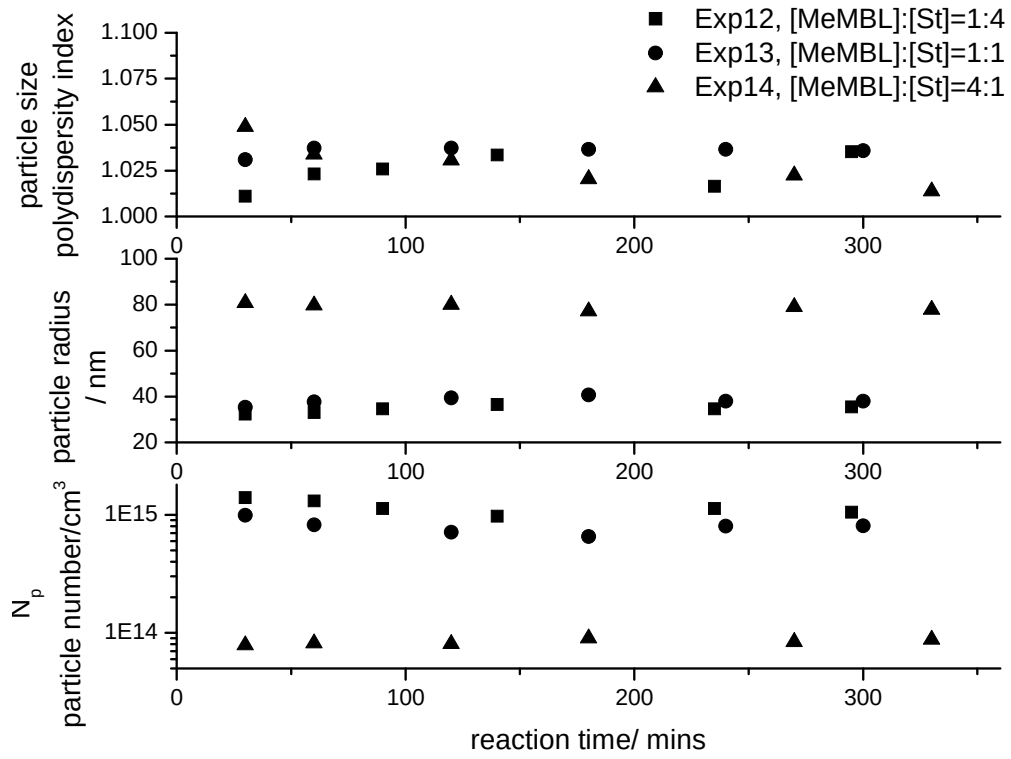

Figure 4.12 Particle radius, particle number and polydispersity index of free-radical miniemulsion copolymerization with different ratios of MeMBL and styrene at 70ºC.

A stable latex of poly(MeMBL-co-styrene) was obtained in the free-radical miniemulsion copolymerizations. However, severe coagulation was observed in the RAFT miniemulsion copolymerization when the molar ratio of MeMBL to styrene was 4:1. The stability of RAFT miniemulsion polymerizations is usually inferior to free-radical miniemulsion polymerizations, as noted above. This has been suggested to be due to a super-swelling effect in RAFT miniemulsion polymerizations.[86] Therefore, the kinetics of the RAFT copolymerizations were studied only when the molar ratio of MeMBL to styrene was less than 1. The conversion-time curves of RAFT bulk and RAFT miniemulsion polymerization of MeMBL/styrene are shown in Figure 4.13. Compared with the data in Figure 4.11 describing free-radical miniemulsion polymerizations (Exp. 12 and Exp. 13), the RAFT miniemulsion polymerizations (Exp. 17 and Exp. 18) show a significant rate retardation in the polymerization. Rate retardation

is a well known phenomenon in RAFT chemistry. [195, 196] The cause of the retardation in RAFT polymerizations is still under vigorous debate, with a particular focus on the fate of the RAFT intermediate radicals that are formed in the pre-equilibrium and main equilibrium of the RAFT process. Two theories, slow fragmentation of the RAFT initial intermediate radical, [197] and termination of the intermediate radical, were proposed by different groups to explain the retardation. [197] Some recent data support the theory that the retardation is caused, at least in part, by intermediate termination.[159] A higher radical desorption rate in RAFT miniemulsion polymerization could be another reason for the retardation in miniemulsion polymerizations.[198] For ideal RAFT miniemulsion polymerizations, all oligomeric chains grow slowly into polymeric chains in the particles at the same time. These oligomeric chains have a higher probability of desorption from the particles and the probability decreases as the molecular weight increases and as the chains become more hydrophobic. Desorbed radicals can terminate in the continuous phase. As a result, the effective number of propagating radicals in the particle can decrease and thus rate retardation can ensue. The exact cause of the rate retardation in the present system is not yet clear, but may be due to a combination of the factors described above.

The RAFT miniemulsion polymerizations (Exp. 17 and Exp. 18) also exhibited a retardation effect compared with their RAFT bulk polymerization counterparts (Exp. 15 and Exp. 16). The composition of the organic phase of the miniemulsion polymerizations was the same as that of RAFT bulk copolymerizations. In the case of appropriately formulated miniemulsions, the polymerization takes place in the droplets and ideally the droplets act as individual batch reactors. As a result, the RAFT miniemulsion polymerization rate of MeMBL should be comparable to or higher to its RAFT bulk polymerization due to the segregation effect of miniemulsion polymerizations.[197] Therefore, the retardation indicated that there were certain atypical mechanisms slowing down the RAFT miniemulsion polymerization.

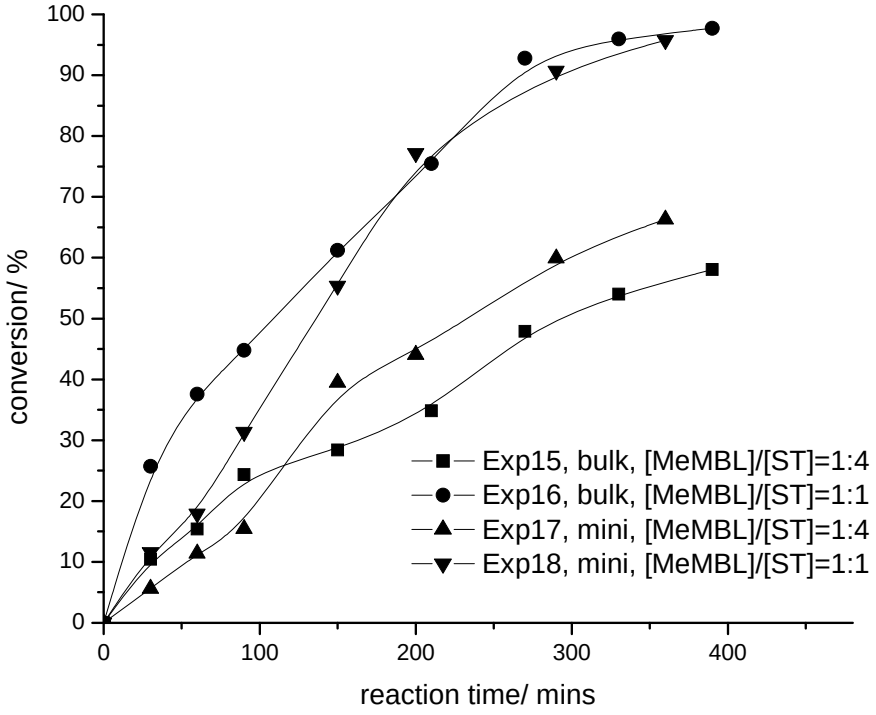

Figure 4.13 RAFT bulk copolymerization and RAFT miniemulsion copolymerization at 70ºC with different ratios of MeMBL and styrene.

Several possible mechanisms could contribute to the retardation. First it may result from a lower initiator efficiency of AIBN in the RAFT miniemulsion polymerizations. Despite the fact that AIBN may greatly reduce the possibility of homogeneous nucleation, its use in miniemulsion polymerizations has been limited since it complicates the kinetics of miniemulsion polymerizations. [87] A low initiator efficiency has often been observed,[199] possibly due to a so-called "cage effect" in (mini)emulsion polymerizations.[200] In RAFT bulk polymerization, the pair of primary radicals formed from AIBN are surrounded by a solution domain. Before the radicals diffuse out this "pseudo cage", they may experience a bimolecular termination and cause lower overall initiator efficiency. In the RAFT miniemulsion polymerizations of Exp.17 and Exp.18, on the other hand, the primary radicals have the additional restriction of being inside a polymer droplet or particle, i.e. an "enforced cage." Only the fraction of

primary radicals that survive both the "pseudo cage" and "enforced cage" can effectively participate in particle growth. Therefore it is reasonable to expect a lower initiator efficiency in Exps. 17-18 (RAFT miniemulsion) compared to Exps. 15-16 (RAFT bulk), and thus a rate retardation. Another potential mechanism resulting in the retardation in RAFT miniemulsions is radical desorption from the polymer particles.[201] As mentioned above, the average number of propagating radicals in each particle is expected to be lower due to the radical desorption in the RAFT miniemulsion polymerization, and this may cause rate retardation. The compartmentalization of RAFT miniemulsion polymerization can contribute to the retardation as well.[89] Under a zero-one condition of miniemulsion polymerizations, the intermediate radicals inside particles do not propagate with monomers and thus shorten the time period that is available for the radicals to propagate in the absence of a RAFT agent. Both N_p (number of particles) and $\bar{n}$ (average number of radicals per particle) are significantly decreased in RAFT miniemulsion polymerizations, and therefore, RAFT miniemulsions can have a more pronounced retardation than RAFT bulk polymerizations. Finally, the rates may be retarded by a lower effective concentration of the highly reactive MeMBL in the droplets than the system stoichiometry might suggest due to the high water solubility of the MeMBL.

The relationships between Mn, molecular weight polydispersity index and the conversion for the controlled copolymerizations are shown in Figure 4.14. The theoretical molecular weights for the poly(styrene) and poly(MeMBL) were calculated as:

$$M_n = M_{w,monomer} \cdot x \cdot [monomer] / [RAFT] + M_{w,RAFT} \qquad (4.2)$$

where $M_{w,monomer}$ was the molecular weight of the monomer and x was the conversion. The theoretical molecular weight of the copolymer should fall into the area between the theoretical Mn of poly(MeMBL) and poly(styrene). As shown in Figure 4.14, the Mn of the copolymers made from the RAFT bulk or miniemulsion polymerizations increased linearly with conversion but were lower than the theoretical predications. This linearity suggests some level of controlled polymerization. The deviations of Mn from predictions may result from the GPC method. The Mn of the copolymer is referenced to narrowly distributed poly(styrene) standards. However, poly(MeMBL) and poly(styrene) have different hydrodynamic volumes and this will result in an error in the measured Mn of the copolymers.

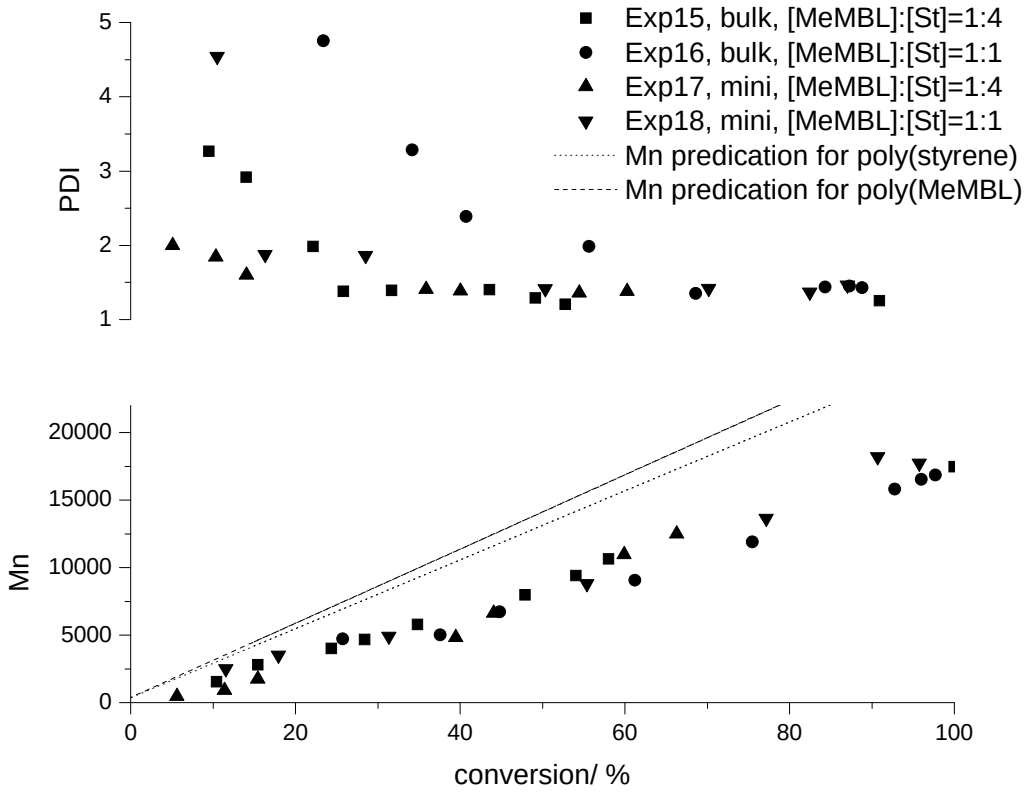

Figure 4.14 Evolution of Mn and PDI with conversion in controlled RAFT copolymerization of MeMBL and styrene at 70°C.

As shown in Figure 4.14, the polydispersity index (PDI) of the polymers from the RAFT bulk and miniemulsion copolymerizations decreased with conversion before reaching a nearly constant value. There are some noteworthy features in the evolution of the PDIs. First, the PDIs were quite broad at low conversions. As shown in Figure 4.15, the molecular weight of the copolymer in Exp.17 was bimodally distributed. In general, the higher the ratio of styrene to MeMBL, the lower the PDI of the resulting polymer. Second, the PDIs of the copolymers made from RAFT miniemulsions (Exp. 17 and Exp 18) were lower than those from RAFT bulk polymerizations (Exp. 15 and Exp. 16) when the conversion was low. As discussed above, PEPDTA allows for good control over styrene but poor control for MeMBL. Thus, in this approach, styrene acts as "translator" monomer to realize controlled copolymerization of MeMBL. The uncontrolled effect from MeMBL was pronounced when the conversion was low, while the degree of control was improved as more styrene units were incorporated in the copolymer and when

MeMBL concentration is decreased at higher conversions. Therefore, the bimodality could be associated with the hypothesized presence of two types of macro-RAFT agents or polymer [(f) and (g)], as shown in Figure 4.10, at the beginning of the copolymerization. It should also be noted that the molecular weight distribution became more monomodal at higher conversions, as shown in Figure 4.15, which is consistent with the macro-RAFT agent (g) being the dominant species at that time. In general, the higher the ratio of styrene to MeMBL, the more the RAFT copolymerization process was like the RAFT homopolymerization of styrene. Therefore, a lower PDI could be achieved in Exp. 15 and Exp. 17 at the beginning of the polymerizations. The PDI in RAFT miniemulsion polymerizations Exp. 17 and Exp. 18 also tended to be lower than their bulk controls Exp. 15 and Exp. 16, respectively, at the beginning of the polymerization. The reason for this phenomenon is still under investigation. One possible reason is the solubility difference in water between styrene and MeMBL, as noted above. Since the real ratio of styrene to MeMBL was higher in the miniemulsion monomer droplets due to the high solubility of MeMBL in water, the RAFT miniemulsion copolymerizations should be under better control than the RAFT bulk polymerizations, therefore, a lower PDI was observed in Exp.17 and Exp.18, respectively, as demonstrated in Figure 4.14.

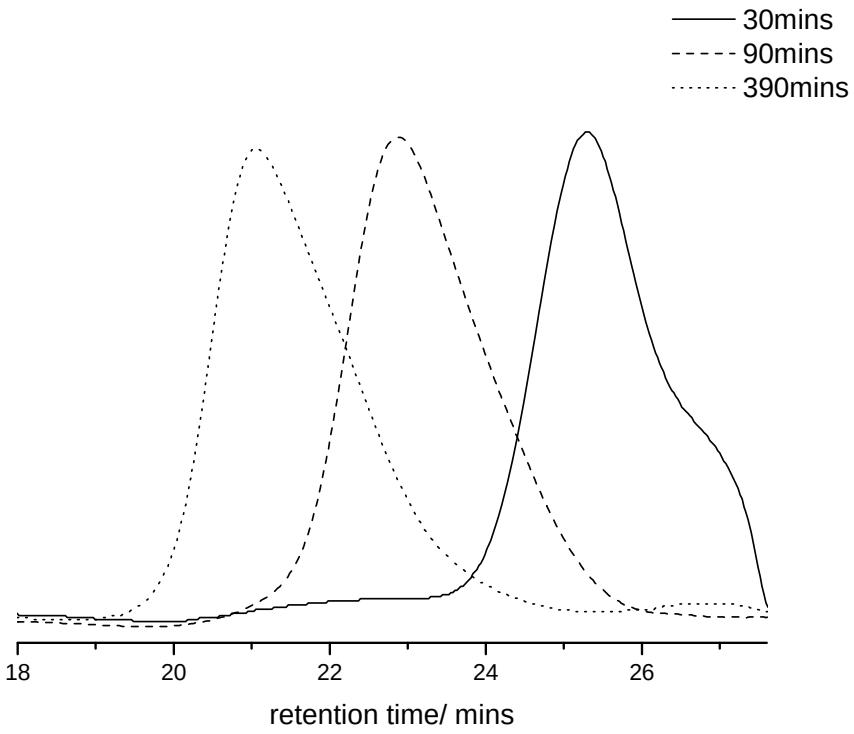

Figure 4.15 Evolution of the RI GPC curve with different reaction times in experiment 17 (RAFT miniemulsion copolymerization. [MeMBL]/[ST]=1:4).

4.3.3.3 Reactivity ratios of MeMBL and styrene in the RAFT bulk copolymerizations

The reactivity ratios of MeMBL and styrene in the RAFT bulk copolymerizations (Exp.15 and Exp. 16) were estimated by both the Kelen-Tudos method and Fineman-Ross method. [202] The composition of the copolymers was measured by ^{1}H NMR at a conversion below 5%. A typical ^{1}H NMR spectrum of a copolymer is shown in Figure 4.16. The copolymer composition can be determined with ^{1}H NMR analysis by using the areas of peak 2 and peaks 1, 3-5.

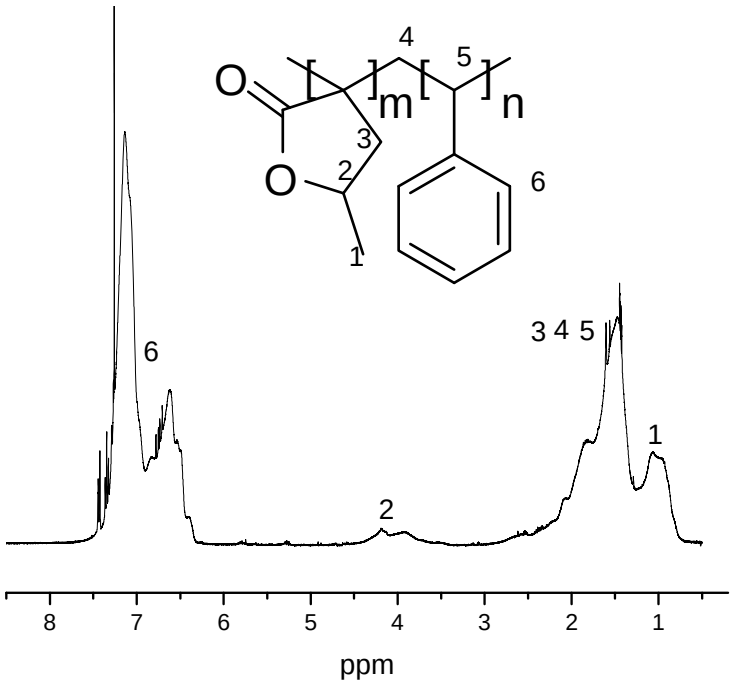

Figure 4.16 Typical ^{1}H NMR spectrum of the copolymer of MeMBL and styrene produced via bulk RAFT copolymerization in experiment 15.

The calculation of reactivity ratios of MeMBL and styrene in the RAFT bulk copolymerizations at 70ºC was shown in Figure 4.17. The reactivity ratio of MeMBL, $r_{MeMBL} = 0.85$ and the reactivity ratio of styrene, $r_{styrene} = 0.39$ were calculated using the Fineman-Ross method and using the Kelen-Tudos method, the ratios were $r_{MeMBL} = 0.75$ and $r_{styrene} = 0.33$. It has been reported that the reactivity ratios are $r_{MMA} = 0.46$ and $r_{styrene} = 0.52$ for the RAFT copolymerization of methyl methacrylate (MMA) and styrene using Mayo-Lewis method.[203] Therefore, the MMA-ended radicals have a higher probability of adding a styrene unit than MeMBL-ended radicals. From the reactivity ratios there is an azeotropic point at $f_{styrene} = 0.20$ for the copolymerization of MeMBL and styrene, where copolymerization occurs without a drift in monomer composition. Since the monomer ratios in Exp. 15 and Exp. 16 were different from the azeotropic point, the copolymer composition drifted during the polymerizations. Therefore, gradient copolymers were expected to be produced in Exp. 15 and Exp. 16.

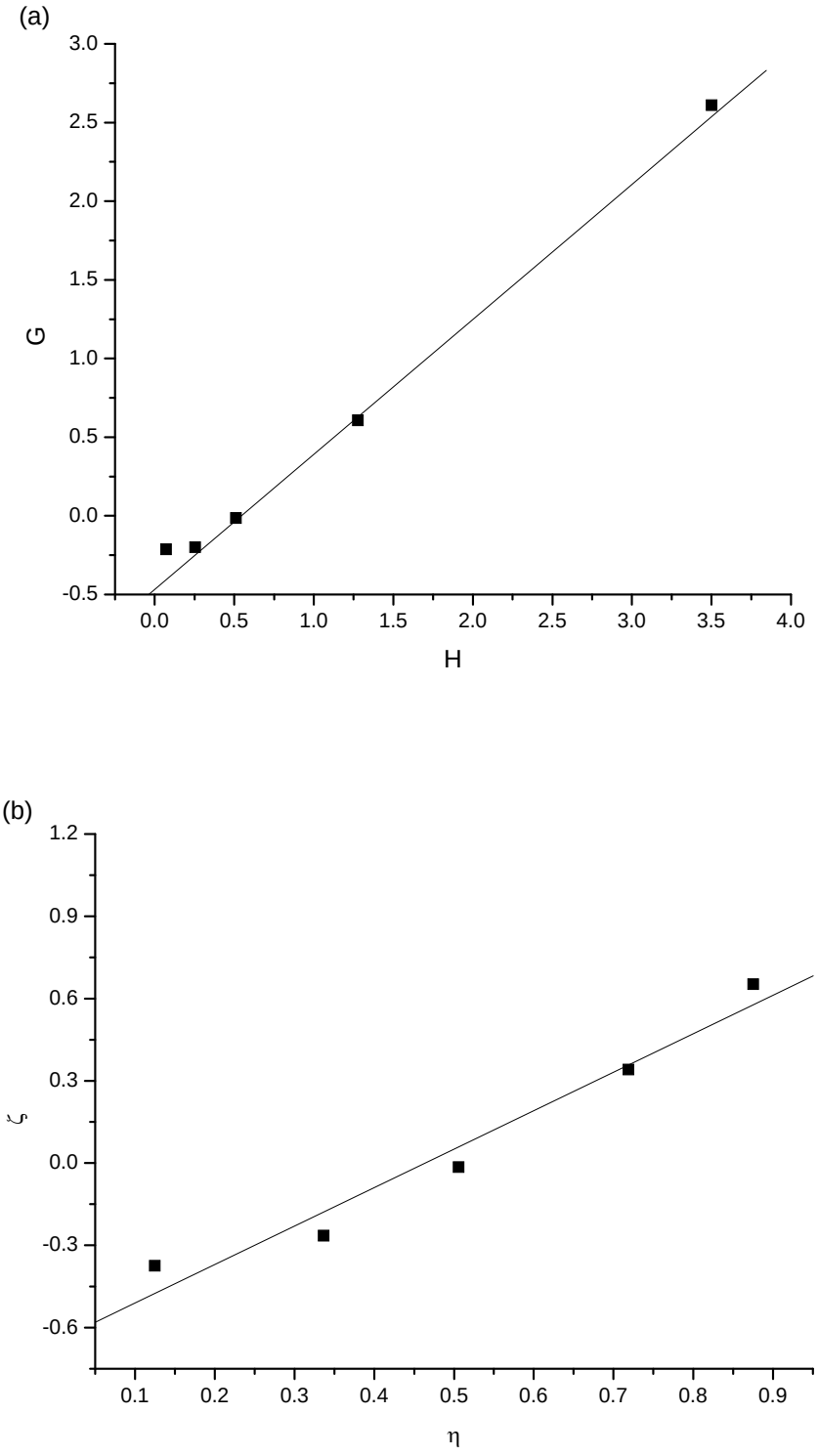

Figure 4.17 Calculations for the reactivity ratios of MeMBL and styrene in the bulk RAFT copolymerization of MeMBL and styrene at 70ºC. (a) Fineman-Ross plots; (b) Kelen-Tudos plots.

4.4 Conclusion

In this study, the kinetics of free-radical miniemulsion polymerization of MeMBL were assessed and stable MeMBL latexes were prepared. The "miniemulsion" polymerization of MeMBL had a significantly different kinetic behavior from conventional miniemulsion polymerization. A emulsifier free emulsion polymerization of MeMBL gave similar results to MeMBL "mimiemulsion" polymerization. As the emulsifier-free emulsion polymerization operates via a homogeneous nucleation mechanism, the similarity between the "miniemulsion" polymerization of MeMBL and the emulsifier-free emulsion polymerization suggest a true "miniemulsion" polymerization, in the traditional sense, may not be taking place and instead that significant homogeneous nucleation may play a role in the "miniemulsion" homopolymerization. The effects of different reaction parameters on free-radical "miniemulsion" homopolymerization were investigated.

In the miniemulsion copolymerizations of MeMBL and styrene using an oil soluble initiator, the potential homogeneous nucleation process appeared limited. Both the RAFT miniemulsion polymerizations and RAFT bulk polymerizations were well controlled and narrow polydispersity copolymers of MeMBL/styrene were produced. Rate retardation was observed in the RAFT miniemulsion polymerizations compared with the free-radical polymerization and RAFT bulk polymerization controls. The reactivity ratios of MeMBL and styrene in RAFT bulk copolymerization were measured and compared with that of MMA and styrene. It was found that the MeMBL radicals were less monomer preferential in the propagation reaction compared with MMA radicals.

CHAPTER 5

RAFT INVERSE MINIEMULSION POLYMERIZATION*

5.1 Introduction

In chapters 3 and 4, we have discussed the RAFT miniemulsion polymerizations of a hydrophobic monomer in CSTR trains and a partially water soluble monomer in batch, respectivly. In this chapter, we will discuss the RAFT miniemulsion polymerizations of hydrophilic monomers.

Synthetic hydrophilic polymers are widely used in numerous applications and are a billon dollar market each year, including uses as flocculants,[204] drag reduction agents, drilling fluids,[205, 206] paper making additives,[207] and in drug delivery.[208-210] However, there are various process challenges such as non-uniform mixing and heat transfer limitations that exist in large scale industrial production of hydrophilic polymers by solution polymerization.[3] Free-radical inverse emulsion polymerization was used to overcome these problems, and has evolved into one of the main routes in industry to produce synthetic hydrophilic polymers. As mentioned in the introduction, understanding of the process originated from the pioneering work of John Vanderhoff and coworkers in 1962.[100] Recently, a free-radical inverse miniemulsion polymerization was developed.[102] An inverse miniemulsion disperses an aqueous monomer or solution in a continuous oil phase and forms droplets range from 50nm to 500nm in radius. Free-radical inverse miniemulsion polymerizations maintain typical properties of conventional miniemulsion polymerizations such as droplet nucleation and are superior to free-radical inverse emulsion polymerizations in process robustness, particle size uniformity, and colloidal stability. However, free-radical inverse miniemulsion polymerization still offers only limited ability to precisely design the structures and properties of the polymer products. As a potential answer to this challenge, RAFT inverse miniemulsion polymerization is proposed here by applying RAFT chemistry to inverse miniemulsion

* Portions of this chapter have been published in Macromol. Rapid Commun., 2007, 28, 1010-1016.

polymerizations.[158] By combining RAFT polymerization with inverse miniemulsion, RAFT inverse miniemulsion polymerization can in principle take the advantages of both of these techniques and offer a convenient way to synthesize unique or well-defined structured copolymers and colloids such as hydrophilic nanogels.

For inverse miniemulsions, the prevailing surfactants have to be steric surfactants or a combination of steric and ionic surfactants. In contrast, conventional miniemulsions are generally stabilized by solely ionic surfactants or a combination of ionic and steric surfactants. When steric surfactants are used, the kinetic behavior of the inverse miniemulsion can be dramatically different from ionically stabilized conventional (o/w) miniemulsion polymerizations. Unfortunately, no effort has been devoted to investigate systematically the polymerization kinetics and mechanism of sterically stabilized inverse systems. Therefore, it is of significant importance from both industrial and academic perspectives to perform a detailed study of RAFT inverse miniemulsion polymerization.

5.2 Experimental Section

5.2.1 Materials

All chemicals were purchased from Aldrich unless otherwise stated. Acrylamide (Am, >99.5%) was recrystallized from chloroform (>99.8%). Acrylic acid (AAc, >99.0%) was distilled under reduced pressure prior to use. B246SF (Uniqema), sodium sulfate (>99.0%), 2,2-azobisisobutyronitrile (AIBN, >99.0%), 4,4'-azobis(4-cyanovaleric acid) (ABCP, >99.0%), 2,2-Diphenyl-1-picrylhydrazyl (DPPH, ~95%), and cyclohexane (>99.5%) were used without further purification. The water soluble initiator, 2,2'-Azobis[2-(2-imidazolin-2-yl)propane]dihydrochloride (VA-044, >98%) was purchased from Wako and used as received. Deionized water was generated with a U.S. Filter Systems Deionizer and was used without further purification.

5.2.2 Synthesis of RAFT agents

The RAFT agent, 2-(2-carboxyethyl-sulfanylthiocarbonylsulfanyl) propionic acid (CTA), was synthesized according to literature procedures,[211] using the following materials without further purification: 3-mercaptopropionic acid (99%) and acetone

(>99.5%) from Alfa Aeser, as well as chloroform (>99.8%) from J. B. Baker. The macro-RAFT agents were synthesized from the above RAFT agent by the solution polymerization of acrylamide in water at 45^{o}C. As an example, in a 50ml flask 1.59g AM, 0.81g CTA, and 0.010g VA-044 were dissolved by 10ml water. The mixture was purged with N_2 and heated to 45^{o}C. After polymerization for 4 h, the reactant mixture was slowly poured into 100ml chilled methanol under rigorous stirring. The macro-RAFT agent was separated by centrifuge at 0^{o}C and then dried in vacuum oven at 40^{o}C for 48 h. For macro-RAFT1, Mn=623, PDI=1.43 and macro-RAFT2, Mn=2305, PDI=1.25, as measured by GPC.

5.2.3 Inverse miniemulsion polymerization

Preparation of inverse miniemulsions

Before performing an in-depth study of RAFT inverse miniemulsion polymerization, a preliminary study was carried out to understand the basic kinetic features. Two kinds of initiators were used in the preliminary study. Hydrophobic initiator, AIBN, was dissolved in the continuous phase while hydrophilic initiator, ABCP in the aqueous phase. The RAFT inverse miniemulsions were prepared by the following procedure. As an example, the continuous phase was a solution of 1.0g B246SF in 50g cyclohexane. In the dispersed phase, 5.0g acrylamide, 0.12g $MgSO_4$, 0.089g RAFT and 0.039g ABCP were dissolved in 7.5g water. The inverse emulsion was prepared by dropwise addition of the dispersed phase to the B246SF cyclohexane solution. The emulsion was stirred under nitrogen at 7 °C using an ice-water bath for 90 min and purged with nitrogen, then sonicated with a Fischer Model 30 sonic dismembrator operated at 70% power output for approximately 10 min under nitrogen while cooled in an ice bath. A representative recipe in the preliminary study is shown in Table 5.1.

Table 5.1 Typical recipe for the RAFT inverse miniemulsion polymerization of acrylamide at 60 °C in the preliminary study.

Component		Mass	Notes
Continuous phase	Dispersed phase		
B246		1.00 g	2 Wt% of continuous phase
Cyclohexane		50.0 g	
	H_2O	7.5 g	
	Acrylamide	5.0 g	
	$MgSO_4$	0.12 g	1 Wt% of dispersed phase
	RAFT agent	0.089 g	[monomer]/[RAFT]=200
	ABCP (85 Wt %)	0.039 g	[RAFT]/[ABCP]=3

In the subsequent detailed study of RAFT inverse miniemulsion polymerizations, an optimized water soluble initiator, VA-044, was employed in the aqueous phase. The RAFT inverse miniemulsions were prepared according to the following procedure. As an example, 0.6g B246SF was dissolved in 40g cyclohexane to prepare the continuous phase of the inverse miniemulsion. The dispersed phase was prepared separately by adding 2.5g acrylamide, 0.028g VA-044, 0.089g RAFT agent and 0.10g $MgSO_4$ (costabilizer) to 7.5g water and degassed under vacuum for 5 min. The inverse emulsion was prepared by dropwise addition of the dispersed phase to the B246SF cyclohexane solution and stirred under nitrogen at 10 °C for 40 min. The coarse inverse emulsion was then ultrasonicated with a Fischer Model 30 sonic dismembrator operated at 70% power output for approximately 5 min under nitrogen. The free-radical inverse miniemulsions were prepared in a similar manner as RAFT inverse miniemulsions except that no RAFT agent was added in the aqueous phase. A typical recipe for the inverse miniemulsions is shown in Table 5.2.

Table 5.2 Typical recipe for free-radical and RAFT inverse miniemulsion polymerizations of acrylamide at 60 °C in the in-depth study.

	Component		Mass	Notes
	Free-radical mini	RAFT mini	(g)	
	cyclohexane	cyclohexane	40	
Surfactant	B246	B246	0.60	1.5 wt% based on oil
Monomer	acrylamide	acrylamide	2.5	3.62 M
Initiator	VA-044	VA-044	0.028	[AM]:[initiator]=400:1
Costabilizer	$MgSO_4$	$MgSO_4$	0.10	1 wt% of aqueous phase
RAFT	-	CTA	0.089	[AM]:[CTA]=100:1

Polymerization

The RAFT inverse miniemulsion prepared above was transferred into a 100ml flask with a magnetic stirring bar. Inverse miniemulsion polymerizations were carried out in an oil bath preheated to 60 ^{o}C unless otherwise specified. The stirring rate was kept around 300rpm. Samples were taken during the polymerizations to provide kinetic data. For RAFT inverse miniemulsion polymerizations, the samples were separated into two parts, one part for particle size determination and another was quenched with drops of 1wt% hydroquinone acetone solution for conversion measurements. For free-radical inverse miniemulsion polymerizations, the samples were also divided into two parts. A small portion of the samples was diluted with cyclohexane for particle size analysis and the other was quickly precipitated in excess chilled acetone containing 0.1wt% hydroquinone for measurements of conversion.

5.2.4 Characterization

The molecular weight of the poly(acrylamide) samples was measured by aqueous gel permeation chromatography (GPC) at 30°C. In the preliminary study, the GPC system was comprised of a Shimadzu LC-20AD pump, a Shimadzu RID-10A RI detector, a Shimadzu SPD-20A UV detector, a Shimadzu CTO-20A column oven, and Viscotek TSK Viscogel PWXL Guard, G3000, G4000 and G6000 columns mounted in series. In the in-depth study, it was found that G3000 and G6000 have a high resolution of polymer separation. Therefore, the column G4000 was removed in the in-depth study to save analysis time.

The mobile phase was 0.05M Na_2SO_4 and the flow rate was maintained at 0.5 mL/min. Poly(ethylene oxide) narrow standards were used to calibrate the GPC by the universal calibration method. The Mark-Houwink parameters of poly(acrylamide) in 0.05M Na_2SO_4 aqueous are: α=0.66 and K=0.000373; for poly(ethylene oxide), α=0.693 and K=0.000365.[212] The GPC samples were prepared according to the following procedure: latex aliquots of 1 ml were removed during the polymerization, quenched with drops of 0.1wt% hydroquinone acetone solution and ice bath, followed by vacuum drying at 30°C to remove the volatile organics and water. The dried samples were redispersed in 10ml 0.05M Na_2SO_4 aqueous solution, stored in the dark for 24 h at 5^{o}C and then filtered

with a 0.2μm nylon filter. Shimadzu EZ-start V7.3 software was used for the analysis of molecular weight and polydispersity of poly(acrylamide).

For RAFT inverse miniemulsion polymerizations, the conversions of the monomer were determined with GPC by comparing the area of the RI signal corresponding to the monomer and the polymer.[213] For free-radical inverse miniemulsion polymerization, the conversions were measured gravimetrically: 3ml miniemulsion aliquots were taken at certain intervals during the polymerizations, and precipitated with chilled acetone containing 0.1wt% hydroquinone. The polymers were washed with copious chilled acetone and separated by centrifuge. The polymer samples were then vacuum dried at 70°C for 48 h and the conversion was measured gravimetrically. Low molecular weight poly(acrylamide) has a finite solubility in the precipitating solvent, which lead to significant errors using the gravimetric method for the RAFT polymerizations at a low conversions, that is why GPC method was used for conversion measurement for RAFT polymerizations.

Latex particle radius and polydispersities were analyzed using quasi-elastic light scattering (QELS, Protein Solutions DynaPro with DynaPro DCS v 5.26 software). The inverse latexes were diluted with filtered pure cyclohexane to a volume fraction of 0.5% of the dispersed phase. The total particle number N_p was estimated with the following equation:

$$N_p = \frac{m}{\frac{4}{3}\pi \bar{r}^3 \rho} \tag{5.1}$$

where m is the initial mass of the dispersed phase (g), ρ is the density of the particles, and $\bar{r}$ is the average particle radius.

5.3 Results and Discussion

5.3.1 Preliminary study of RAFT inverse miniemulsion polymerization

All the experiments in the preliminary study were carried out at 60°C and the ratio of monomer, RAFT agent and initiator was fixed to 600: 3: 1, as outlined in Table 5.3. The recipe for RAFT solution polymerization (Table 5.3, Exp. P1) was the same as

the dispersed phase of the inverse miniemulsion polymerizations (Table 5.3, Exps. P2 and P3).

Table 5.3 Experimental recipe for the RAFT inverse miniemulsion polymerization of acrylamide at 60 °C in the preliminary study.

Exp	Polymerization type	Initiator	[B246]/[$(CH_2)_6$]	[monomer]/[RAFT]/[initiator]
P1	RAFT solution	ABCP	0	600:3:1
P2	RAFT radical mini	AIBN	2 Wt%	600:3:1
P3	RAFT radical mini	ABCP	2 Wt%	600:3:1

The RAFT solution polymerization (Exp. P1) was first performed to check the polymerization recipe since the appropriate selection of the RAFT agent is important for achieving well controlled RAFT polymerizations, especially for RAFT polymerizations in an aqueous environment.[138, 139] As shown in Figure 5.1, the polymerization initially followed pseudo first order kinetics, followed by a deviation with a lower polymerization rate after about 60 min.

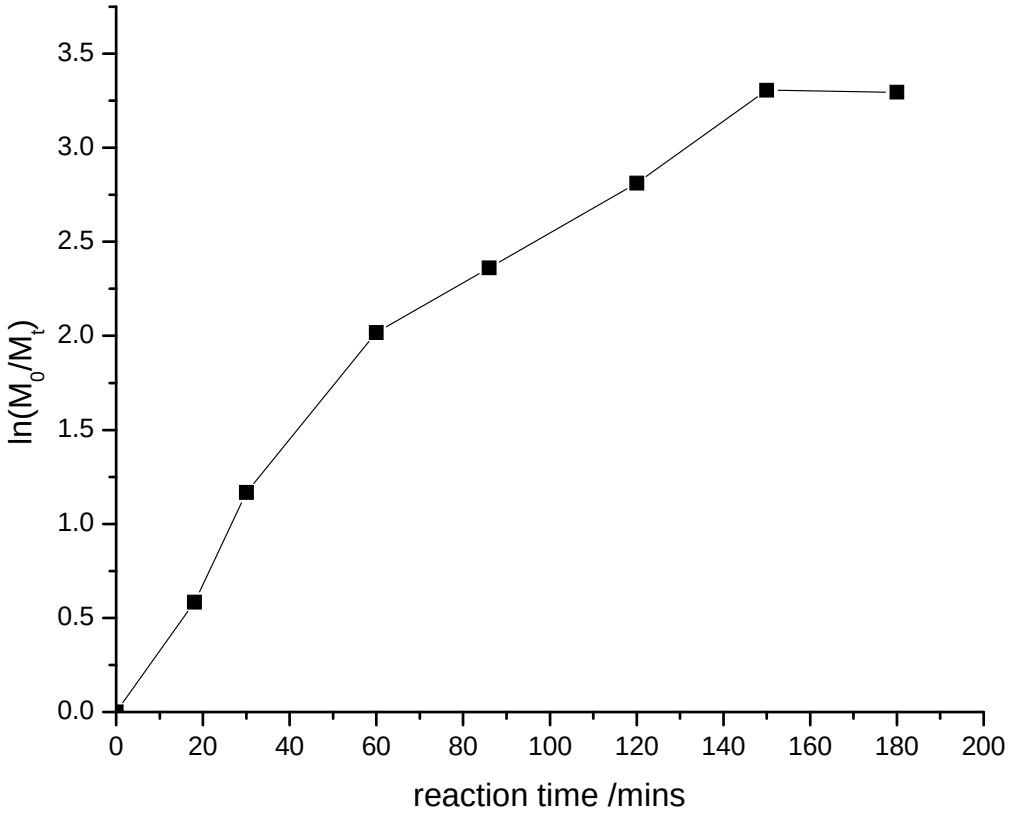

Figure 5.1 Evolution of the conversion as a function of reaction time in RAFT solution polymerization of acrylamide (Table 5.3, Exp. P1).

The molecular weight of poly(acrylamide), as shown in Figure 5.2, falls on the theoretical line at first and then deviates from the predicted line with a higher value. The PDIs also show an increasing trend with the conversion up to 1.35, although it is still far below the typical PDI of about two for free-radical polymerization of acrylamide with disproportionation termination. The reduced control at higher conversions could result from the hydrolysis and aminolysis of the RAFT agent, among other factors, a common problem in aqueous RAFT polymerizations.[139] McCormick and coworkers have reported very similar behavior in systems where RAFT agent hydrolysis and aminolysis were shown to be problematic.[139] Albertin et al. also observed the above phenomena in the RAFT polymerization of methacrylic glycomonomer in the presence of added base. They claimed that hydrolysis of the free RAFT agent and the end-of-chain dithiobenzoyl

groups was promoted by the high pH of the solution and this process could lead to the deviation from a well-controlled RAFT process.[214]

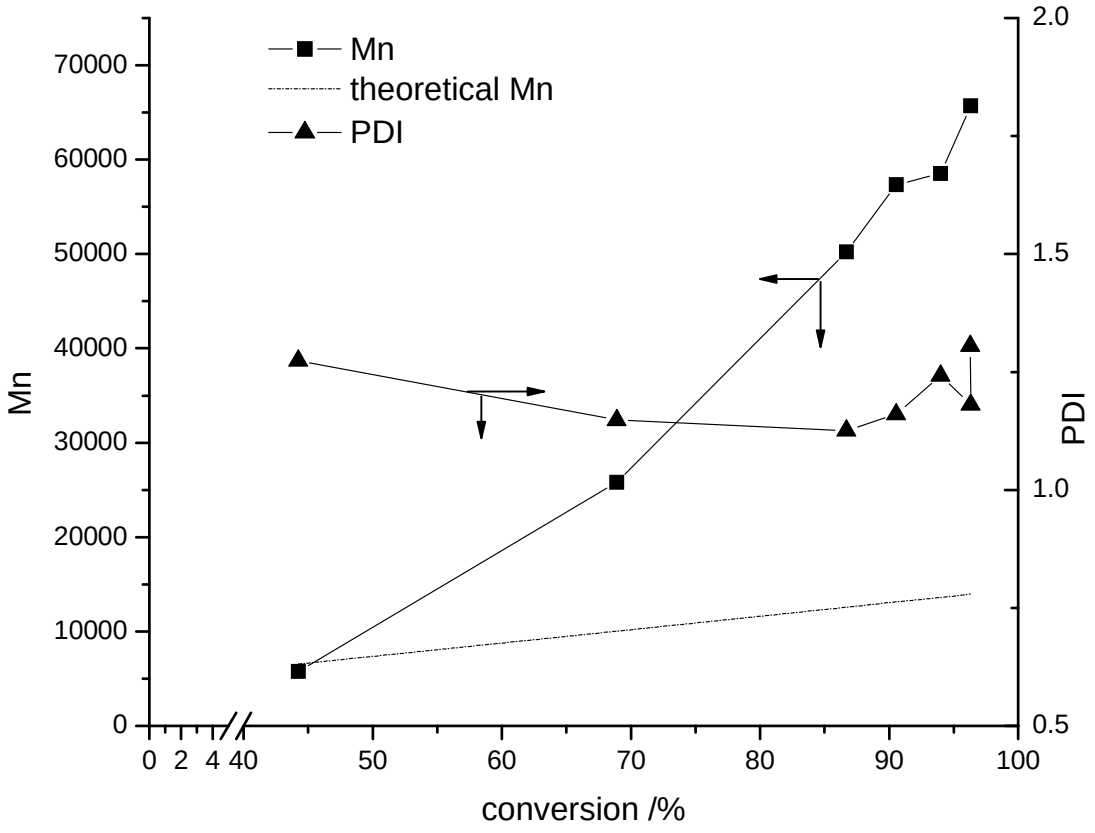

Figure 5.2 Evolution of Mn and PDI as a function of conversion in RAFT solution polymerization of acrylamide (Table 5.3, Exp. P1).

Figure 5.3 shows the RI curve from the gel permeation chromatograph (GPC) overlaid with the UV curve monitored at 311nm. The UV curve monitored at 311nm corresponds to the C=S bond in the RAFT agent. The absorption indicates the polymer chains contain a RAFT agent functional group and they could be 'living chains'.[194] It is worth noting that there is a small shoulder in the RI curve with a shorter retention time in the GPC. This likely corresponds to the dead chains associated with the coupling termination of the polymeric radicals or terminated RAFT intermediates. The increase of this shoulder with prolonged reaction time suggests a loss of control, which might be

attributable to hydrolysis or aminolysis of the RAFT agent and/or a higher content of terminated RAFT intermediates.[86,159,232-234] The overall RI signal has a very good overlay with the UV curve throughout the RAFT solution polymerization of acrylamide in spite of the small shoulder, which suggests that a species with a C=S bond is associated with most polymer chains, even at long times where the kinetics and molecular weight deviate from the theoretical curve. Therefore, the same recipe was utilized as the dispersed phase in inverse miniemulsion polymerizations of P2 and P3 (as shown in Table 5.3).

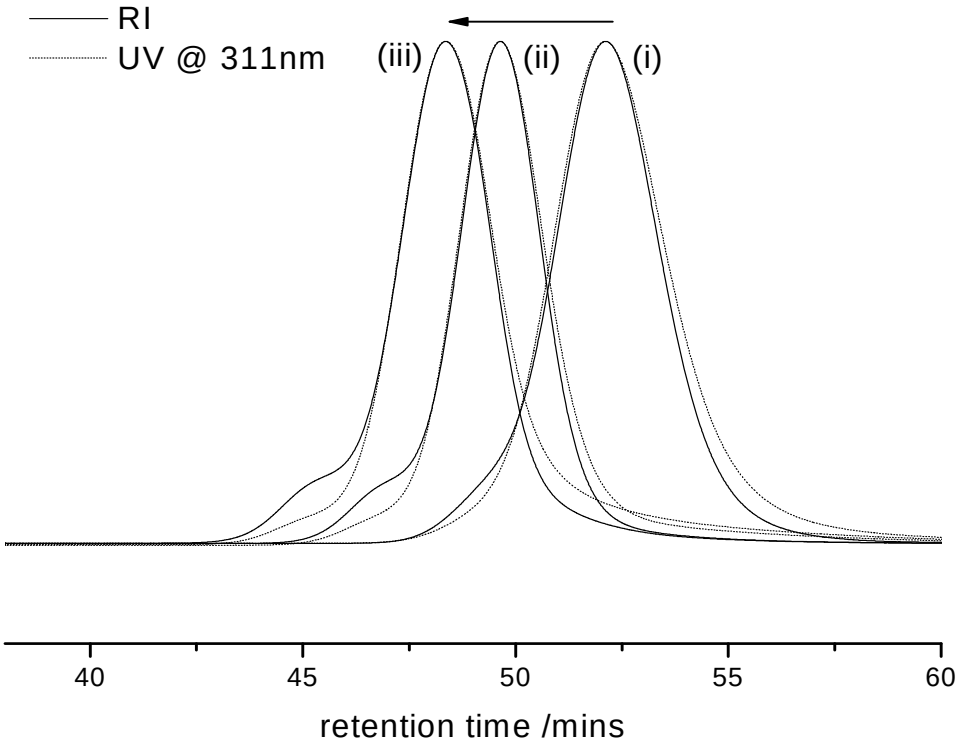

Figure 5.3 GPC chromatogram (RI and UV traces at 311nm) evolution during the polymerization RAFT solution polymerization of acrylamide (Exp. P1): (i) 18min, conversion=44%, Mn=5774, PDI=1.27; (ii) 30min, conversion=69%, Mn= 25802, PDI=1.15; (iii) 86min, conversion=91%, Mn= 57329, PDI=1.16).

The results of RAFT inverse miniemulsion polymerization of acrylamide with AIBN as initiator (Table 5.3, Exp. P2) and ABCP as initiator (Table 5.3, Exp. P3) are

shown in Figure 5.4-5.9. The two systems behaved similarly in some aspects. As shown in Figure 5.4, the poly(acrylamide) latexes produced in both experiments had good colloidal stability, with no phase separation observed after 5 days. From Figure 5.5, there was an induction time in both inverse miniemulsion polymerizations, probably due to a small amount of O_2 or other impurities trapped in the aqueous phase.[215, 216] Another cause of the induction time may be related to radical desorption from the particles, which will be discussed later in this chapter.

a b

Figure 5.4 Poly(acrylamide) latexes produced from (a). Exp. P2; (b) Exp. P3 after the completion of polymerization for 5 days.

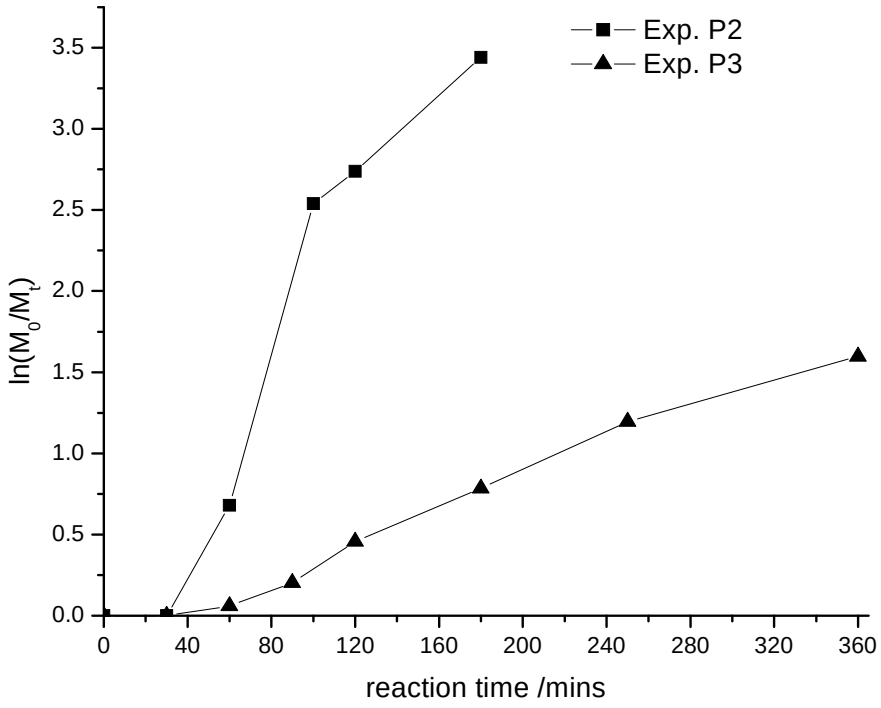

Figure 5.5 Evolution of the conversion as a function of reaction time in RAFT inverse miniemulsion polymerization of acrylamide with AIBN (Exp. P2), and ABCP (Exp. P3) as initiator.

The polymerization rates in experiments of P2 and P3, as shown in Figure 5.5, both decreased with reaction time. As in the RAFT solution polymerization, Figure 5.6 showed the molecular weights in both Exp. P2 and Exp. P3 had a deviation from the predicted value after the conversions reached ~50%. However, despite these similarities, there were some significant differences between the two inverse miniemulsion polymerizations. The molecular weight of poly(acrylamide) in Exp. P2 was much higher than that of Exp.P3 at the same conversion. The PDIs in Exp. P2, as high as 1.7, were much broader than in Exp. P3, indicative of less control in Exp. P2.

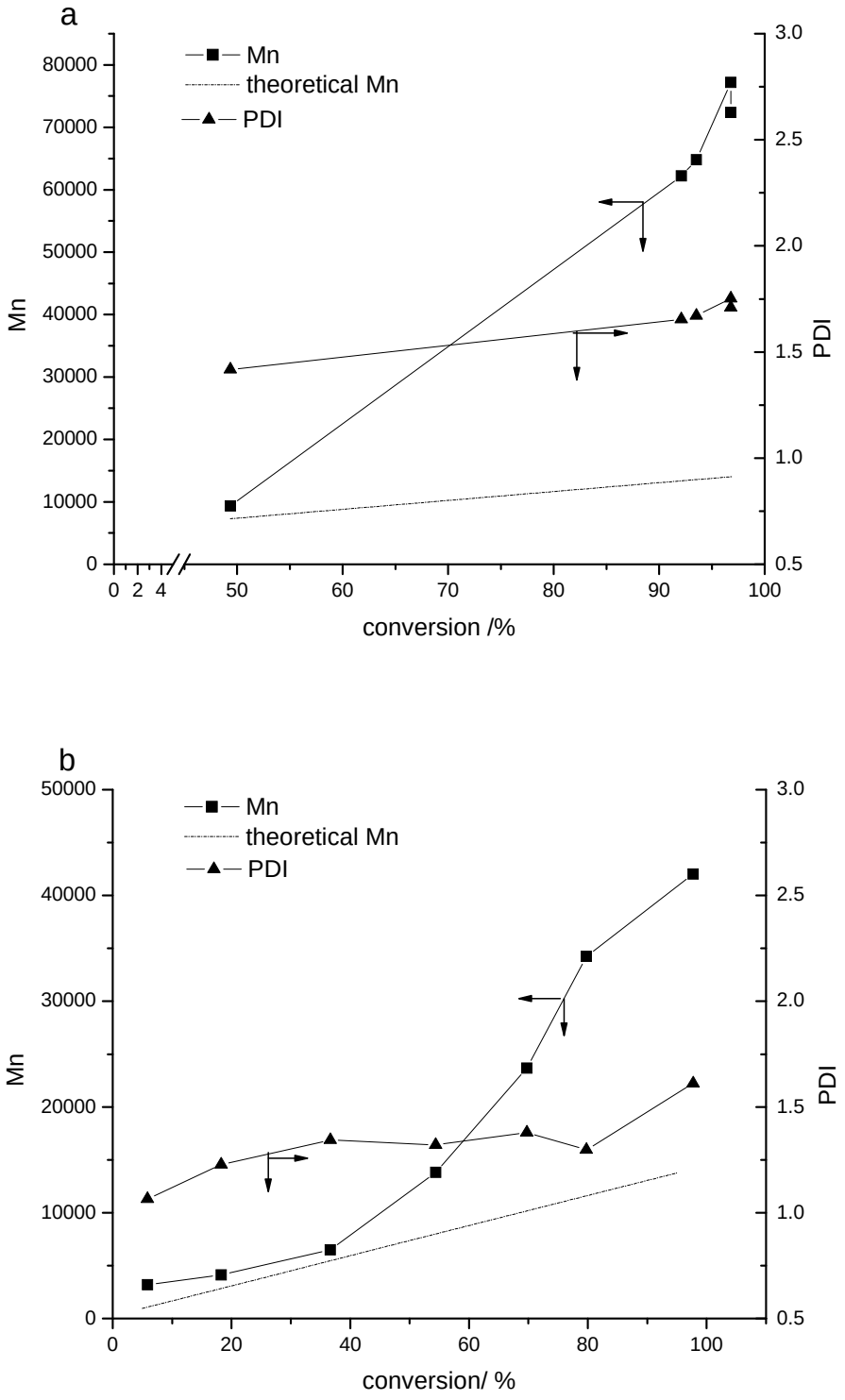

Figure 5.6 Evolution of Mn and PDI as a function of conversion in the RAFT inverse miniemulsion polymerization of acrylamide. (a). AIBN as initiator (Exp. P2), and (b). ABCP as initiator (Exp. P3).

Furthermore, the overlay of the RI and UV GPC curves from Exp. P2 and Exp. P3, as shown in Figure 5.7 and Figure 5.8 respectively, suggest a significant loss of control in Exp. P2. A bimodality in the RI signal and poor overlay of the RI and UV curves were observed in Exp. P2, suggesting AIBN, an oil-based initiator, leads to poor control in this system. In contrast, a good overlay of the curves was achieved in Exp. P3. Several potential reasons could contribute to the difference in the overlay of the RI and UV curves. The first that we considered is homogeneous nucleation in the continuous phase. The acrylamide radicals can diffuse out of the droplets,[105] and the most likely fate these radicals is to propagate in the continuous phase. Any homogeneous nucleated polymers could lead to a different controlled behavior in each locale. The water soluble initiator, ABCP, would greatly suppress the chance of homogeneous (organic phase) nucleation while the use of AIBN could result in an increase in this occurrence, and thus increased termination in the continuous phase where the primary radicals are generated. A second cause we considered was a boundary layer barrier of the nonionic surfactant between the cyclohexane continuous phase and the aqueous droplets. The desorbed radicals may reenter the particles after growth to a critical degree in the continuous phase; However, these propagated radicals will have a much lower diffusion coefficient than the initially desorbed monomeric radicals, an this should greatly limit the reentry rate of radicals.[216, 217] This could also lead to an increase in termination in the continuous phase if oil soluble initiators are utilized.

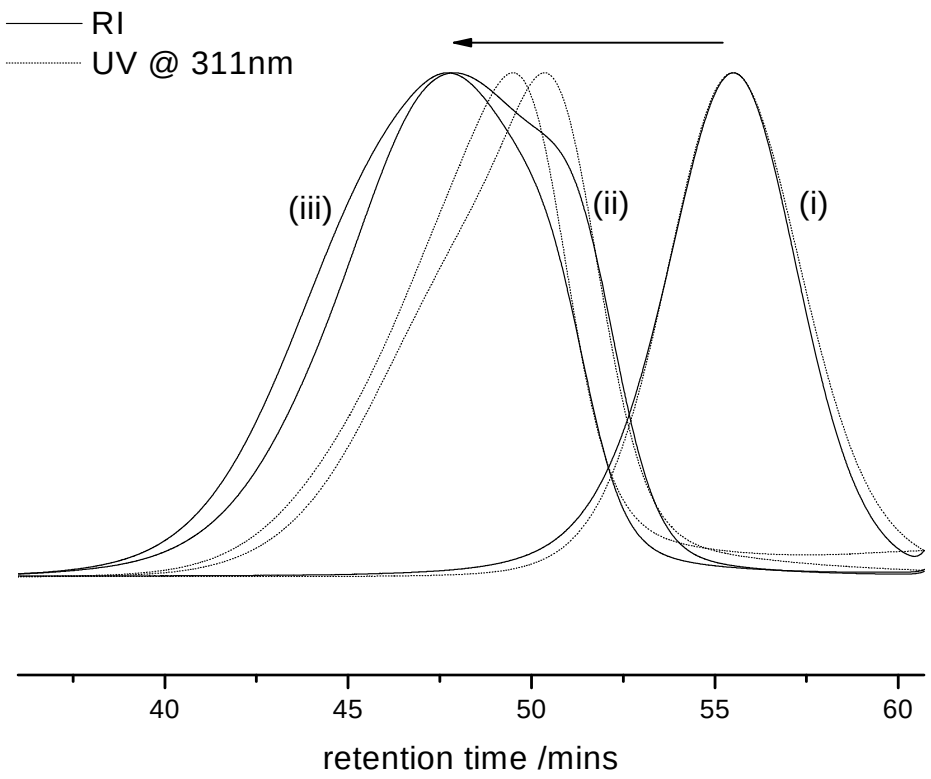

Figure 5.7 GPC chromatograms (RI and UV traces at 311nm) evolution in RAFT inverse miniemulsion polymerization of acrylamide with AIBN as initiator (Exp. P2): (i) 60min, conversion=49%, Mn=9320, PDI=1.42; (ii) 100min, conversion=92%, Mn= 62218, PDI=1.65; (iii) 186min, conversion=97%, Mn= 74235, PDI=1.70).

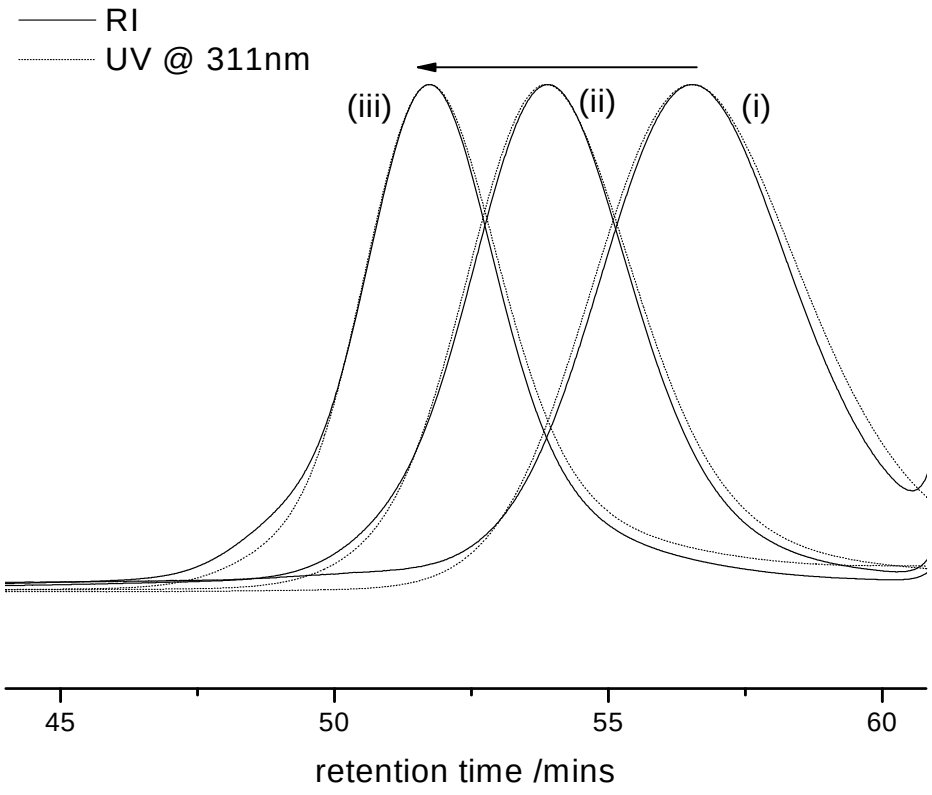

Figure 5.8 GPC chromatograms (RI and UV traces at 311nm) evolution in RAFT inverse miniemulsion polymerization of acrylamide with ABCP as initiator (Exp. P3). (i) 120min, conversion=37%, Mn=6530, PDI=1.34. The RI curve deviated slightly from the baseline in this case due to a partial overlap of the salt peak at the retention time around 63 min; (ii) 180min, conversion=54%, Mn= 13828, PDI=1.32; (iii) 250min, conversion=70%, Mn= 23677, PDI=1.38).

The above data suggest that ABCP-initiated inverse miniemulsion RAFT polymerization of acrylamide produces polymer chains with kinetics and molecular weights that deviate from the theoretical line at high conversion but that still contain the C=S bond on most chains. To further probe this, the polymers from Exp. P2 and P3 were extended with another aliquot of acrylamide. The final polymer products of Exps. P2 and P3 were collected, precipitated with acetone and dried in vacuum at 40 °C for 4 days. After fully dissolving the dried RAFT-bearing polymers in water, acrylamide and ABCP were added and the mixture polymerized at 60 °C. These chain extension experiments clearly showed a difference in the 'livingness' of the poly(acrylamide)s made in Exps. P2

and P3. As shown in Figure 5.9, only the relatively low molecular weight poly(acrylamide) chains were extended when using the samples prepared by AIBN initiation in Exp. P2, while nearly all the poly(acrylamide) chains prepared via ABCP initiation in Exp. P3 grew in Figure 5.9b. These data suggest that like the solution polymerization, the ABCP-initiated inverse miniemulsion polymerization proceeds in a controlled manner up to about 40% conversion, after which the polymerization proceeds in a pseudo-living manner.[218] Thus, ABCP is a suitable initiator for RAFT inverse miniemulsion polymerization, which is demonstrated to proceed under pseudo-living conditions here for the first time.

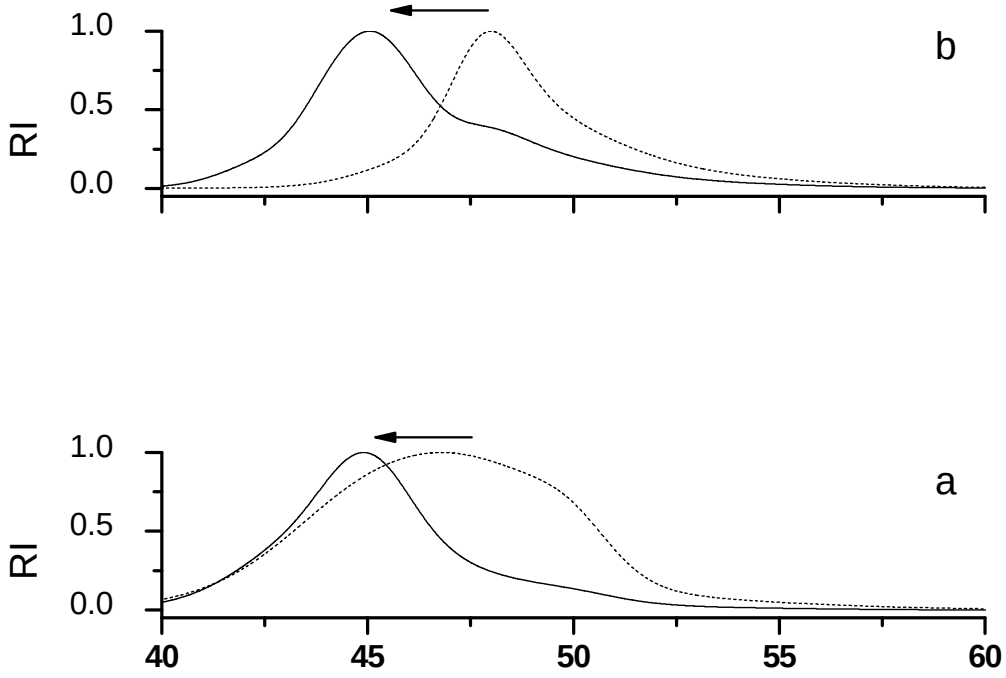

Figure 5.9 RI traces of GPC chromatograms for the chain extension of poly(acrylamide) in solution at 60°C. The poly(acrylamide)s made from the final products of Exp. P2 (Mn=79975, PDI=1.66) and Exp. P3 (Mn=49926, PDI=1.43) were used as the chain transfer agents. [Acrylamide]/[CTA]= 800 and [CTA]/[ABCP]=0.5. (a) Chain extension of the poly(acrylamide) from Exp. P2 and (b) Chain extension of the poly(acrylamide) from Exp. P3.

5.3.2 In-depth study of RAFT inverse miniemulsion polymerization

From the above preliminary study, a formulation for RAFT inverse miniemulsion polymerization was developed and used to successfully synthesize stable hydrophilic polymer latexes. The preliminary study also made progress in the understanding of the kinetics of inverse miniemulsion polymerization in the following aspects:

1. The RAFT inverse miniemulsion polymerizations followed similar kinetics to RAFT solution polymerizations.
2. The nature of the initiator had a great effect on the kinetics and controllability of RAFT inverse miniemulsion polymerization of acrylamide. Hydrophilic initiators can have certain advantages over hydrophobic ones in the control of the inverse miniemulsion polymerizations. When the water soluble initiator ABCP was used, the polymerization proceeded in a controlled/living manner at low conversion and pseudo-living manner at high conversion, both in inverse miniemulsion and solution. When the oil soluble initiator AIBN was utilized, however, a significant loss of control was observed with prolonged reaction time.
3. A deviation from well controlled polymerization was observed at higher conversions, e.g. a nonlinear increase of Mn with the conversion. However, it should be noted that the degree of livingness/control at low conversions is comparable to the only other report of controlled inverse miniemulsion polymerization where ATRP was used as the control methodology.[188,189] In those works, good control was achieved up to a conversion of 65-80%. The RAFT polymerizations in this preliminary work appear well-controlled at conversions up to 40% and only deviate at higher conversions. RAFT agent hydrolysis could be the problem that caused the loss of control.[138, 139, 219]

Based on the preliminary study, a recipe for a follow-up in-depth study (Table 5.2) was optimized with the goal of suppressing the uncontrolled behavior. Compared with the recipe in the preliminary study (Table 5.1), another hydrophilic initiator VA-044 was used. VA-044 has a much faster radical generation rate than ABCP, and this can allow completion of the polymerizations in a shorter reaction time and thus less time for the hydrolysis of the RAFT agent. In addition, the pH of the aqueous phase in Table 5.2 was adjusted to 4 instead of pH=8 used in the preliminary study to further slow down the

hydrolysis of RAFT agent. With these changes in recipe, a detailed study of RAFT inverse miniemulsion polymerizations was carried out. The effect of the reaction parameters on the kinetics was first studied. The polymerization mechanism, including the possible fates of desorbed monomeric radicals and the effect of steric surfactant on the desorption rate of radicals, was then investigated.

5.3.2.1 Effect of reaction parameters

Table 5.4 Recipes for RAFT inverse miniemulsion polymerization of acrylamide in the in-depth study.

Exp	reaction	Monomer (M)	initiator (mM)	CTA (mM)	$\frac{\text{CTA}}{\text{initiato}}$	$\frac{\text{monomer}}{\text{CTA}}$	B246 (wt%)	temp ^{o}C	pH	$\bar{r}_w$ (nm)
1	RAFT solution	3.62	9.08	36.2	3.99	100		60	4	
2	free-radical mini	3.62	9.08				1.5	60	4	98
3	RAFT mini	3.62	9.08	36.2	3.99	100	1.5	52	4	102
4	RAFT mini	3.62	9.08	36.2	3.99	100	1.5	60	4	105
5	RAFT mini	3.62	4.54	36.2	7.98	100	1.5	60	4	103
6	RAFT mini	3.62	9.08	36.2	3.99	100	1.5	60	7	107
7	RAFT mini	3.62	9.08	36.2	3.99	100	1.5	60	10	99
8	RAFT mini	3.62	9.08	57.9	6.37	63	1.5	60	4	108
9	RAFT mini	3.62	9.08	36.2	3.99	100	1.0	60	4	112
10	RAFT mini	3.62	9.08	36.2	3.99	100	2.5	60	4	103
11[a]	RAFT mini	3.62	9.08	36.2	3.99	100	1.5	60	4	110
12[b]	RAFT mini	3.62	9.08	36.2	3.99	100	1.5	60	4	114

[a] macro-RAFT1 was used as CTA.

[b] macro-RAFT2 was used as CTA.

Experiments 1-10, as shown in Table 5.4, explored the effects of different reaction parameters on the kinetics of RAFT inverse miniemulsion polymerization. The effect of temperature on the polymerization is shown in Figure 5.10. The rate of polymerization increased with increasing temperature. A longer induction time was observed at the lower temperature of 52^{o}C. This is likely due to both a lower propagation rate constant and a smaller population of free-radicals generated from initiator at lower temperatures.

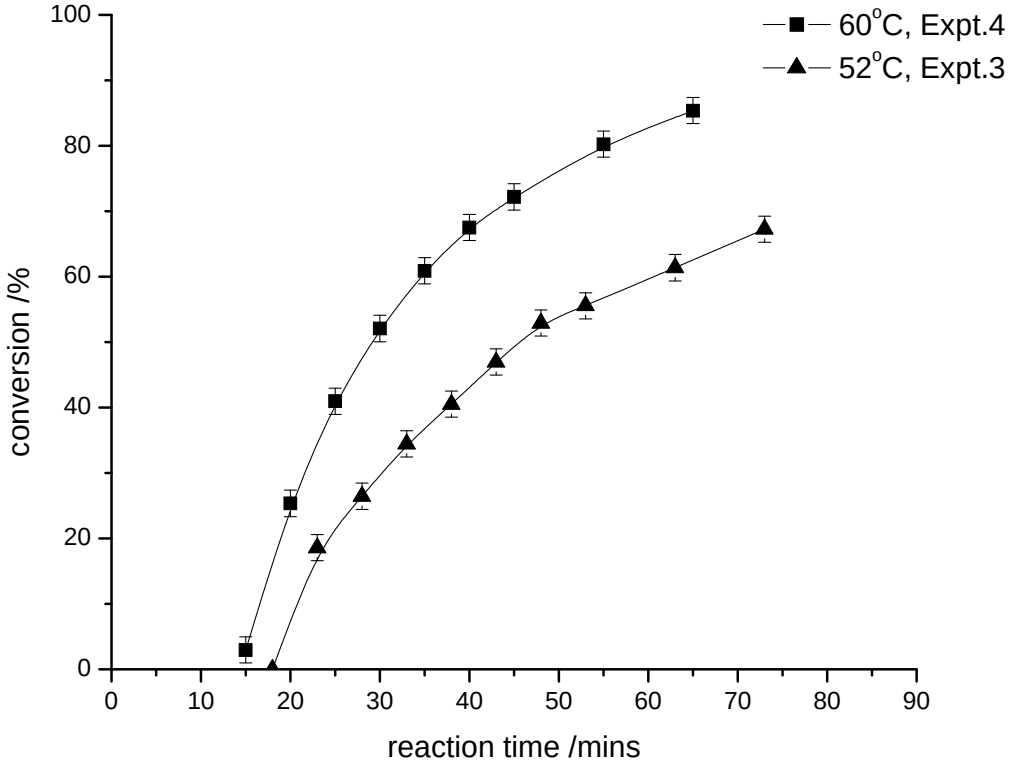

Figure 5.10 RAFT inverse miniemulsion polymerization of acrylamide at different reaction temperatures.

Figure 5.11 shows the conversion-time curves at two different initiator concentrations. The polymerization rate increased with an increasing amount of initiator since more radicals can be generated. The amount of initiator seemed have no effect on the final particle radius, as shown in Table 5.4. This is consistent with droplet nucleation. The entire particle radius in Exp. 4 and Exp. 5 were close to 100nm throughout the polymerization.

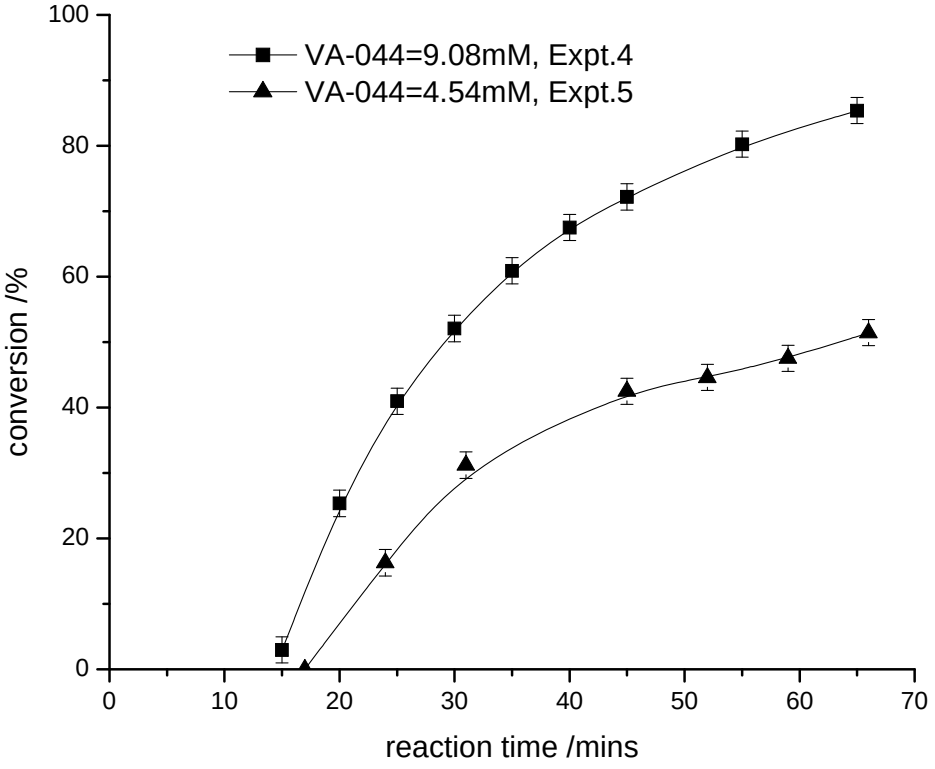

Figure 5.11 RAFT inverse miniemulsion polymerization of acrylamide at 60°C with different amount of initiator.

The pH of the dispersed phase is one of the key parameters that can affect the kinetics of RAFT inverse miniemulsion polymerizations. The aqueous solutions of Exp. 4, Exp. 6 and Exp. 7 were adjusted to a pH of 4, 7 and 10, respectively, before the preparation of the inverse miniemulsions, with all other recipe variables kept constant, as shown in Table 5.4. Figure 5.12 shows the evolution of monomer conversion with reaction time at the different pHs. When the aqueous solution was in a weak acidic or neutral environment, the conversion-time curves overlaid very well. At pH=10, the polymerization rate was trivially affected by pH before the conversion reached around 50% when a higher polymerization rate was observed compared to the lower pH runs. The relationship between molecular weight and conversion is shown in Figure 5.13. There is a deviation of the experimental Mn from the theoretical prediction that may be

caused by the GPC calibration method.[220] The Mn generally increased with conversion in a linear manner except that slightly higher Mn was found at high conversions in Exp. 7 (pH=10). The PDI in Exp. 7, however, showed a significant difference from Exp. 4 and Exp. 6 (Figure 5.13). The PDI at pH=10 remained below 1.5 before 50% in conversion, although it was slightly larger than in the experiments at pH=4 and pH=7, followed by a sharp increase of PDI up to 3.5. The evolution of the RI curve from the GPC compared with the UV curve monitored at 311nm is shown in Figure 5.14 for the experiments at different pH values. As mentioned in the preliminary study, the UV curve corresponds to the signal from the C=S bond in the RAFT agent, giving a measure of the polymer chains that contain a RAFT functional group (potentially "living chains"), while the RI curve accounts for all the polymer species in the system.[194] Therefore, the content of living chains among all the polymer chains can be estimated by the overlapping degree of the two curves. At pH=4 and pH=7, the overall RI signal had a very good overlay with the UV curve throughout the RAFT inverse miniemulsion polymerization in spite of the small shoulder in the RI curve with shorter retention time. This is likely caused by the termination between the propagating radicals or propagating radicals and RAFT intermediates. However, significant deviation of RI and UV curves was observed at pH=10 with increasing conversion. The RI curve skewed to high molecular weight and this resulted in a much broader PDI. The reduced control at higher conversions at pH=10 may result from the hydrolysis of the RAFT agent, among other factors, a well known issue in aqueous RAFT polymerizations.[139] Different groups have reported very similar behavior in RAFT solution polymerizations as a result of RAFT agent hydrolysis.[141-143,149] Although trithiocarbonate was found to be a more preferable RAFT agent than dithioesters for the polymerization of acrylamide and is thought to be fairly stable when the pH is lower than 7, it can be hydrolyzed in basic solution. [112,113] The good overlap between the RI and UV signals in Exp. 4 and Exp. 6 and the significant increase in the high molecular weight shoulder with prolonged reaction time in Exp. 7 at pH=10 suggests a loss of control in Exp. 7 is likely attributable to hydrolysis of the RAFT agent. The poor overlap of the GPC curves at pH=10 is also consistent with the significantly broader PDI in Exp. 7.

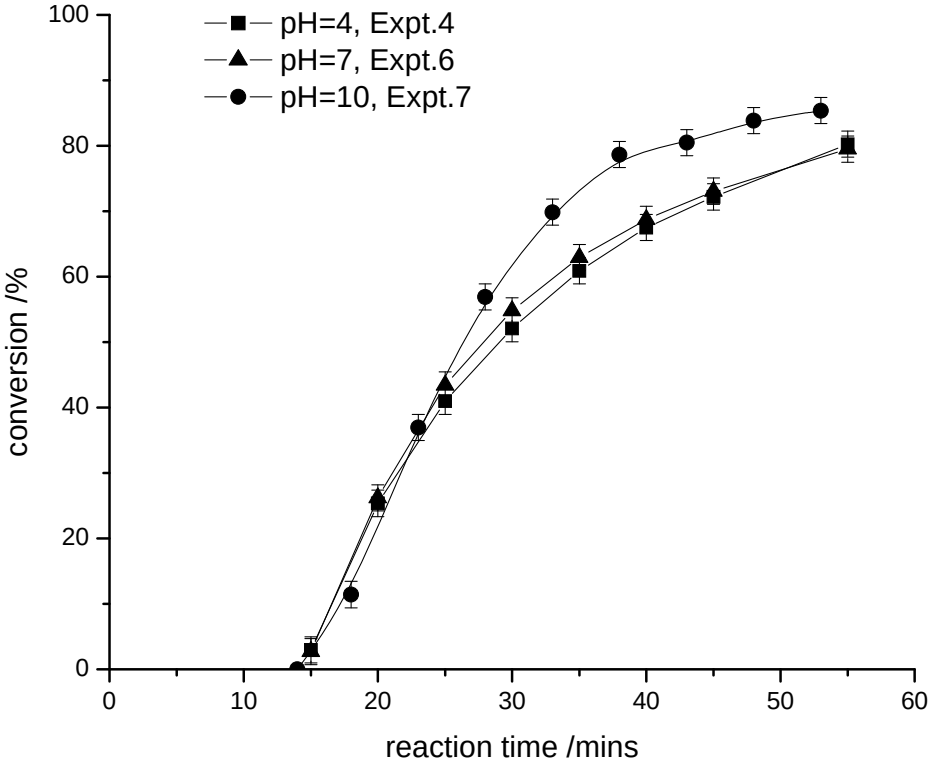

Figure 5.12 RAFT inverse miniemulsion polymerization of acrylamide at 60^{o}C at different pH values.

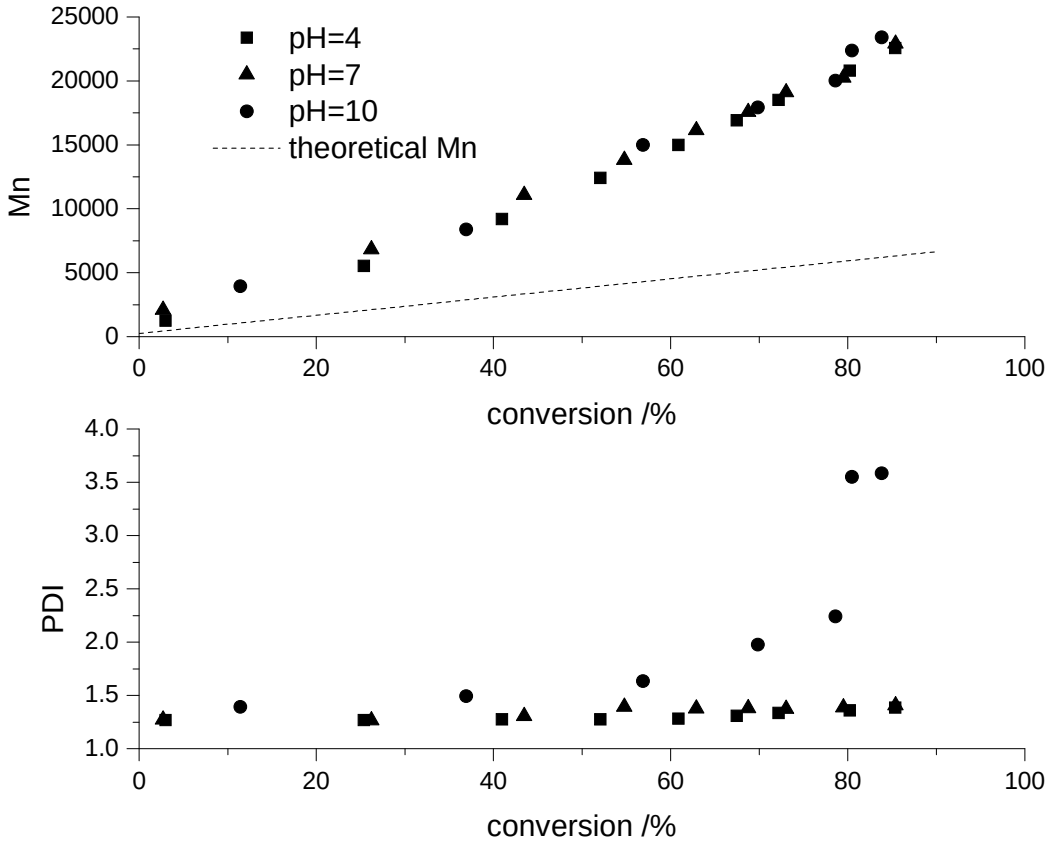

Figure 5.13 Relationship between Mn, PDI and conversion in RAFT inverse miniemulsion polymerization of acrylamide at 60^{o}C at different pH values.

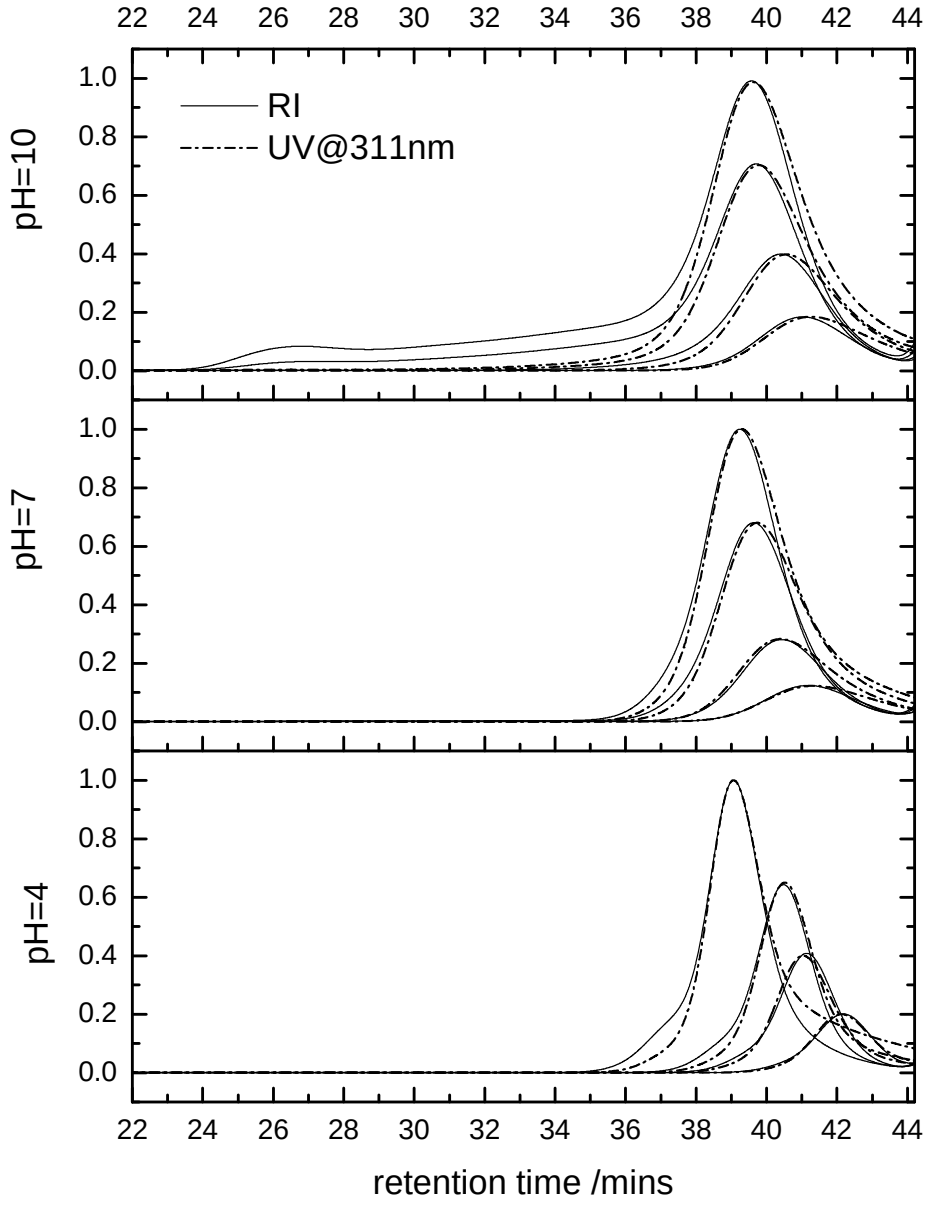

Figure 5.14 GPC chromatograms (RI and UV traces at 311 nm) showing the evolution of the RAFT inverse miniemulsion polymerization of acrylamide at different pH values.

The effect of RAFT on the polymerization was studied by the comparison of Exp. 4 and Exp. 8. With an increase of RAFT concentration from 36.2mM (Exp. 4) to 57.9mM (Exp.8), Figure 5.15 shows significant rate retardation in Exp. 8 compared with Exp. 4.

More retardation is usually observed in conventional o/w miniemulsion polymerizations in the presence of a larger amount of RAFT agent. Different reasons have been proposed for such a phenomenon and these may be applicable to the RAFT inverse miniemulsion polymerization studied here. First, a retardation effect may come from the RAFT chemistry because of cross-termination of intermediate and propagating radicals. The retardation factor for bulk RAFT polymerization has been evaluated by: [81]

$$\frac{R_{p,RAFT}}{R_{p,blank}} = (1 + \frac{2k_{ct}}{k_{tc}} K[RAFT]_0)^{-0.5} \tag{5.2}$$

From this equation, retardation would be more pronounced at a higher concentration of RAFT agent. Second, RAFT-induced exit and oligomeric radical desorption from the polymer particles may lead to retardation.[156, 221] More shorter chain radicals will be produced at a higher concentration of RAFT agent and these are more likely to desorb from the particles and lead to a lower average number of propagating radicals in each particle. From the conversion-time curves of Exp. 4 and Exp. 8, the apparent total propagating radical concentration [$P\bullet$] during the polymerizations of Exp. 4 and Exp. 8 can be roughly estimated by the following equation: [144]

$$[P\bullet] = \frac{d[-\ln(1-x)]}{k_p dt} \tag{5.3}$$

Where x is the conversion of monomer and the apparent propagating coefficient of the monomer at 60°C is $k_p = 2.58 \times 10^6$ L/mol·min^{-1}. [222] To avoid the potential influences of the gel effect and chain length dependence of k_p in the polymerizations, only the conversion data between 25-55% were used for analysis. As shown in Figure 5.16, the apparent total propagating radical concentration [$P\bullet$] in Exp. 4 and Exp. 8 appeared to decrease slightly with reaction time but still remained on the same order of 10^{-8} mol/L. When a higher concentration of RAFT agent was used, a lower [$P\bullet$] resulted in the system. Third, the compartmentalization of RAFT miniemulsion polymerization can also contribute to the retardation. [87] If the RAFT miniemulsion polymerization is a zero-one system, the intermediate and propagating radicals are segregated in separate particles. There is a quantitative relationship between the average number of radicals per particle of

a RAFT miniemulsion polymerization, $\overline{n}_{RAFT}$, and that of free-radical miniemulsion polymerization $\overline{n}_{free-radical}$:[87]

$$\frac{1}{\overline{n}_{RAFT}} = \frac{1}{\overline{n}_{free-radical}} + 2K[RAFT]_0 \tag{5.4}$$

A larger RAFT concentration will result in a lower average number of radicals per particle and thus a more pronounced retardation. It should be noted that it is difficult to tell conclusively based on the data here whether RAFT chemistry, radical desorption or both caused the lower apparent total propagating radical concentration at the higher RAFT concentration.

It is helpful to compare the change of average number of radicals per particle with the concentration of RAFT and shed some light on the above compartmentalization assumption. The average number of radicals per particle, $\overline{n}$, can be calculated with the following equation:

$$\overline{n} = \frac{M_0 N_A}{k_p [M]_p N_t} \frac{dx}{dt} \tag{5.5}$$

Where M_0 is the initial total monomer amount (mol) in the system, N_A is Avogadro's constant, k_p is the propagation coefficient of the monomer (L/mol·min), $[M]_p$ is the monomer concentration in the latex particles (mol/L), N_t is the total particle number, and x is the conversion of the monomer. From Figure 5.17, the $\overline{n}$ values in both Exp. 4 and Exp. 8 were far below 0.5. The theoretical predication of the average number of radicals per particle for Exp. 4 and Exp. 8 with Eqn. 5.4 is in very good agreement with the experimental results.

Figure 5.18 shows the relationship between Mn and the conversion in Exp. 4 and Exp. 8. The Mn increased linearly with the conversion and as expected, decreased with an increase in RAFT agent concentration. In both cases, the PDIs remained below 1.3 until the end of the polymerizations.

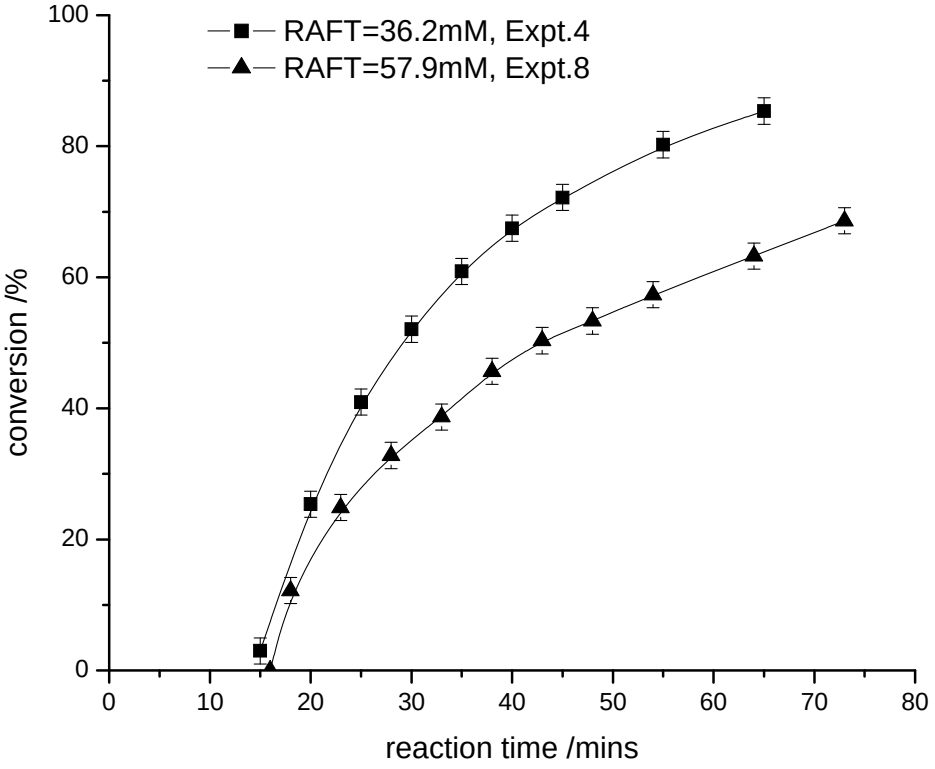

Figure 5.15 RAFT inverse miniemulsion polymerization of acrylamide at 60°C with different RAFT agent concentrations.

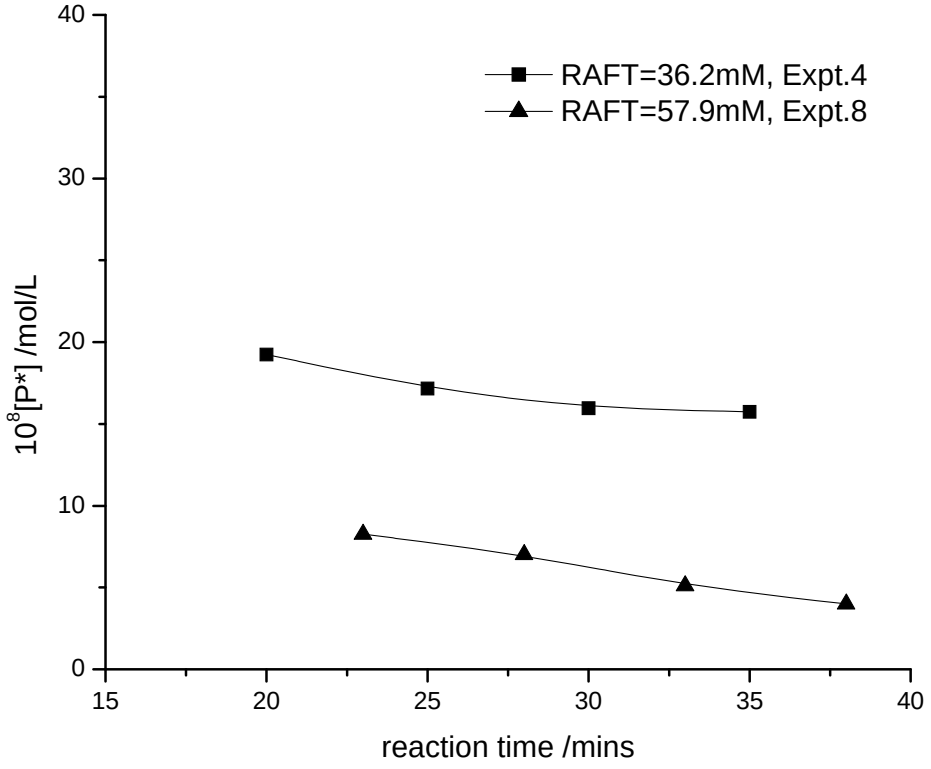

Figure 5.16 Apparent total propagating radical concentrations in RAFT inverse miniemulsion polymerization of acrylamide with varying RAFT agent concentration.

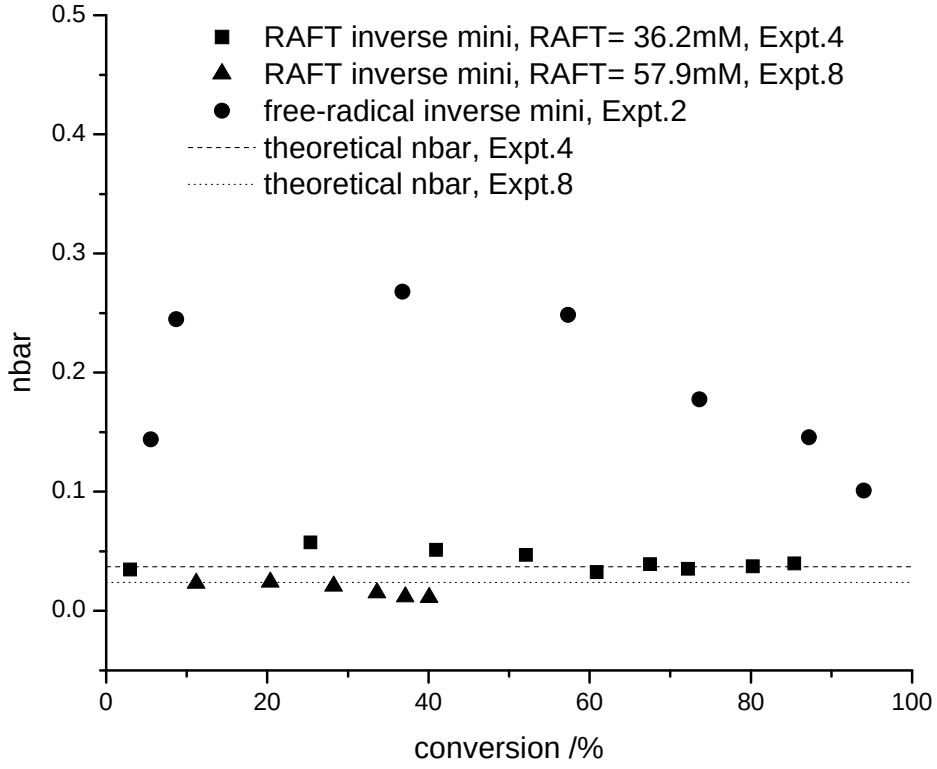

Figure 5.17 Evolution of the average number of propagating radicals per particle as a function of conversion in RAFT inverse miniemulsion polymerizations at 60°C. The theoretical average number of propagating radicals per particle was calculated from Eqn.5.4 using the following parameters: $\bar{n}_{free-radical} = 0.2$, and K=300.

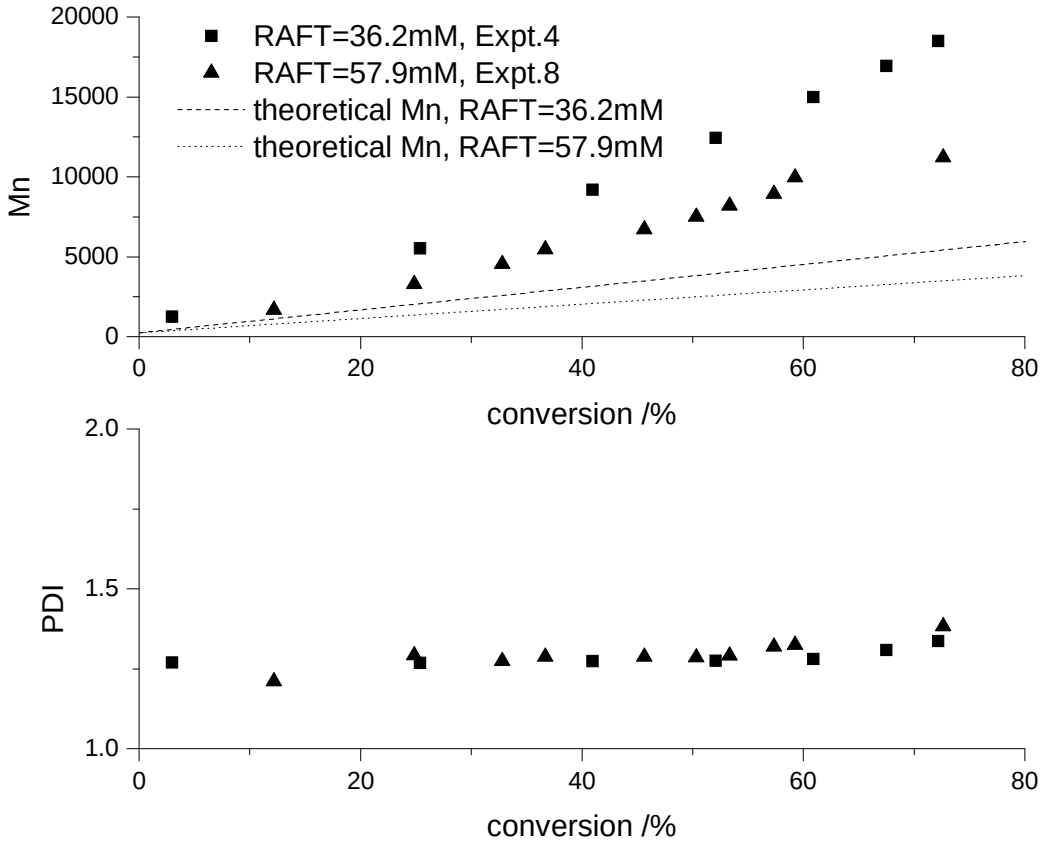

Figure 5.18 Relationship of Mn, PDI and conversion in RAFT inverse miniemulsion polymerization of acrylamide at 60^{o}C with different RAFT concentrations.

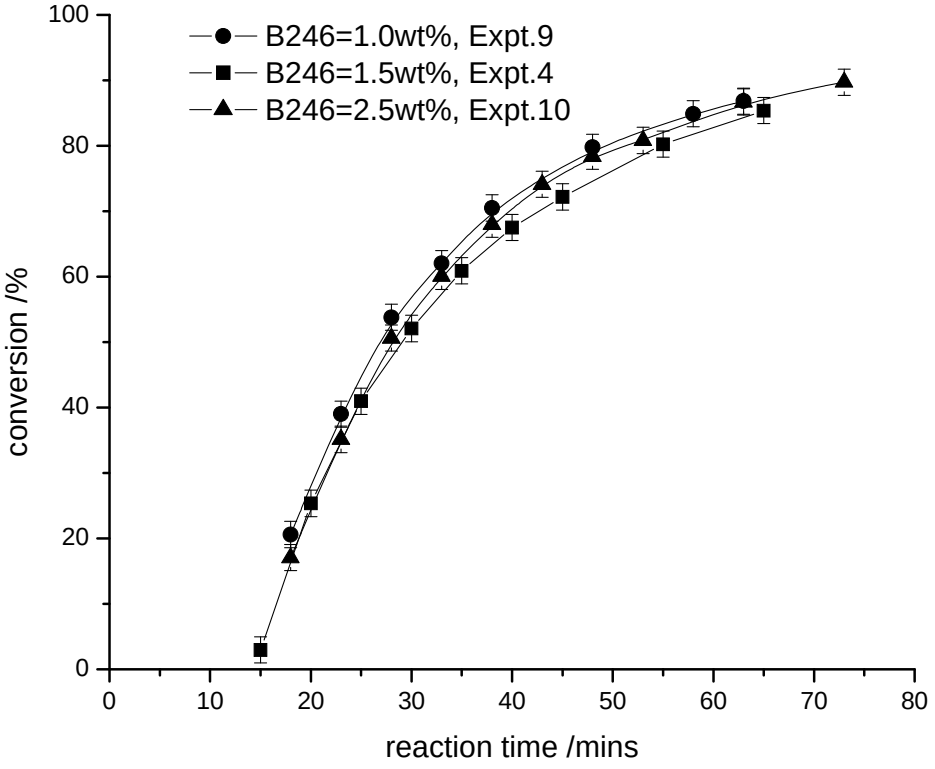

Figure 5.19 RAFT inverse miniemulsion polymerization of acrylamide at 60°C with different surfactant concentrations.

The effect of the surfactant concentration on the polymerization kinetics was evaluated in Exp. 4, Exp. 9 and Exp. 10 with an increasing amount of surfactant from 1wt% to 2.5wt% based on the oil phase. Compared to normal emulsion polymerizations, the correlation of the polymerization rates with the surfactant concentration is complicated in inverse emulsion polymerizations by the reaction temperature, the continuous oil solvent (temperature and the oil solvent can affect the micelle formation and the interaction between surfactants and droplets) and the nature of the initiator (which affects the primary radical location, in the continuous phase vs. in the monomer droplets). It was found that when oil soluble initiators were used, polymerizations carried out at higher temperatures and using aromatic solvents as the continuous phase tended to have positive reaction orders with respect to surfactant concentration, while negative

reaction orders can occur when using aliphatic media at low reaction temperatures and with high surfactant levels; [223-225] If water soluble initiators are used, the polymerization kinetics of inverse emulsion polymerizations are similar to the solution or bulk polymerization controls.[223-225] Steric surfactants used in inverse emulsion or miniemulsion polymerizations can dramatically change the reaction kinetics because of the barrier effects of the surfactant, as well as potential chain transfer reactions to the surfactant molecules. [224, 226] As shown in Figure 5.19, there seems to be no significant change in the polymerization rate at the different surfactant concentrations in our study. The average particle radius remained almost constant at ~105nm under different surfactant concentration levels, as shown in Table 5.4. These results agree with previous inverse microsuspension polymerizations of acrylamide where the polymerization rate, the average particle diameter, and the radical capture efficiency were essentially independent of the emulsifier,[224] indicative of the pure physical role of B246 and the dominant droplet nucleation feature in our inverse miniemulsion polymerizations.

5.3.2.2 Location of radical generation for particle nucleation and fate of desorbed monomeric radicals in inverse miniemulsion polymerization

For emulsion or miniemulsion polymerizations, initiators are usually dissolved in the continuous phase and the polymerization mechanism has been well studied.[197,198] When an initiator in the dispersed phase of an emulsion or miniemulsion (e.g. 2,2'-azobis(isobutyronitrile) [AIBN] is used in the conventional oil-in-water emulsion polymerization of styrene), the polymerization kinetics are more complicated. Although the kinetic behavior of such emulsion or miniemulsion polymerizations is known to be very similar to that with water-soluble initiators, the apparent initiation efficiency is usually significantly lower than that of solution and bulk polymerizations.[227] To clarify the reason for the low initiation efficiency, two primary theories have been proposed and have been subject of a vigorous debate over the last decade. The focus has been on the dominant radical generation location resulting in particle nucleation. Nomura et al. claimed that the fraction of initiator partitioned in the continuous phase plays a decisive role in radical generation since these radicals produced in a pairwise manner in the particles may result in geminate termination instantaneously.[228] Asua et al., however,

suggested that the locus of radical generation is in the particles due to initiator decomposition in the particles, followed by desorption of one of the radicals.[229] Both of the two theories have been supported by various, and in many cases conflicting experimental evidence and theoretical simulations.[230-233]

The initiator used in this study, VA-044, was dissolved in the dispersed phase since the preliminary study showed that using a water-soluble initiator had some advantage over an oil-soluble initiator in achieving controlled polymerization by limiting homogeneous nucleation.[158] Identification of the main radical source for particle nucleation and the fate of desorbed radicals is, therefore, very important in understanding the mechanism of RAFT inverse miniemulsion polymerizations. A set of experiments (Table 5.5, Exp. 13-22) was used to explore this issue.

Table 5.5. Effects of radical scavengers on the inverse miniemulsion polymerizations.

Exp	Monomer (M)	initiator (mM)	CTA (mM)	$\frac{\text{CTA}}{\text{initiator}}$	$\frac{\text{monomer}}{\text{CTA}}$	DPPH amount (mM)	acrylic acid (mM)	addition conversion (%)
13	3.62	9.08	36.2	3.99	254	1.24		24
14	3.62	9.08	36.2	3.99	254	1.24		42
15	3.62	9.08	36.2	3.99	254	1.24		56
16	3.62	9.08	36.2	3.99	254		195	39
17	3.62	9.08				1.24		37
18	3.62		36.2		254	2.32		0
19		9.08				2.32		0
20		9.08	36.2	3.99		2.32		0
21	3.62	9.08				2.32		0
22	3.62	9.08	36.2	3.99	254	2.32		0

DPPH, a water insoluble radical scavenger, was added to the cyclohexane to trap the active radicals in the continuous phase. The effects of DPPH on the kinetics of RAFT inverse miniemulsion polymerizations were quite different from the free-radical inverse miniemulsion polymerizations. For the RAFT inverse miniemulsion polymerizations Exp. 13, Exp. 14 and Exp. 15, DPPH was added to the continuous phase at a conversion of 24%, 42%, and 56% respectively. As shown in Figure 5.20, the conversion-time curves generally were all identical, up to the point of DPPH addition when a plateau occurred. The duration of the plateau period was shorter in Exp. 13, compared with Exp. 14 and

Exp. 15, where DPPH was added at a higher conversion, but the plateau periods were similar. Once the added DPPH was consumed, the polymerization continued again and the conversion increased with reaction time. These results indicate that radicals in the continuous phase may be the dominant source of initiation of the controlled polymerizations. Since there was a concern that a trace fraction of DPPH might diffuse into the particle and terminate the polymerizations, Exp. 16 used acrylic acid instead of DPPH to check the main radical location. In this experiment, 0.72g of acrylic acid was added to cyclohexane (~195mM) when the conversion of RAFT inverse miniemulsion polymerization was at ~39%. No loss of colloidal stability and particle radius change was observed in the experiment. In Exp. 16, the aqueous phase had a pH=4 and the volume ratio of the aqueous phase to cyclohexane was around 0.19, therefore, it is estimated that most of acrylic acid was partitioned in the cyclohexane.[102] The active radical species in the continuous phase preferred to react with acrylic acid due to its significant concentration in cyclohexane. The portion of acrylic acid dissolved in the aqueous phase should not inhibit the polymerization in the particles. A plateau was observed again once acrylic acid was added and no copolymer of acrylamide and acrylic acid formed during the plateau period. This evidence further suggests that the continuous phase cyclohexane is the main source of radical generation for the particle nucleation in the controlled polymerizations.

When DPPH was added to a free-radical inverse miniemulsion system, however, there is no such plateau (Exp17). Indeed the polymerization continued, but at a slower rate than in the control (Exp2). This result suggests that a portion of the radicals was produced inside the particles and there was another fraction of radicals in the continuous phase that appeared to terminate due to reaction with DPPH, with these also contributing to the polymerization under normal circumstances. Clearly, the dominant locus of radical generation for nucleation changes with the presence of the RAFT agent.

The variation of the dominant locus of radical generation for nucleation could be attributed to the chain transfer reaction of initiator-derived radicals with RAFT agent within the particles. For free-radical inverse miniemulsion polymerizations, the newly-born radicals from the initiator inside the particles will propagate by adding monomer units, terminate via radical recombination or with an incoming radical from the oil phase,

or desorb from the particle into the continuous phase. For RAFT inverse miniemulsion polymerizations, other than the above fates, those initiator-derived radicals may suffer an additional chain transfer reaction with the RAFT agent and form a leaving radical which can desorb into the continuous phase. Thus, the overall effect of the RAFT agent is to decrease the chance of formation of propagating radicals in the particles for nucleation. Therefore, the donation of radicals within the particle for nucleation was lessened in RAFT inverse miniemulsion polymerizations compared with free-radical inverse miniemulsion polymerizations.

On the other hand, the difference of viscosity and diffusivity between free-radical and RAFT inverse miniemulsion polymerizations can also lead to a change in the primary radical production. The average molecular weight of polymer is much higher in the free-radical inverse miniemulsion polymerization. The higher viscosity and lower diffusivity in the free-radical inverse miniemulsion polymerization can lead to a pronounced gel effect, limiting the mutual termination reaction of radicals in the particles. The higher radical survival probability makes free-radical inverse miniemulsion polymerizations more like a "pseudo-bulk" polymerization.[13] Thus, the fraction of radicals generated in the particles for nucleation can be "magnified" in free-radical inverse miniemulsion polymerization compared with RAFT inverse miniemulsion polymerizations.

One advantage of using DPPH as radical scavenger is the significant color change with the consumption of DPPH.[234] Depending on the consumption of DPPH, the color of a DPPH solution can change significantly: from the original purple color to grey, and brown. Then, once all the DPPH is consumed, it turns into an orange color. The color evolution of DPPH seems to be independent of DPPH radical consumption resources.[234, 235] To further exam the correlation between the color of DPPH solution and DPPH consumption, AIBN and benzoyl peroxide (BPO) were dissolved in DPPH cyclohexane solution and heated to 70^{o}C to produce different radicals. As shown in Figure 21a and 21b, the color evolution of DPPH followed the same trend in spite of the difference of radicals. Therefore, the consumption rate of DPPH can be qualitatively assessed from the color change of DPPH. Figure 21c-21g shows the color evolution of inverse miniemulsions with the addition of DPPH in the oil phase. Initially, all the inverse miniemulsions were purple in the presence of DPPH. Figure 21c shows that the

miniemulsion in Exp18 remained purple after 100 min, suggesting that RAFT and acrylamide by themselves cannot generate radicals, as expected. For Exp19, VA-044 was added to the aqueous phase without RAFT agent and monomer, and in this case the miniemulsion color became brown (as shown in Figure 21d) after 100 min, suggesting no significant radical flux was produced into the continuous phase, i.e. there was significant geminate termination (two radicals generated in the particle were terminated pairwise) of VA-044 radicals in the particles.

From Figure21c and 21d, no significant amount of desorbed radicals was generated when either RAFT agent or VA-044 was used separately. However, a combination of RAFT agent and VA-044 in Exp20 did result in a fast color change of DPPH, as shown in Figure 21e, indicative of a significant flux of desorbed radicals into the continuous phase. Comparing Figure 21e with 21c and 21d, it can be inferred that the initiator radicals can react with the RAFT agent and increase the radical desorption rate into the continuous phase, providing support for the above assumption of the chain transfer reaction of initiator-derived radicals with the RAFT agent resulting in the significantly different behavior of RAFT and free-radical inverse miniemulsion in the presence of DPPH. From Figure 21f and 21g, the loss of radicals in free-radical inverse miniemulsion polymerization (Exp21) was significantly lower than in the RAFT inverse miniemulsion polymerization (Exp22) since the RAFT inverse miniemulsion turned orange in a much shorter period. The brown color of Exp21 suggested there was certain amount of unreacted DPPH remaining. Besides, poly(acrylamide) was produced in Exp21, while no polymerization occurred in Exp22 until the complete DPPH consumption after ~40 min, as indicated by the orange color of the miniemulsion at that time. Exp21 and Exp22 suggest that free-radical inverse miniemulsion polymerization has more “pseudo-bulk” character than RAFT inverse miniemulsion polymerization.

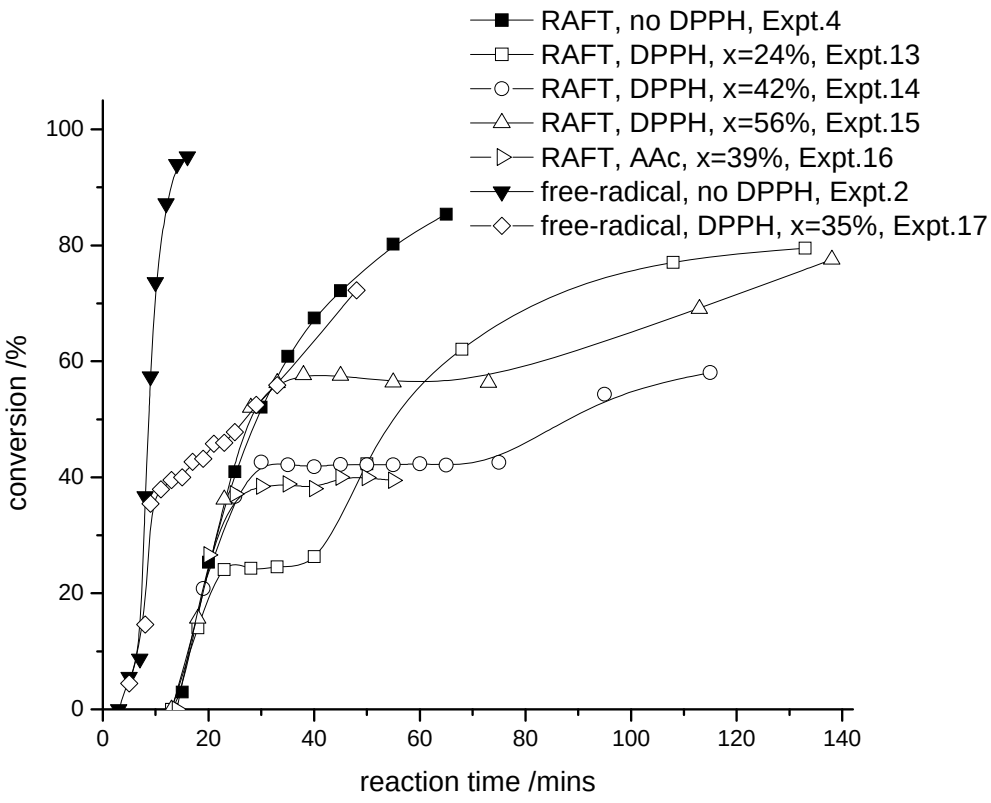

Figure 5.20 Effect of radical scavenger on the RAFT and free-radical inverse miniemulsion polymerizations.

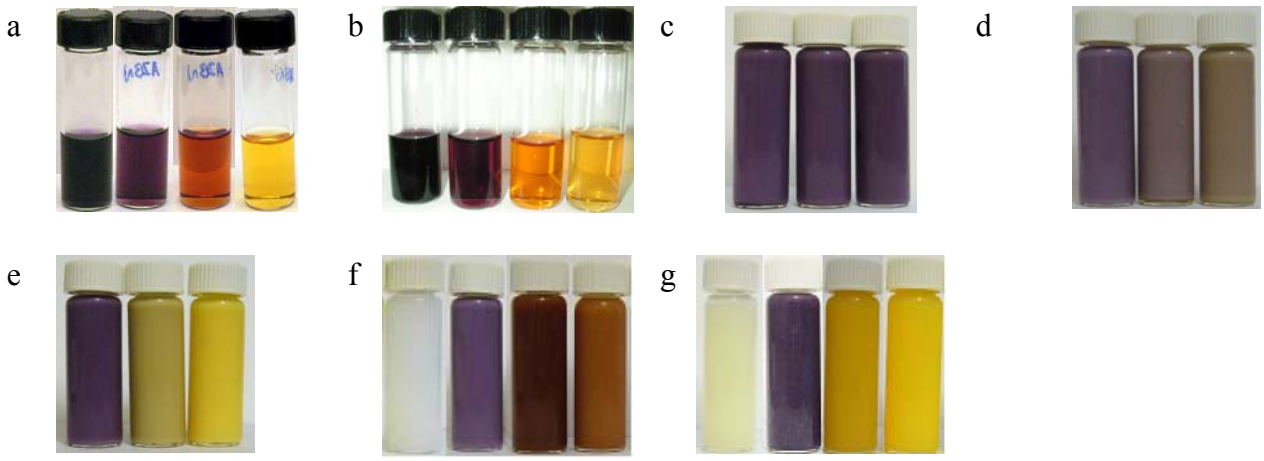

Figure 5.21 Evolution of color change of DPPH cyclohexane solution using different initiators. (a). AIBN; (b). BPO; and the evolution of color of inverse miniemulsions after the addition of DPPH at reaction time= 0 min. (c). Exp18, with only RAFT agent and AM in the aqueous phase. From left to right: t=0, 50min, 100min; (d). Exp19, with only VA-044 in the aqueous phase. From left to right: t=0, 50min, 100min; (e) Exp20, with only RAFT agent and VA-044 in the aqueous phase. From left to right: t=0, 30min, 40min; (f) Exp21, free-radical inverse miniemulsion polymerization of AM. DPPH was added in the continuous phase at the beginning of the polymerization. From left to right: t=0 (before adding DPPH), t=0 (after adding DPPH), 30 min, 60 min; (g) Exp22, RAFT inverse miniemulsion polymerization of AM. DPPH was added in the continuous phase at the beginning of the polymerization. From left to right: t=0 (before adding DPPH), t=0 (after adding DPPH), 30 min, 40 min.

Steric surfactants can significantly change the kinetics of emulsion polymerizations and result in a barrel effect, a sharp decrease both in the exit and entry rate of oligomeric radicals. [13, 216, 226, 233, 236-238] Since the desorption of oligomeric radicals and RAFT induced radical loss can cause retardation of RAFT miniemulsion polymerizations, [197, 221] it is important to understand the fate of oligomeric radicals exiting to the continuous phase. Generally, these radicals can either reenter into the particle, propagate in the continuous phase to a critical degree, or suffer a termination with other radicals or dormant species in the continuous phase, as can be estimated by the following equations:[12,255,256]

For the entry rate of monomeric radicals R_{ads}

$$R_{ads} = k_{ads} \frac{N_p}{V_{oil} N_{Av}} [R\bullet] = 4\pi \frac{r_s (r_s + \delta)}{\delta + r_s D_h / D_{oil}} D_h \frac{N_p}{V_{oil}} [R\bullet]$$

Where k_{ads} is the absorption coefficient, N_p is the particle number, and N_{Av} is the Avogadro constant. r_s , δ are the average radius of particles and thickness of the surfactant hairy layer. D_h , D_{oil} are the diffusion coefficient of monomeric radicals in the surfactant layer and in oil phase. $[R\bullet]$ is the concentration of monomeric radicals in the oil phase. V_{oil} is the volume of the continuous phase.

The propagation rate R_p

$$R_p = k_p [M]_{oil} [R\bullet] \tag{5.6}$$

The termination rate R_t

$$R_t = k_t [T\bullet]_{oil} [R\bullet] \tag{5.7}$$

And the total radical concentration in the continuous phase $[T\bullet]$ can be estimated by

$$[T\bullet] \approx \sqrt{\frac{k_d [I]_{oil}}{k_t}} \tag{5.8}$$

where k_p , and k_t are the coefficient of propagation, and termination reactions in the continuous phase. k_d is the decomposition coefficient of the initiator in the oil phase. $[I]_{oil}$ is the concentration of the initiator partitioned in the oil phase.

Figure 5.22 compares the relative values of the three rates with a variation of D_h and the related parameters listed in Table 5.6. The absorption rate decreases with a lower D_h while propagation, and termination reactions remained constant. Considering that the D_h usually has a value around 10^{-11} to 10^{-12} m^2/s,[123, 124] the most likely fate of monomeric radicals is to propagate in the continuous phase. The particle number and radius did not change significantly during the RAFT inverse miniemulsion polymerizations. Therefore, it is suggested that the radicals of a critical degree chain length are captured by the particles, reentry into the particles or are terminated in or around the surfactant hairy layer instead of precipitating from the continuous phase.

Table 5.6 Parameters value for the evaluation of the fate of desorbed monomeric radicals.

parameter	value (units)	ref
r_s	105nm	This work
δ	11nm	[224]
D_{oil}	2.9×10^{-9} m^2/s	[105]
N_{Av}	6.0×10^{23} mol^{-1}	
N_p	2.0×10^{15} /L	This work
k_p	4.3×10^{4} Lmol^{-1}s^{-1}	[222]
k_d	1.4×10^{-4} s^{-1}	[222]
k_t	1.5×10^{5} Lmol^{-1}s^{-1}	[222]
$[I]_{oil}$	4.5×10^{-4} molL^{-1}	This work
$[M]_w$	0.0069 molL^{-1}	This work
V_{oil}	51 mL	This work

Since D_h decreases with an increase of chain length, the barrel effect of the steric surfactant would be more pronounced for these oligomeric radicals. As shown in Figure 5.22, the termination rate of the critical chain length radical is very close or even higher than the entry rate when $D_h < 1.1\times10^{-13}$ m^{2}s^{-1}. Therefore, the fate of desorbed monomeric radicals could be propagation in the continuous phase to a critical degree and then reentry into the particles. At the same time, a significant number of radicals may suffer a termination during the reentry step. The overall barrel effect on the monomeric radicals is to decrease significantly the reentry rate while boosting the termination rate.

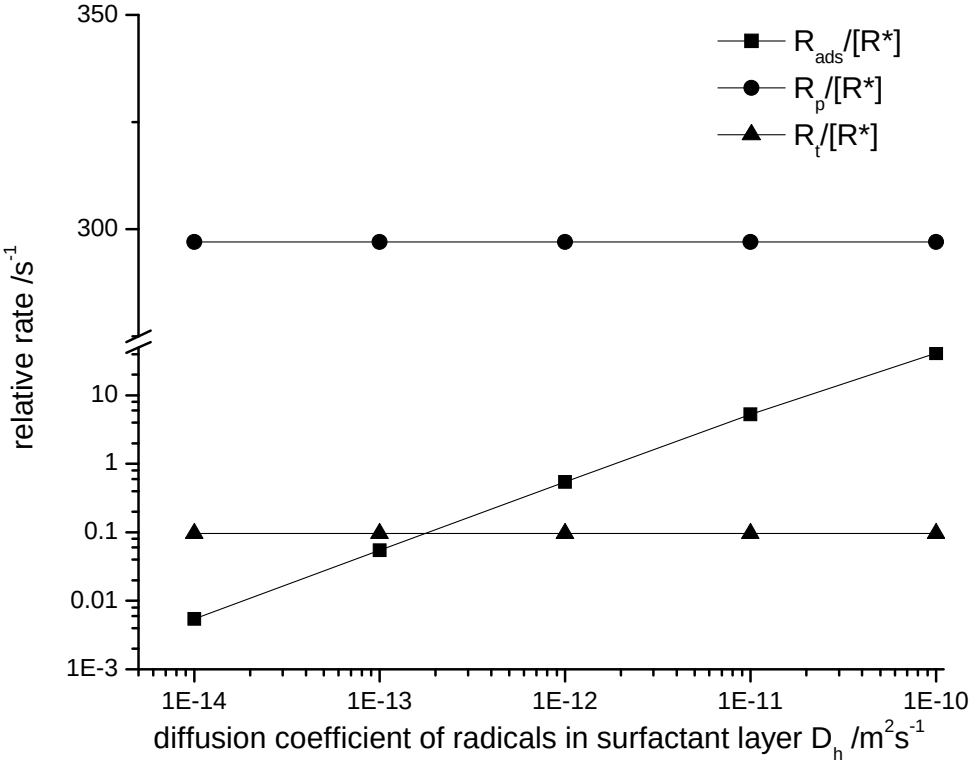

Figure 5.22 Relative rates of absorption, propagation and termination reactions of monomeric radicals in the continuous phase.

Figure 5.23 shows the induction times in the inverse miniemulsion polymerizations. Unlike benzyl dithioesters, trithiocarbonates usually do not result in a significant induction time for RAFT polymerizations since their RAFT intermediate radicals are less stable.[44,138] There was no induction time in the RAFT solution polymerization (Exp.1). Compared with the free-radical inverse miniemulsion polymerization of Exp.2, the RAFT inverse miniemulsion polymerization of Exp.4 had a much longer induction time of ~15mins. The induction time of Exp.11 and Exp.12 using macro-RAFT agents tended to be shorter than Exp.4. The polymerization degree of the R group in macro-RAFT1 (Exp.11) was about 5 while for macro-RAFT2 (Exp.12) it was ~28. The shorter induction times in Exp.11 and Exp.12 indicate that the induction time can be affected by the chain length of the R group of RAFT agent. It was reported that the critical chain length of acrylamide in isooctane was 3.6. [222] Thus, there can be a significant loss of monomeric

R group radicals from the RAFT agent as well as oligomeric radicals; As mentioned above, after propagation in the continuous phase, these radicals can have a very low reentry rate but a high termination rate. Therefore, the loss of oligomeric radicals, among other potential reasons, can contribute to the induction time in the RAFT inverse miniemulsions.

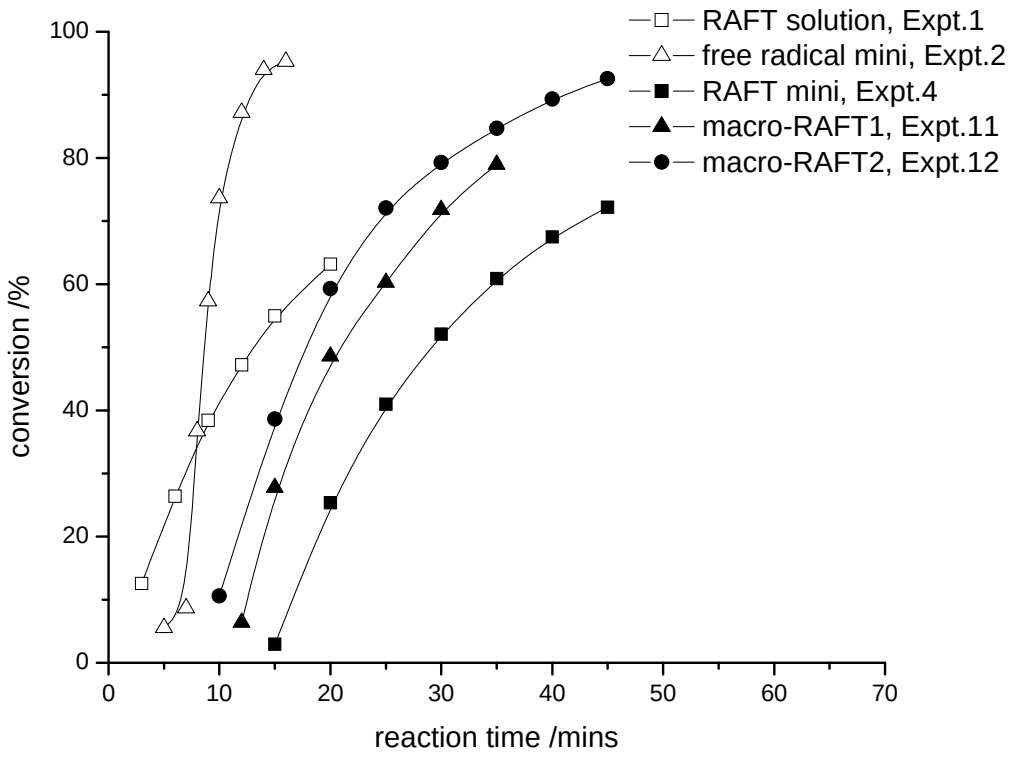

Figure 5.23 Comparison of induction times in RAFT inverse miniemulsion polymerizations with different RAFT agents, along with the RAFT solution polymerization and free-radical inverse miniemulsion polymerization.

5.4 Conclusion

In this contribution, RAFT inverse miniemulsion polymerization was proposed as one way to synthesize well defined hydrophilic polymer latexes. The kinetics of RAFT inverse miniemulsion polymerization were investigated in detail. Under the optimized conditions in the in-depth study, the RAFT inverse miniemulsion polymerization of acrylamide exhibited typical behavior of controlled polymerizations when limited

hydrolysis of the RAFT agent is taking place up to high conversions. These include a linear relationship between Mn and the conversion, narrow PDI, and overlap of the RI and UV traces in the GPC curves. The effects of different reaction parameters on RAFT inverse miniemulsion polymerization were studied. Under the reaction conditions employed, a higher reaction temperature, and a larger amount of the initiator increases the polymerization rate. When the aqueous phase is a neutral or slightly acidic environment, the RAFT inverse miniemulsion polymerizations were better controlled compared with experiments at a pH above 7 (due to hydrolysis of the RAFT agent at high pH). An increase in the RAFT agent concentration tended to retard the polymerization and lower the average radical number per particle. The surfactant concentration had no significant effect on the polymerization rate and particle radius.

The dominant location of radical generation for particle nucleation in the inverse miniemulsion polymerizations was studied by the use of radical scavengers. It was found that the dominant locus of radical generation for particle nucleation varied depending on whether the polymerizations were conducted in the presence or absence of RAFT agent. In the RAFT inverse miniemulsion polymerizations, the radicals leading to particle nucleation mainly came from the fraction of the dissolve initiator in the continuous phase. In the free-radical inverse miniemulsion polymerizations, both initiator in the continuous phase and inside the particles contribute to the particle nucleation. The fate of desorbed monomeric radicals in inverse miniemulsion polymerizations was evaluated by the relative rates of propagation, reentry and termination. One of the potential reasons for the induction time observed in the RAFT inverse miniemulsion polymerizations is suggested to be associated with desorption of oligomeric radicals below a critical chain length.

CHAPTER 6

SUMMARY AND RECOMMENDATIONS FOR FURTHER STUDY*

6.1 Summary of Current Work

Conventional free-radical miniemulsion polymerization has been well studied since its birth in early 1970s. In spite of numerous advantages over macroemulsion polymerizations, conventional free-radical miniemulsion polymerizations have some inherent limitations, e.g. an inability to achieve precise control of polymer structure. This work extended the applications of free-radical miniemulsion polymerizations and helps to overcome these limitations. By introduction of new techniques to miniemulsion systems, new types of various kinds of unconventional miniemulsion polymerization techniques were developed. At the same time, the kinetics and mechanism of these unconventional miniemulsion polymerizations were explored in this work.

In Chapter 2, enzyme initiated free-radical miniemulsion polymerization was proposed for the first time as an answer to the challenges associated with aqueous enzymatic polymerization of hydrophobic vinyl monomers. A recipe for HRP initiated free-radical miniemulsion polymerization was formulated and stable poly(styrene) latexes were successfully synthesized. Compared with enzymatic polymerizations performed with homogeneous cosolvents, enzyme initiated free-radical miniemulsion polymerization in the work achieved much higher monomer conversion and higher polymer molecular weight. The kinetics of enzyme initiated free-radical miniemulsion polymerization was briefly studied. The effect of reaction conditions on the polymerization was investigated. It was shown that only a very small amount of H_2O_2 and ACAC was required for HRP to facilitate the miniemulsion polymerizations.

In chapters 3-5, to precisely control polymer properties and latex morphology, RAFT chemistry was employed in miniemulsion systems to polymerize monomers of different hydrophilicities. Chapter 3 described RAFT miniemulsion polymerization of

* Portions of this chapter are to be submitted.

styrene in CSTR trains, focusing on the transient states observed in a previous Gatech study.[2] Potential causes of the transient states were summarized and solutions were suggested. Two categories of factors potentially contributing to unstable transients in CSTR trains were examined in this work. Possibilities from equipment design and operation were first checked. When keeping the CSTR train under nitrogen pressure and a constant concentration of initiator feed, no significant transient states were observed. Other causes related to the polymerization mechanism were then evaluated. However, such possibilities were ruled out after careful analysis. Therefore, the transient states in previous work appear to result from the previous equipment design and operation rather than from mechanistic issues associated with RAFT miniemulsion polymerizations. A steady state in RAFT miniemulsion polymerization in a CSTR train was achieved in this work.

In chapter 4, RAFT miniemulsion polymerization of MeMBL, a partially water soluble lactone monomer derived from renewable resources, was successfully formulated and a stable poly(MeMBL) latex was produced. The water-solubility limit of monomers in the oil-in-water miniemulsion polymerization technique was extended from ~7wt% (acrylonitrile) to ~9wt% (MeMBL). The kinetics of free-radical "miniemulsion" polymerization of MeMBL were assessed. The effects of reaction parameters on free-radical "miniemulsion" homopolymerization were investigated. Homogeneous nucleation was found to play an important role in the free-radical "miniemulsion" homopolymerization. RAFT miniemulsion polymerizations of MeMBL were achieved by the use of styrene as a comonomer. In the miniemulsion copolymerizations of MeMBL and styrene using an oil soluble initiator, the homogeneous nucleation process appeared limited. The RAFT miniemulsion polymerizations of MeMBL and styrene were well controlled and narrow polydispersity copolymers of MeMBL/styrene were produced. Rate retardation was observed in the RAFT miniemulsion polymerizations compared with the free-radical polymerization and RAFT bulk polymerization controls. The reactivity ratios of MeMBL and styrene in RAFT bulk copolymerization were measured and compared with that of MMA and styrene. It was found that the MeMBL radicals were less monomer preferential in the propagation reaction compared with MMA radicals.

In Chapter 5, a RAFT inverse miniemulsion polymerization technique is developed for the first time to synthesize well defined hydrophilic polymer latexes. The kinetics of RAFT inverse miniemulsion polymerization were investigated in detail. After optimizing the recipe, the RAFT inverse miniemulsion polymerization of acrylamide exhibited typical behavior of controlled polymerizations up to high conversions. The effects of reaction parameters, such as reaction temperature, initiator amount, pH value of the aqueous phase, concentration of RAFT agent and surfactant, on the polymerization rate and particle radius were investigated. The dominant location of radical generation for particle nucleation in the inverse miniemulsion polymerizations was studied by the use of radical scavengers. It was found that the dominant locus of radical generation for particle nucleation varied depending on whether the polymerizations were conducted in the presence or absence of a RAFT agent. In the RAFT inverse miniemulsion polymerizations, the radicals causing particle nucleation mainly came from the fraction of the dissolved initiator in the continuous phase. The fate of desorbed monomeric radicals in inverse miniemulsion polymerizations was evaluated by the comparison the relative rates of propagation, reentry and termination.

6.2 Recommendations for Further Inquiry

6.2.1 Enzymatic miniemulsion polymerization

The kinetics of HRP initiated miniemulsion polymerization was preliminarily studied in Chapter 2. Figure 2.1 showed there was an initialization period at the beginning of HRP initiated miniemulsion polymerization in which the polymerization rate was relatively slow. We suggested that the slow polymerization rate could be the result of ACAC partitioning leading to an atypical initiation mechanism using HRP. In-depth investigation of the enzymatic polymerization mechanism, especially understanding the fundamental reasons resulting in the initial slower polymerization rate, is needed before drawing a conclusive answer.

The enzymatic polymerizations can also be applied to inverse miniemulsions to immobilize enzymes *in situ*. Compared to free enzymes, immobilized enzymes are superior in maintenance of their activity, storage convenience, and tolerance to undesired

reaction conditions.[239] As an example, the enzyme (HRP), H_2O_2 and hydrophilic monomers such as acrylamide can be dissolved in the aqueous phase of an inverse miniemulsion. HRP will initiate the polymerization of acrylamide and simultaneously be immobilized *in situ* by the poly(acrylamide) gel formed. A tentative recipe is shown in Table 6.1.

Table 6.1 Tentative recipe for in situ immobilization of HRP at room temperature.

Component		Mass
Continuous phase	Dispersed phase	(g)
B246		1.00
Cyclohexane		50.0
	H_2O	7.5
	Acrylamide	1.0
	N,N'-methylene bisacrylamide	0.2
	$MgSO_4$	0.12
	H_2O_2(30wt%)	0.015
	HRP	0.005

6.2.2 RAFT miniemulsion polymerizations of MeMBL

In Chapter 4, styrene was used as comonomer to improve the stability of the miniemulsions and gain control over the polymerization of MeMBL. The introduction of styrene also allows one to tune the glass transition temperature of the copolymer and increase its solubility in common solvents. However, one may prefer a homopolymer of MeMBL to the copolymer for certain applications because of the unique properties of poly(MeMBL), e.g. solvent resistance and an extremely high Tg above 200 ^oC.

RAFT miniemulsion homopolymerization of MeMBL can be a promising way to prepare well defined poly(MeMBL) and at the same time, avoid processing challenges such as heat transfer and polymer solubility. As mentioned in Chapter 4, the stability of a miniemulsion of MeMBL can be a significant concern in achieving the miniemulsion homopolymerization. Two tentative strategies are proposed here to improve the stability of miniemulsions of MeMBL.

1. Dissolve MeMBL in a nonreactive hydrophobic solvent and then prepare the miniemulsion. This strategy is similar to the use of styrene. The hydrophobic

solvent, however, doesn't react with MeMBL, therefore, a homopolymer of MeMBL will be produced.

2. Addition of a proper amount of poly(MeMBL) as a costabilizer to improve the stability of miniemulsions of MeMBL. As mentioned in Chapter1, poly(MeMBL) may also enhance the nucleation of MeMBL droplets. If most of the MeMBL droplets are nucleated fast enough before the miniemulsion loses its stability, a stable poly(MeMBL) can be produced.

Other than the miniemulsion stability issue, selection of a suitable RAFT agent is another challenge in RAFT miniemulsion homopolymerization of MeMBL. As mentioned in Chapter 4, PEPDTA has shown little control of the homopolymerization, therefore, the Z group of the suitable RAFT must be a group that is better than the phenyl group to promote the formation of the intermediate RAFT radicals.[79] Potential RAFT agents for homopolymerization of MeMBL are shown in Figure 6.1. However, these RAFT agents may result in an induction time in the homopolymerization of MeMBL. A compromise of the two factors, i.e. miniemulsion stability and control of the polymerization, must be achieved to prepare a stable, well-defined poly(MeMBL) latex.

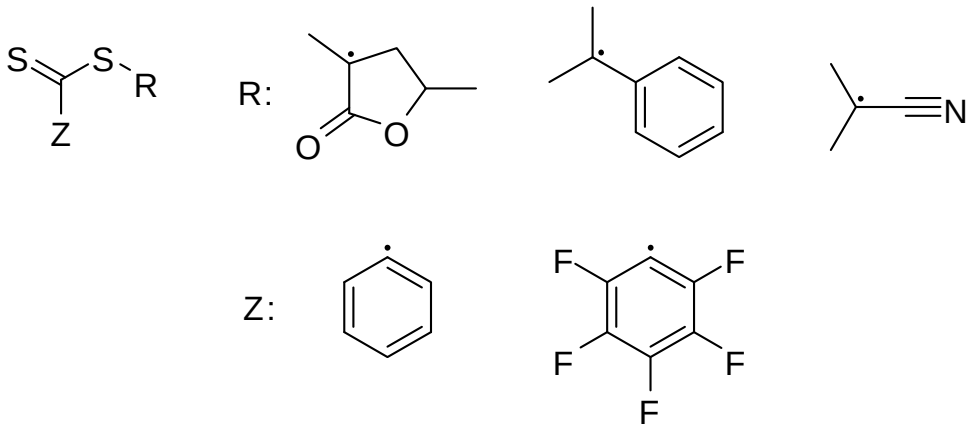

Figure 6.1 Potential RAFT agents for homopolymerization of MeMBL.

6.2.3 RAFT inverse miniemulsion polymerization

Chapter 5 has reported a detailed experimental investigation on the kinetics of RAFT inverse miniemulsion polymerization of acrylamide. A schematic mathematical modeling on the RAFT inverse miniemulsion polymerization needs to be developed since

it can help to further understand the mechanism and related phenomena such as the induction time in the polymerizations.

As mentioned in Chapter 5, the dominant radical source for particle nucleation comes from the small fraction of initiator dissolved in the continuous phase. The average number of radical per particle is significantly lower than 0.5. There is no rapid reentry and redesorption of monomeric radicals due to the barrel effect of the steric surfactant. Therefore, RAFT inverse miniemulsion polymerization of acrylamide can be approximated as a "0-1" (instantaneous termination) system, i.e. a poly(acrylamide) particles contain either one or no radical during the polymerization. Based on the RAFT polymerization mechanism (as shown in Figure 1.2), there are six kinds of particles in the system, as shown in Figure 6.2: (1) $N_{0,0}$, particles containing no radical; (2) $N_{1,0}^{m}$, particles containing only one monomeric radical; (3) $N_{1,0}^{p}$, particles containing only one polymeric radical; (4) $N_{0,1}^{m}$, particles containing one RAFT intermediate radical whose two arms are less than critical degree; (5) $N_{0,1}^{mp}$, particles containing one RAFT intermediate radical whose one arm is less than critical degree while the other is larger than critical degree; and (6) $N_{0,1}^{p}$, particles containing one RAFT intermediate radical whose two arms are larger than critical degree.

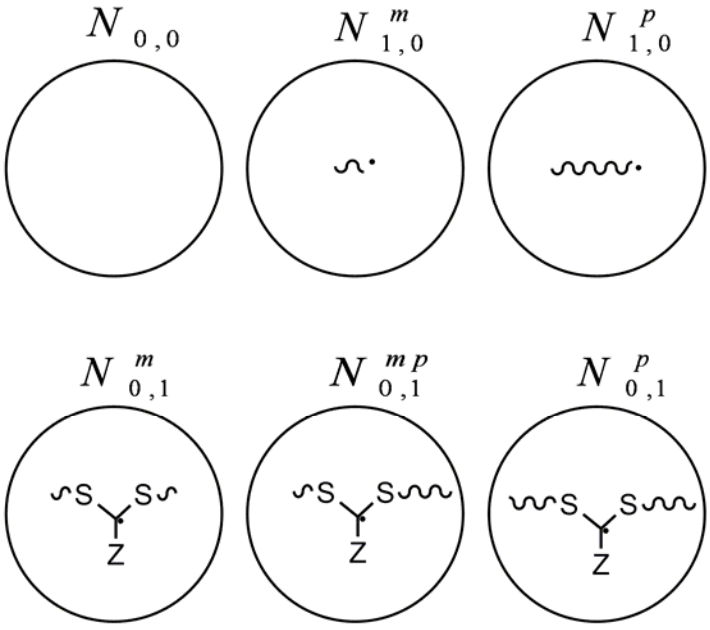

Figure 6.2 Different kinds of particles in the RAFT inverse miniemulsion polymerization of acrylamide.

A few of assumptions are required for the model:

1. Monomeric radicals are the only radical species within the particles that can desorb to the continuous phase;
2. Initiator-derived oligomeric radicals are irreversibly captured by the particles once their chain length is larger than the critical degree;
3. All RAFT intermediate radicals stay in the particles and undergo either fragmentation or termination, but no propagation.

From these assumptions, we can derive the following equations for "0-1" RAFT inverse miniemulsion polymerization systems:

$$\frac{dN_{0,0}}{dt} = \rho(N_{1,0}^{m} + N_{1,0}^{p} + N_{0,1}^{m} + N_{0,1}^{mp} + N_{0,1}^{p} - N_{0,0}) + k_f N_{1,0}^{m} \tag{6.1}$$

$$\begin{aligned}\frac{dN_{1,0}^{m}}{dt} &= \rho_{re} N_{0,0} - \rho N_{1,0}^{m} + k_{mf}[M]_p N_{1,0}^{p} + k_{frag}{}^{m} N_{0,1}^{m} + k_{frag}{}^{mp} N_{0,1}^{mp} \\ &- k_f N_{1,0}^{m} - k_p^{1}[M]_p N_{1,0}^{m} - k_{-add}[RAFT]_m N_{1,0}^{m} - k_{-add}[RAFT]_p N_{1,0}^{m}\end{aligned} \tag{6.2}$$

$$\begin{aligned}\frac{dN_{1,0}^{p}}{dt} &= \rho_I N_{0,0} + k_p^{1}[M]_p N_{1,0}^{m} + k_{-frag}{}^{mp} N_{0,1}^{mp} + k_{frag}{}^{p} N_{0,1}^{p} \\ &- \rho N_{1,0}^{p} - k_{mf}[M]_p N_{1,0}^{p} - k_{add}[RAFT]_m N_{1,0}^{p} - k_{add}[RAFT]_p N_{1,0}^{p}\end{aligned} \tag{6.3}$$

$$\frac{dN_{0,1}^{m}}{dt} = -\rho N_{0,1}^{m} + k_{-add}[RAFT]_m N_{1,0}^{m} - k_{frag}{}^{m} N_{0,1}^{m} \tag{6.4}$$

$$\begin{aligned}\frac{dN_{0,1}^{mp}}{dt} &= -\rho N_{0,1}^{mp} + k_{add}[RAFT]_m N_{1,0}^{p} + k_{-add}[RAFT]_p N_{1,0}^{m} \\ &-(k_{frag}{}^{mp} + k_{-frag}{}^{mp}) N_{0,1}^{mp}\end{aligned} \tag{6.5}$$

$$\frac{dN_{0,1}^{p}}{dt} = -\rho N_{0,1}^{p} + k_{add}[RAFT]_p N_{1,0}^{p} - k_{frag}{}^{p} N_{0,1}^{p} \tag{6.6}$$

$$\frac{d[RAFT]_p}{dt} = k_{frag}{}^{p} N_{0,1}^{p} + k_{frag}{}^{mp} N_{0,1}^{mp} - k_{-add}[RAFT]_p N_{1,0}^{m} - k_{add}[RAFT]_p N_{1,0}^{p} \tag{6.7}$$

$$\frac{d[RAFT]_m}{dt} = k_{frag}{}^m N_{0,1}^m + k_{-frag}{}^{mp} N_{0,1}^{mp} - k_{-add}[RAFT]_m N_{1,0}^m - k_{add}[RAFT]_m N_{1,0}^p \quad (6.8)$$

The above equations 6.1-6.8 describe the evolution of different types of particles in the RAFT inverse miniemulsion polymerization. From these equations, the average number of radical per particle $\bar{n}$ can be derived and related to the polymerization rate R_p:

$$\bar{n} = N_{1,0}^m + N_{1,0}^p \approx N_{1,0}^p \quad (6.9)$$

$$R_p = k_p[M]_p N_p \bar{n} / N_A \quad (6.10)$$

Therefore, the kinetics of RAFT inverse miniemulsion polymerization can be predicted quantitatively from equations 6.1-6.10. Currently, the modeling of the kinetics of RAFT inverse miniemulsion polymerization is under investigation.

The study in Chapter 5 focused on the kinetic aspects of RAFT inverse miniemulsion polymerizations. The practical applications of RAFT inverse miniemulsion polymerization in different fields, such as the synthesis of polymer-inorganic nanocomposites, are worth further study. As an example, the synthesis of ZnO-polymer nanocomposites by RAFT inverse miniemulsion polymerization is under investigation. The first step towards this aim has been achieved by using free-radical inverse miniemulsion polymerization. A typical recipe is shown in Table 6.2. The prepared stable composite latex is shown in Figure 6.2. The next step will use RAFT chemistry to control the properties of the polymer matrix and the morphology of the nanocomposite.

Table 6.2 Typical recipe for the synthesis of ZnO nanocomposite.

Component		Mass
Continuous phase	Dispersed phase[a]	(g)
B246		0.5
Cyclohexane		40.0
	H_2O	12
	Acrylamide	1.0
	VA-044	0.05
	$Zn(NO_3)_2$	0.10
	NH_4NO_3	0.30

[a] The pH of dispersed phase was adjusted to 10 by NaOH.

Figure 6.3 Stable ZnO/(polyacrylamide) nanocomposite latex prepared from the recipe in Table 6.2.

APPENDIX A

EFFECT OF RAFT AGENT ON THE STABILITY OF MINIEMULSION FEED*

The effect of RAFT agent on the stability of the miniemulsion feed (as discussed in Chapter 3) is evaluated here. It should be pointed out that the following derivation describes a different situation from the superswelling theory.[86] The situation here is from a purely physical process before the onset of oligomerization in the miniemulsion feed. The superswelling theory describes a situation after the oligomerization or polymerization when there is an uneven oligomerization in the RAFT miniemulsion. The RAFT oligomers are assumed to have interaction with the monomers in the superswelling theory.

As mentioned in the first chapter, a miniemulsion is a metastable emulsion of fine oil droplets dispersed in water. The droplets must be stabilized against coalescence by collisions and against Ostwald ripening by diffusion processes. Stabilization against coalescence can be achieved by adding appropriate surfactants, such as sodium dodecyl sulfate (SDS). Diffusional stabilization is achieved by adding a small quantity of a highly monomer-soluble and extremely hydrophobic costabilizer such as hexadecane. Since only a small amount of RAFT agent is utilized in controlled miniemulsion polymerization, which is partitioned in the monomer droplets and structurally different from surfactants, the addition of RAFT agent has very limited effects, if any, on changing the collision environment around the droplets. Therefore, we will focus on the Ostwald ripening process after introduction of RAFT agents. In the following, subscripts 1, 2, 3 refer to the monomer, RAFT agent and costabilizer respectively.

The following derivation is based on the Lifshitz-Slyozov-Wagner (LSW) theory.[240, 241] The main results of LSW theory are the following:

---

* Portions of this appendix have been published in *Langmuir*, 2006, 22, 9075-9078.

(1) During the ripening process, there exists a critical radius a_c in polydisperse droplets. Particles with a larger radius grow while smaller ones shrink. For those radius equals a_c, the radius of the particle does not change. a_c increases during the ripening process.

(2) The Ostwald ripening rate w is constant

$$w = \frac{d\bar{a}^{-3}}{dt} = \frac{8V_{mi}\sigma}{9RT} D_i C_i^{'} \tag{A.1}$$

(3) The particle radius distribution $P_\infty(u)$ is independent of time and the droplet sizes are scaled to a_c.

$$P_\infty(u) = P_\infty(\frac{a}{a_c}) = \frac{81eu^2 \exp[1/(2u/3-1)]}{\sqrt[3]{32}(u+3)^{\frac{7}{3}}(1.5-u)^{\frac{11}{3}}}, 0 \le \mu \le 1.5 \tag{A.2}$$

and $P_\infty(u) = 0, \mu > 1.5$

The derivation proposed here is based on the following assumptions:

(1) The surfactants will not interfere with the mass transfer of different species. The present of RAFT agent does not change the surface tension of the miniemulsions.

(2) The molar fraction of RAFT agent and costabilizer in a RAFT miniemulsion system is small. There is no reaction between RAFT agent and the monomer.

(3) The concentration of the dispersed phase is the same throughout the medium except the neighborhood of the droplet surfaces.

(4) The dispersed phase transport is by molecular diffusion from one droplet to the others, following the Fick's first law.

(5) The solubility of RAFT agent in water is comparable or less than that of the monomer.

The chemical potential of component *i* in one droplet of miniemulsion is

$$\mu_i^{drop} = \mu_i^{'} + \frac{2\sigma V_{mi}}{a} + RT \ln x_i \tag{A.3}$$

The chemical potential of component *i* in bulk is

$$\mu_i^{'} = \mu_i^0 + RT \ln C_i^{'} \tag{A.4}$$

When the droplets and the medium reach equilibrium, the chemical potential of composition i in the droplets should equal that close to the surface of the droplets.

$$\mu_i^{drop} = \mu_i^{surf} \tag{A.5}$$

The chemical potential of component *i* around the droplet surface can be written as

$$\mu_i^{surf} = \mu_i^0 + RT \ln C_i^{surf} \tag{A.6}$$

From the above equations,

$$C_i^{surf} = C_i^{'} \exp(\frac{\alpha_i}{a}) x_i \tag{A.7}$$

in which

$$\alpha_i = \frac{2\sigma V_{mi}}{RT}$$

From Fick's first law, the mass transfer rate

$$J_i = -4\pi a^2 D_i \left.\frac{\partial C_i}{\partial r}\right|_{r=a} = 4\pi a D_i (C_i - C_i^{surf}) \tag{A.8}$$

At every instant, there exists a critical radius a_c in the polydisperse distribution of droplet radius at which the flux of the droplets close to zero. For an arbitrary droplet, the mass flux of costabilizer is:

$$J_3 = 4\pi a D_3 C_3^{'} [x_{3,c} \exp(\frac{\alpha_3}{a_c}) - x_3 \exp(\frac{\alpha_3}{a})] \tag{A.9}$$

Since miniemulsions can be stable for a relatively long time, there should be a quasi-stationary state in which $J_1 \approx 0$ (J_2 and J_3 are therefore close to zero too since the monomer flux J_1 accounts for the main part of the total mass transfer), that is

$$C_1^{'} \exp(\frac{\alpha_1}{a_c})(1 - x_{2c} - x_{3c}) \approx C_1^{'} \exp(\frac{\alpha_1}{a})(1 - x_2 - x_3) \tag{A.10}$$

From the Equation (A10), considering that the molar fraction of RAFT agent and costabilizer in a RAFT miniemulsion system is typically quite small, by expanding the exponents in a Taylor series truncated at the second term, we have

$$x_{2c} - x_2 + x_{3c} - x_3 = \frac{\alpha_1}{a_c} - \frac{\alpha_1}{a} \tag{A.11}$$

Two observations have been made in previous reports of RAFT miniemulsions: [2, 83, 159, 197]

(1) The stability of RAFT miniemulsions was found to be reduced to some extent compared with those without RAFT; however, the stability was still quite good in these situations. There is no obvious phase separation or cream except a thin layer of oil at the vortex over a long storage times.

(2) The molecular weight distribution (PDI) of the polymer product is very narrow. The particle size distribution (PSD) of the final polymer latex is also quite narrow though slightly broader than the free-radical miniemulsion protocol. The living non-growing chains in RAFT miniemulsion polymerization only accounts for a very small part of the total polymer produced.[2]

The above phenomena indicate that the relative concentration change of the components in RAFT miniemulsion droplets is relatively small for most cases. Therefore, the ratio of the component fluxes is assumed to be approximately equal to the volume fractions ϕ_i of the components in the droplets though it is a multivariable function of volume fractions, diffusion coefficient and solubility of the components:

$$J_1 / J_2 / J_3 = \phi_1 / \phi_2 / \phi_3 \tag{A.12}$$

This leads to:

$$J_1 + J_2 + J_3 = -\frac{dV^{droplet}}{dt} = 4\pi\alpha_1 a\left(\frac{\phi_2}{D_2 C_2^{'}} + \frac{\phi_3}{D_3 C_3^{'}}\right)^{-1}\left(\frac{1}{a_c} - \frac{1}{a}\right) \tag{A.13}$$

Note that Equation (A.13) has a form similar to that of one-component particle evolution equation described decades before by Lifshitz, et al.[240] From LSW theory, the rate of droplet growth should be:

$$w_1 = \frac{d\bar{a}^3}{dt} = \frac{8V_{m1}\sigma}{9RT}\left(\frac{\phi_2}{D_2 C_2^{'}} + \frac{\phi_3}{D_3 C_3^{'}}\right)^{-1} \tag{A.14}$$

The one-component droplet system without costabilizer and RAFT agent should be:

$$w = \frac{d\bar{a}^{3}}{dt} = \frac{8V_{m1}\sigma}{9RT} D_1 C_1^{'} \tag{A.15}$$

A retardation factor F, defined as the droplet growth rate ratio of a miniemulsion and an emulsion, could evaluate the relative stability of a miniemulsion system.

So the retardation factor F for miniemulsions with both RAFT agent and costabilizer is:

$$F_{2,3} = \frac{w}{w_1} = D_1 C_1^{'} \left(\frac{\phi_2}{D_2 C_2^{'}} + \frac{\phi_3}{D_3 C_3^{'}} \right) \tag{A.16}$$

and the retardation factor F for a miniemulsion system having only costabilizer is:

$$F_3 = \frac{w}{w_1^{'}} = D_1 C_1^{'} \frac{\phi_3^{'}}{D_3 C_3^{'}} \tag{A.17}$$

The effect of RAFT agent can be evaluated by a factor R

$$R = \frac{F_{2,3}}{F_3} = \left(\frac{\phi_2}{D_2 C_2^{'}} + \frac{\phi_3}{D_3 C_3^{'}} \right) / \frac{\phi_3^{'}}{D_3 C_3^{'}} \tag{A.18}$$

Unfortunately, there is no experimental report of diffusion coefficient of RAFT agents so far. Since the diffusion coefficient is around 0.5×10^{-9} to 2×10^{-9} m^2/s for a wide range of systems, for simplification, by assuming $D_2 \approx D_3$ the above equation can be simplified as

$$R = \left(\phi_2 \frac{C_3^{'}}{C_2^{'}} + \phi_3 \right) / \phi_3^{'} \tag{A.19}$$

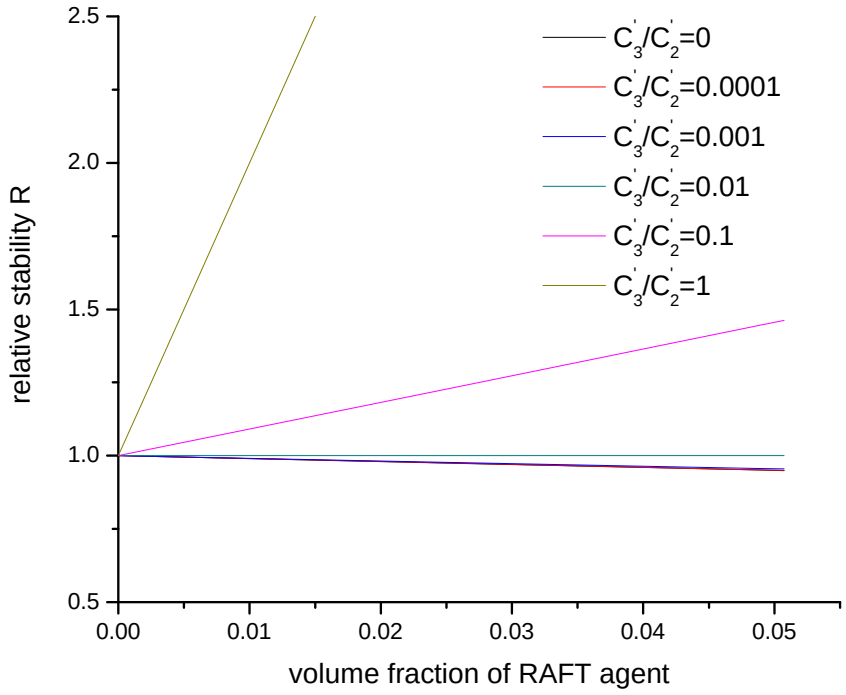

Figure A.1. Relative stability comparison R of the miniemulsion containing RAFT agent with the miniemulsion without RAFT agent. Assuming that the volume of monomer equals 100, and costabilizer equals 1.

Figure A.1 shows the effect of RAFT agent on the stability of miniemulsions. With higher hydrophilicity of the RAFT agent, the miniemulsions tend to be less stable. It is noteworthy that there is a low boundary when $C_3^{'}/C_2^{'}=0$, that is, when the costabilizer has zero solubility. However, when the hydrophobicity of the RAFT agent is comparable to that of the costabilizer, the miniemulsions are even more stable than conventional miniemulsions. To understand the above result, RAFT agent can be considered to be a special costabilizer, but not of the same stabilizing effectiveness as costabilizers such as hexadecane. On one hand, RAFT agent improves the stability of miniemulsions as when its solubility is comparable to hexadecane; on the other hand, when the RAFT agent is more hydrophilic than the costabilizer, it dilutes the costabilizer, making the miniemulsion less stable and contributing to oil phase separation. Considering

that typically the solubility of RAFT is much higher than that of hexadecane, the stability of miniemulsions with RAFT should be close to the lower boundary $C_3^{'}/C_2^{'}=0$.

There are some supplementary explanations that need to be made for the derivation:

(1) It is worthy of pointing out here that even after introducing RAFT agents, the critical radius $a_c=\bar{a}$, which is similar to the conventional emulsions. [242] This relationship can be derived easily from the mass conservation. For N droplets,

$$\sum_i^N (J_1+J_2+J_3)_{dropleti}=\sum_i^N [4\pi\alpha_1(\frac{\phi_2}{D_2C_2^{'}}+\frac{\phi_3}{D_3C_3^{'}})^{-1}(\frac{1}{a_c}-\frac{1}{a})]_{dropleti}=0 \quad \text{(A.20)}$$

Thus

$$a_c=\frac{1}{N}\sum_i^N a=\bar{a} \quad \text{(A.21)}$$

(2) The derivation is not limited to miniemulsions with RAFT agents. Actually it can be applied to evaluate the stability of miniemulsions with any small amount of controlled agents similar to RAFT agents, such as, many controlled agents utilized in ATRP. [243]

(3) Although the assumption that the ratio of the component fluxes is approximately equal to the volume fractions of the components in the droplets works well for most of RAFT miniemulsion systems previously reported; there maybe few cases the assumption does not apply under certain conditions. For example, when the RAFT agent is extremely hydrophilic or there is a significant different diffusion behavior between RAFT agent and the other components in the droplets. In these cases, RAFT agent will redistribute in the droplets due to Oswald ripening and cause an unevenly distribution of RAFT concentration in the droplets. The high concentration of RAFT in certain droplets could favor the retard the following polymerization process in these droplets which leads to a much broader PDI in the final latex.[134, 146, 244, 245]

REFERENCES

1. Smulders, W., C. Jones, and F. Schork, *Macromolecules*, **2004**, 37(25), 9345-9354.

2. Smulders, W.W., C.W. Jones, and F.J. Schork, *AIChE J.*, **2005**, 51(3), 1009-1021.

3. Lovell, P.A. and M.S. El Aasser, *Emulsion Polymerization and Emulsion Polymers*. 1997, Chichester: Wiley.

4. Chow, P.Y. and L.M. Gan, *Microemulsion polymerizations and reactions*, in *Polymer Particles*. 2005, Springer-Verlag Berlin: Berlin. p. 257-298.

5. Chou, Y.J., M.S. El-Aasser, and J.W. Vanderhoff, *J. Disper. Sci. Technol.*, **1980**, 1(2), 129-150.

6. Chamberlain, B., D. Napper, and R. Gilbert, *J. Chem. Soc., Faraday Trans.*, **1982**, 78, 591.

7. Barnette, D.T. and F.J. Schork, *Chem. Eng. Comm.*, **1989**, 80, 113-125.

8. Choi, Y., et al., *J. Polym. Sci., Part A: Polym. Chem.*, **1985**, 23(12), 2973-2987.

9. Mouran, D., J. Reimers, and F.J. Schork, *J. Polym. Sci., Part A: Polym. Chem.*, **1996**, 34(6), 1073-1081.

10. Reimers, J. and F.J. Schork, *Polym. React. Eng.* , **1996**, 4(2-3), 135-152.

11. Reimers, J.L. and F.J. Schork, *J. Appl. Polym. Sci.*, **1996**, 59(12), 1833-1841.

12. Ostwald, W., *Z.Phys.Chem.*, **1901**, 37, 385.

13. Gilbert, R.G., *Emulsion Polymerization: A Mechanistic Approach*. 1995, London: Academic.

14. Priest, W.J., *J. Phys. Chem.*, **1952**, 56(9), 1077-1082.

15. Jansson, L., *test*. 1983, L. Jansson , Masters Thesis, Georgia Institute of Technology, 1983.: Atlanta.

16. Smith, W.V. and R.H. Ewart, *J. Chem. Phys.*, **1948**, 16, 592-599.

17. Caruso, F., ed. *colloids and colloidal assemblies*. 2004, Wiley: Weinheim.

18. Ugelstad, J., M.S. Elaasser, and Vanderho.Jw, *J. Polym. Sci., Part C: Polym. Lett.*, **1973**, 11(8), 503-513.

19. Ugelstad, J., F.K. Hansen, and S. Lange, *Makromol. Chem.*, **1974**, 175(2), 507-521.

20. Hansen, F.K. and J. Ugelstad, *J. Polym. Sci., Part A: Polym. Chem.*, **1979**, 17(10), 3069-3082.

21. Azad, A.R.M., et al., *Acs Symposium Series*, **1976**(24), 1-23.

22. Boyd, J.V., et al., *Theory and Practice of Emulsion Technology*. 1976, London: Academic.

23. Miller, C.M., et al., *J. Polym. Sci., Part A: Polym. Chem.*, **1994**, 32(12), 2365-2376.

24. Miller, C.M., et al., *J. Polym. Sci., Part A: Polym. Chem.* , **1995**, 33(8), 1391-1408.

25. Miller, C.M., et al., *Macromolecules*, **1995**, 28(8), 2772-2780.

26. Miller, C.M., et al., *Macromolecules*, **1995**, 28(8), 2765-2771.

27. Blythe, P.J., et al., *Langmuir*, **2000**, 16(3), 898-904.

28. Blythe, P.J., et al., *Macromolecules*, **1999**, 32(21), 6944-6951.

29. Blythe, P.J., et al., *Macromolecules*, **1999**, 32(21), 6952-6957.

30. Blythe, P.J., et al., *Macromolecules*, **1999**, 32(13), 4225-4231.

31. Delgado, J., M.S. Elaasser, and J.W. Vanderhoff, *J. Polym. Sci., Part A: Polym. Chem.*, **1986**, 24(5), 861-874.

32. Delgado, J., et al., *J. Polym. Sci., Part B: Polym. Phys.*, **1988**, 26(7), 1495-1517.

33. Delgado, J., et al., *J. Polym. Sci., Part A: Polym. Chem.*, **1989**, 27(1), 193-202.

34. Delgado, J., et al., *J. Polym. Sci., Part A: Polym. Chem.*, **1990**, 28(4), 777-794.

35. Chern, C.S. and J.C. Sheu, *J. Polym. Sci., Part A: Polym. Chem.*, **2000**, 38(17), 3188-3199.

36. Chern, C.S. and J.C. Sheu, *Polymer*, **2001**, 42(6), 2349-2357.

37. Barnette, D.T. and F.J. Schork, *Chem. Eng. Prog.*, **1987**, 83(6), 25-30.

38. Samer, C. and F. Schork, *Ind. Eng. Chem. Res.*, **1999**, 38(5), 1792-1800.

39. Samer, C.J. and F.J. Schork, *Polym. React. Eng.*, **1997**, 5(3), 85-124.

40. Durant, Y.G., *Abstracts of Papers of the American Chemical Society*, **1999**, 217, U484-U484.

41. Ouzineb, K., C. Graillat, and T. McKenna, *J. Appl. Polym. Sci.*, **2004**, 91(4), 2195-2207.

42. Kobayashi, S., S. Shoda, and H. Uyama, *Enzymatic polymerization and oligomerization*, in *Polymer Synthesis/Polymer Engineering*. 1995, Springer-Verlag Berlin: Berlin 33. p. 1-30.

43. Wang, Y.F., et al., *J. Am. Chem. Soc.*, **1988**, 110(21), 7200-7205.

44. Okumura, S., M. Iwai, and Y. Tominaga, *Agric. Bio. Chem.*, **1984**, 48(11), 2805-2808.

45. Wallace, J.S. and C.J. Morrow, *J. Polym. Sci., Part A: Polym. Chem.*, **1989**, 27(10), 3271-3284.

46. Gross, R.A., A. Kumar, and B. Kalra, *Chem. Rev.* , **2001**, 101(7), 2097-2124.

47. Gross, R.A. and B. Kalra, *Science*, **2002**, 297(5582), 803-807.

48. Al-Azemi, T.F., L. Kondaveti, and K.S. Bisht, *Macromolecules*, **2002**, 35(9), 3380-3386.

49. Kobayashi, S., H. Uyama, and M. Ohmae, *Bull. Chem. Soc. Jpn.*, **2001**, 74(4), 613-635.

50. Kobayashi, S., *J. Polym. Sci., Part A: Polym. Chem.*, **1999**, 37(16), 3041-3056.

51. Stryer, L., *Biochemistry*. 1995, New York: W.H. Freeman and Company.

52. Reihmann, M. and H. Ritter, *Synthesis of phenol polymers using peroxidases*, in *Enzyme-Catalyzed Synthesis of Polymers*. 2006, Springer-Verlag Berlin: Berlin. p. 1-49.

53. Blinkovsky, A.M. and J.S. Dordick, *J. Polym. Sci., Part A: Polym. Chem.* , **1993**, 31(7), 1839-1846.

54. Yaropolov, A.I., et al., *Appl. Biochem. Biotechnol.*, **1994**, 49(3), 257-280.

55. Kobayashi, S., et al., *Macromol. Chem. Phys.* , **1998**, 199(5), 777-782.

56. Tonami, H., et al., *Macromol. Chem. Phys.* , **1999**, 200(10), 2365-2371.

57. Ichinohe, D., et al., *J. Polym. Sci., Part A: Polym. Chem.* , **1998**, 36(14), 2593-2600.

58. Singh, A. and D.L. Kaplan, *J. Polym. Environ.* , **2002**, 10(3), 85-91.

59. Kalra, B. and R.A. Gross, *Biomacromolecules*, **2000**, 1(3), 501-505.

60. Kobayashi, S., H. Uyama, and S. Kimura, *Chem. Rev.*, **2001**, 101(12), 3793-3818.

61. Jerome, C. and P. Lecomte, *Adv. Drug Delivery Rev.* , **2008**, 60(9), 1056-1076.

62. Albertsson, A.C. and R.K. Srivastava, *Adv. Drug Delivery Rev.* , **2008**, 60(9), 1077-1093.

63. Uyama, H. and S. Kobayashi, *Enzymatic synthesis of polyesters via polycondensation*, in *Enzyme-Catalyzed Synthesis of Polymers*. 2006, Springer-Verlag Berlin: Berlin. p. 133-158.

64. Matsumura, S., *Enzymatic synthesis of polyesters via ring-opening polymerization*, in *Enzyme-Catalyzed Synthesis of Polymers*. 2006, Springer-Verlag Berlin: Berlin. p. 95-132.

65. Taden, A., M. Antonietti, and K. Landfester, *Macromol. Rapid Commun.* , **2003**, 24(8), 512-516.

66. Szwarc, M., *Nature*, **1956**, 178(4543), 1168-1169.

67. Szwarc, M., M. Levy, and R. Milkovich, *J. Am. Chem. Soc.*, **1956**, 78(11), 2656-2657.

68. Solomon, D.H., E. Rizzardo, and P. Cacioli, 1986, U.S. 4581429

69. Georges, M.K., et al., *Polym. Mater. Sci. Eng.*, **1993**, 69, 305.

70. Wang, J. and K. Matyjaszewski, *J. Am. Chem. Soc.*, **1995**, 117(20), 5614-5615.

71. Chiefari, J., et al., *Macromolecules*, **1998**, 31(16), 5559-5562.

72. Chong, Y.K., et al., *Macromolecules*, **1999**, 32(6), 2071-2074.

73. Hutson, L., et al., *Macromoleculs*, **2004**, 37(12), 4441-4452.

74. Meijs, G.F., E. Rizzardo, and S.H. Thang, *Polym. Bull.*, **1990**, 24(5), 501-505.

75. Rizzardo, E., G.F. Meijs, and S.H. Thang, 1988, EP0333758

76. Meijs, G.F., et al., *Macromoleculs*, **1991**, 24(12), 3689-3695.

77. Le, T.P.T., et al., 1998, PCT Int. Appl. WO 9801478

78. Corpart, P., et al., 1998, WO 9858974

79. Chiefari, J., et al., *Macromolecules*, **2003**, 36(7), 2273-2283.

80. Chong, Y., et al., *Macromolecules*, **2003**, 36(7), 2256-2272.

81. Kwak, Y., A. Goto, and T. Fukuda, *Macromolecules*, **2004**, 37(4), 1219-1225.

82. Chernikova, E., et al., *Macromolecules*, **2004**, 37(17), 6329-6339.

83. de Brouwer, H., et al., *Macromolecules*, **2000**, 33(25), 9239-9246.

84. Lansalot, M., T.P. Davis, and J.P.A. Heuts, *Macromolecules*, **2002**, 35(20), 7582-7591.

85. Vosloo, J.J., et al., *Macromolecules*, **2002**, 35(13), 4894-4902.

86. Luo, Y., J. Tsavalas, and F.J. Schork, *Macromolecules*, **2001**, 34(16), 5501-5507.

87. Luo, Y., et al., *Macromolecules*, **2006**, 39(4), 1328-1337.

88. Luo, Y.W., et al., *J. Polym. Sci., Part A: Polym. Chem.* , **2007**, 45(11), 2304-2315.

89. Luo, Y.W. and X.Z. Liu, *J. Polym. Sci., Part A: Polym. Chem.* , **2004**, 42(24), 6248-6258.

90. Yang, L., Y. Luo, and B. Li, *J Polym Sci Pol Chem*, **2006**, 44(7), 2293-2306.

91. Zhang, F., et al., *J. Polym. Sci., Part A: Polym. Chem.* , **2005**, 43(13), 2931-2940.

92. Bowes, A., J.B. McLeary, and R.D. Sanderson, *J. Polym. Sci., Part A: Polym. Chem.* , **2007**, 45(4), 588-604.

93. Bussels, R., et al., *J. Polym. Sci., Part A: Polym. Chem.* , **2006**, 44(21), 6419-6434.

94. Mcleary, J.B., et al., *J. Polym. Sci., Part A: Polym. Chem.* , **2004**, 42(4), 960-974.

95. Matahwa, H., J.B. McLeary, and R.D. Sanderson, *J. Polym. Sci., Part A: Polym. Chem.* , **2006**, 44(1), 427-442.

96. Schork, F.J. and W. Smulders, *J. Appl. Polym. Sci.*, **2004**, 92(1), 539-542.

97. Russum, J.P., C.W. Jones, and F.J. Schork, *Macromol. Rapid Commun.*, **2004**, 25(11), 1064-1068.

98. Russum, J.P., C.W. Jones, and F.J. Schork, *Ind. Eng. Chem. Res.*, **2005**, 44(8), 2484-2493.

99. Russum, J.P., C.W. Jones, and F.J. Schork, *AIChE J.*, **2006**, 52(4), 1566-1576.

100. Vanderhoff, J.W., *Polymerization and Polycondensation Processes* ACS Advances in Chemistry Series. 1962, Washington: ACS.

101. Graillat, C., et al., *J. Polym. Sci., Part A: Polym. Chem.*, **1986**, 24(3), 427-449.

102. Landfester, K., M. Willert, and M. Antonietti, *Macromolecules*, **2000**, 33(7), 2370-2376.

103. Willert, M. and K. Landfester, *Macromol. Chem. Phys.*, **2002**, 203(5-6), 825-836.

104. Wang, Y.J., et al., *Polym. Int.* , **2001**, 50, 326-330.

105. Capek, I., *Des. Monomers Polym.*, **2003**, 6(4), 399-409.

106. Kobayashi, S., S.-i. Shoda, and K. Kashiwa. *Enzymatic polymerization. The first in vitro synthesis of cellulose via non-biosynthetic path catalysed by cellulase*. 1991. Atlanta, GA, USA: Publ by ACS, Washington, DC, USA.

107. Dordick, J.S., M.A. Marletta, and A.M. Klibanov, *Biotechnology and Bioengineering*, **1987**, 30(1), 31-36.

108. Kobayashi, S., et al., *Macromolecules*, **1992**, 25(12), 3237-3241.

109. MacDonald, R.T., et al., *Macromolecules*, **1995**, 28(1), 73-78.

110. Henderson, L.A., et al., *Macromolecules*, **1996**, 29(24), 7759-7766.

111. Knani, D., A.L. Gutman, and D.H. Kohn, *J. Polym. Sci., Part A: Polym. Chem.*, **1993**, 31(5), 1221-1232.

112. Knani, D. and D.H. Kohn, *J. Polym. Sci., Part A: Polym. Chem.*, **1993**, 31(12), 2887-2897.

113. Uyama, H., et al., *Chem. Lett.* , **1994**, 3, 423-426.

114. Akkara, J.A., K.J. Senecal, and D.L. Kaplan, *J. Polym. Sci., Part A: Polym. Chem.*, **1991**, 29(11), 1561-1574.

115. Akkara, J.A., P. Salapu, and D.L. Kaplan. *Polyaniline synthesized by enzyme-catalyzed reactions in organic solvents*. 1992. San Francisco, CA, USA: Publ by ACS, Washington, DC, USA.

116. Liu, W., et al., *J. Am. Chem. Soc.*, **1999**, 121(1), 71-78.

117. Samuelson, L.A., et al., *Macromolecules*, **1998**, 31(13), 4376-4378.

118. Singh, A., D. Ma, and D.L. Kaplan, *Biomacromolecules*, **2000**, 1(4), 592-596.

119. Shan, J., Y. Kitamura, and H. Yoshizawa, *Colloid. Polym. Sci.*, **2005**, 284(1), 108-111.

120. Derango, R.A., et al., *Biotechnol. Tech.* , **1992**, 6(6), 523-526.

121. Durand, A., et al., *Polymer*, **2001**, 42(13), 5515-5521.

122. Kalra, B. and R.A. Gross. *HRP-mediated polymerization of acrylamide and sodium acrylate*. 2000. Washington, DC, USA: American Chemical Society, Washington, DC, USA.

123. Lalot, T., M. Brigodiot, and E. Marechal, *Polym. Int.* , **1999**, 48(4), 288-292.

124. Tsujimoto, T., H. Uyama, and S. Kobayashi, *Macromol. Biosci.* , **2001**, 1(6), 228-232.

125. Durand, A., et al., *Polymer*, **2000**, 41(23), 8183-8192.

126. Uyama, H., et al., *Macromolecules*, **1998**, 31(2), 554-556.

127. Andrews, L.J. and R.M. Keefer, *J. Am. Chem. Soc.*, **1950**, 72(11), 5034-5037.

128. Nicell, J.A., et al., *Can. J. Civ. Eng.*, **1993**, 20(5), 725-735.

129. Enright, T.E., M.F. Cunningham, and B. Keoshkerian, *Macromol. Rapid Commun.*, **2005**, 26(4), 221-225.

130. Shen, Y.Q., S.P. Zhu, and R. Pelton, *Macromol. Rapid Commun.*, **2000**, 21(14), 956-959.

131. Shen, Y.Q. and S.P. Zhu, *AIChE J.*, **2002**, 48(11), 2609-2619.

132. Tsavalas, J., et al., *Macromolecules*, **2001**, 34(12), 3938-3946.

133. Quinn, J.F., E. Rizzardo, and T.P. Davis, *Chem. Commun.*, **2001**(11), 1044-1045.

134. McLeary, J.B., et al., *Macromolecules*, **2004**, 37, 2383-2394.

135. Schork, F., et al., *Colloids Surf., A* **1999**, 153(1-3), 39-45.

136. Fang, S.J., W. Xue, and M. Nomura, *Polym. React. Eng.* , **2003**, 11(4), 815-827.

137. Aizpurua, I. and M.J. Barandiaran, *Polymer*, **1999**, 40(14), 4105-4115.

138. Thomas, D.B., et al., *Macromolecules*, **2003**, 36(5), 1436-1439.

139. Thomas, D.B., et al., *Macromolecules*, **2004**, 37(5), 1735-1741.

140. Levesque, G., et al., *Biomacromolecules*, **2000**, 1(3), 400-406.

141. Baussard, J., et al., *Polymer*, **2004**, 45(11), 3615-3626.

142. Mertoglu, M., et al., *Macromolecules*, **2005**, 38(9), 3601-3614.

143. Monteiro, M.J. and H. de Brouwer, *Macromolecules*, **2001**, 34(3), 349-352.

144. Kwak, Y., et al., *Macromolecules*, **2002**, 35(8), 3026-3029.

145. Perrier, S., et al., *Macromolecules*, **2002**, 35(22), 8300-8306.

146. Calitz, F.M., et al., *Macromolecules*, **2003**, 36(26), 9687-9690.

147. Mayadunne, R.T.A., et al., *Macromolecules*, **2000**, 33(2), 243-245.

148. Plummer, R., et al., *Macromolecules*, **2005**, 38(12), 5352-5355.

149. Hasan, S.M., *J. Polym. Sci., Part A: Polym. Chem.*, **1982**, 20(10), 2969-2978.

150. Mitsukami, Y., et al., *Macromolecules*, **2001**, 34(7), 2248-2256.

151. Cunningham, M.F., *Prog Polym Sci*, **2002**, 27(6), 1039-1067.

152. Biasutti, J.D., et al., *J. Polym. Sci., Part A: Polym. Chem.*, **2005**, 43(10), 2001-2012.

153. Nguyen, J. and C. Jones, *Abstracts of Papers of the American Chemical Society*, **2004**, 227, U420-U420.

154. Monteiro, M.J. and J. de Barbeyrac, *Macromolecules*, **2001**, 34(13), 4416-4423.

155. Smulders, W. and M.J. Monteiro, *Macromolecules*, **2004**, 37(12), 4474-4483.

156. Butte, A., G. Storti, and M. Morbidelli, *Macromolecules*, **2000**, 33(9), 3485-3487.

157. Qi, G., C.W. Jones, and J.F. Schork, *Ind. Eng. Chem. Res.*, **2006**, 45(21), 7084-7089.

158. Qi, G.G., C.W. Jones, and F.J. Schork, *Macromol. Rapid Commun.*, **2007**, 28(9), 1010-1016.

159. Russum, J.P., et al., *J. Polym. Sci., Part A: Polym. Chem.* , **2005**, 43(10), 2188-2193.

160. Hoffmann, H.M.R. and J. Rabe, *Angew. Chem. Int. Ed. Engl.*, **1985**, 24(2), 94-110.

161. Grieco, P.A., *Synthesis-Stuttgart*, **1975**(2), 67-82.

162. Manzer, L.E., *Appl. Catal., A* **2004**, 272(1-2), 249-256.

163. Stansbury, J.W. and J.M. Antonucci, *Dent. Mater.*, **1992**, 8(4), 270-273.

164. Park, B.K., et al., *J. Antibiot.*, **1988**, 41(6), 751-758.

165. Akkapeddi, M.K., *Macromolecules*, **1979**, 12(4), 546-551.

166. Pittman, C.U. and H. Lee, *J. Polym. Sci., Part A: Polym. Chem.*, **2003**, 41(12), 1759-1777.

167. Trumbo, D.L., *Polym. Bull.*, **1991**, 26(3), 271-275.

168. Akkapeddi, M.K., *Polymer*, **1979**, 20(10), 1215-1216.

169. Lee, C. and H.K. Hall, *Macromolecules*, **1989**, 22(1), 21-25.

170. Koinuma, H., K. Sato, and H. Hirai, *Makromol. Chem. Rapid*, **1982**, 3(5), 311-315.

171. Brandenburg, C., et al., 2003, U.S. Patent 20030130414

172. Brandenburg, C.J., 2003, WO 2003048220

173. Brandenburg, C., L. Manzer, and P. Subramanian, 2005, WO 2005028529

174. Okumura, A., et al., 1997, JP 09236715

175. Okimoto, Y. and H. Hatakeyama, 2007, JP 2007154072

176. Schwind, H., et al., 1996, DE 19501182

177. Lemonidou, A.A., et al., *Appl. Catal., A*, **2004**, 272(1-2), 241-248.

178. Suenaga, J., D.M. Sutherlin, and J.K. Stille, *Macromolecules*, **1984**, 17(12), 2913-2916.

179. Brandenburg, C.J., 2004, US Patent 20040230019

180. Schork, F., et al., *Polym. Particles*, **2005**, 175, 129-255.

181. Landfester, K. and M. Antonietti, *Macromol. Rapid Commun.*, **2000**, 21(12), 820-824.

182. Qi, G.G., et al., *J. Polym. Sci., Part A: Polym. Chem.*, **2008**, 46(17), 5929-5944.

183. *Miniemulsion homopolymerizations of MeMBL were prepared in a typical manner. However, analysis of the resulting polymerization suggested strongly that primarily homogeneous nucleation occurred, rather than droplet nucleation that would be expected for a true miniemulsion. For such polymerizations, we describe them as "miniemulsions" using quotations, to denote the difference from our later copolymerization studies with styrene, where the droplet nucleation appears to play a more significant role.*

184. Wu, X.Q. and F.J. Schork, *J. Appl. Polym. Sci.*, **2001**, 81(7), 1691-1699.

185. Fitch, R.M., M.B. Prenosil, and K.J. Sprick, *J. Polym. Sci. Polym. Symp.* , **1969**(27), 95-118.

186. Arai, M., K. Arai, and S. Saito, *J. Polym. Sci., Part A: Polym. Chem.*, **1979**, 17(11), 3655-3665.

187. Cox, R.A., et al., *J. Polym. Sci., Part A: Polym. Chem.*, **1977**, 15(10), 2311-2319.

188. Song, Z.Q. and G.W. Poehlein, *J. Colloid Interface Sci.* , **1989**, 128(2), 501-510.

189. Chen, C.Y. and I. Piirma, *J. Polym. Sci., Part A: Polym. Chem.*, **1980**, 18(6), 1979-1993.

190. Song, Z.Q. and G.W. Poehlein, *J. Polym. Sci., Part A: Polym. Chem.*, **1990**, 28(9), 2359-2392.

191. Munro, D., et al., *J. Colloid Interface Sci.* , **1979**, 68(1), 1-13.

192. Qi, G. and F.J. Schork, *Langmuir*, **2006**, 22(22), 9075-9078.

193. Tsavalas, J.G., et al., *Macromolecules*, **2001**, 34(12), 3938-3946.

194. Prescott, S.W., et al., *Macromolecules*, **2002**, 35(14), 5417-5425.

195. Zhou, G.C. and Harruna, II, *Anal. Chem.*, **2007**, 79(7), 2722-2727.

196. Geelen, P. and B. Klumperman, *Macromolecules*, **2007**, 40(11), 3914-3920.

197. Butte, A., G. Storti, and M. Morbidelli, *Macromolecules*, **2001**, 34(17), 5885-5896.

198. Nomura, M., H. Tobita, and K. Suzuki, eds. *Polymeric microspheres science and technology*. 2007, Kyoto university press: Kyoto. P189.

199. Kelen, T. and F. Tudos, *J. Macromol. Sci. Part A Pure Appl. Chem.*, **1975**, A 9(1), 1-27.

200. Fineman, M. and S.D. Ross, *J. Polym. Sci.*, **1950**, 5(2), 259-262.

201. Mahdavian, A.R., et al., *J. Appl. Polym. Sci.*, **2006**, 101(3), 2062-2069.

202. Moad, G. and D.H. Solomon, *Chemistry of Radical Polymerization*. 2nd ed. 2006, Oxford: Elsevier.

203. Lewis, F.M., et al., *J. Am. Chem. Soc.*, **1948**, 70(4), 1519-1523.

204. Wada, T., H. Sekiya, and S. Machi, *J. Appl. Polym. Sci.* , **1976**, 20(12), 3233-3240.

205. Virk, P.S., *J. Fluid Mech.* , **1971**, 45, 225-46.

206. Enright, D.P. and A.C. Perricone, *Petrol. Eng. Int.*, **1988**, 60(4), 55-56.

207. Date, J.L. and J.M. Shute, *Tappi*, **1959**, 42(10), 824-826.

208. Buck, S., et al., *Biomacromolecules*, **2004**, 5(6), 2230-2237.

209. Singh, B., et al., *Carbohydr. Polym.* , **2007**, 67(2), 190-200.

210. Chaw, C.-S., et al., *Biomaterials*, **2004**, 25(18), 4297-4308.

211. Wang, R., C.L. McCormick, and A.B. Lowe, *Macromolecules*, **2005**, 38(23), 9518-9525.

212. Wu, C., *Handbook of Size Exclusion Chromatography and Related Techniques*. 2004: Marcel Dekker.

213. Albertin, L., et al., *Macromolecules*, **2004**, 37(20), 7530-7537.

214. Albertin, L., et al., *Polymer*, **2006**, 47(4), 1011-1019.

215. *Inverse miniemulsions are very difficult to completely free of dissolved oxygen compared to conventional miniemulsions, as oxygen must be transferred from the aqueous droplets across an organic phase in which it has very low solubility.*

216. Baade, W. and K.H. Reichert, *Eur. Polym. J.* , **1984**, 20(5), 505-512.

217. Kurenkov, V.F. and V.A. Myagchenkov, *Polym.-Plast. Technol.*, **1991**, 30(4), 367-404.

218. *We describe the polymerizations here that appear as a typical 'living/controlled' RAFT polymerization at low conversion but that deviate from the theoretical line at high conversion while (i) maintaining RAFT groups associated with most if not all polymer chains, where (ii) those chains can be extended, as 'pseudo-living'.*

219. Thomas, D.B., et al., *Macromolecules*, **2004**, 37(24), 8941-8950.

220. *One narrow distributed poly(acrylamide) GPC standard (Mw=15000, Mn=12800) was used to estimate the error due to the calibration method. The universal calibration method gives Mw=18357 and Mn=14081, an error about 22% higher than the true molecular weight of the GPC standard.*

221. Prescott, S.W., et al., *Macromolecules*, **2005**, 38(11), 4901-4912.

222. Platkowski, K., A. Pross, and K.H. Reichert, *Polym. Int.* , **1998**, 45(2), 229-238.

223. Kobyakova, K.O., V.F. Gromov, and E.N. Teleshov, *Polym. Sci.*, **1993**, 35(2), 151-155.

224. HernandezBarajas, J. and D.J. Hunkeler, *Polymer*, **1997**, 38(2), 437-447.

225. Hunkeler, D., A.E. Hamielec, and W. Baade, *Polymer*, **1989**, 30(1), 127-142.

226. Thickett, S.C. and R.D. Gilbert, *Macromolecules*, **2007**, 40, 4710-4720.

227. Alshahib, W.A.G. and A.S. Dunn, *Polymer*, **1980**, 21(4), 429-431.

228. Nomura, M. and K. Fujita, *Makromol. Chem. Rapid*, **1989**, 10(11), 581-587.

229. Asua, J.M., et al., *Journal of Polymer Science Part a-Polymer Chemistry*, **1989**, 27(11), 3569-3587.

230. Alduncin, J.A., et al., *J. Polym. Sci., Part A: Polym. Chem.*, **1991**, 29(9), 1265-1270.

231. Luo, Y. and F. Schork, *J. Polym. Sci., Part A: Polym. Chem.*, **2002**, 40(19), 3200-3211.

232. Nomura, M. and K. Suzuki, *Ind. Eng. Chem. Res.* , **2005**, 44(8), 2561-2567.

233. Autran, C., J.C. de la Cal, and J.M. Asua, *Macromolecules*, **2007**, 40(17), 6233-6238.

234. Espin, J.C., C. Soler-Rivas, and H.J. Wichers, *J. Agric. Food. Chem.*, **2000**, 48(3), 648-656.

235. Schwarz, K., et al., *Eur. Food Res. Technol.*, **2001**, 212(3), 319-328.

236. Thickett, S.C. and R.G. Gilbert, *Macromolecules*, **2006**, 39(6), 2081-2091.

237. Thickett, S.C. and R.G. Gilbert, *Macromolecules*, **2006**, 39(19), 6495-6504.

238. Asua, J.M., *Macromolecules*, **2003**, 36(16), 6245-6251.

239. Bickerstaff, G.F. and SpringerLink, *Immobilization of enzymes and cells*. 1997: Humana Press Totowa, NJ.

240. Lifshitz, I.M. and V.V. Slyozov, *J. Phys. Chem. Solids*, **1961**, 19(1-2), 35-50.

241. Kabalnov, A.S. and E.D. Shchukin, *Adv. Colloid Interface Sci.* , **1992**, 38, 69-97.

242. Finsy, R., *Langmuir*, **2004**, 20(7), 2975-2976.

243. Qiu, J., B. Charleux, and K. Matyjaszewski, *Prog. Polym. Sci.* , **2001**, 26(10), 2083-2134.

244. Barner-Kowollik, C., et al., *J. Polym. Sci., Part A: Polym. Chem.*, **2001**, 39, 1353-1365.

245. Vana, P., T.P. Davis, and C. Barner-Kowollik, *Macromol. Theory Simul.* , **2002**, 11(8), 823-835.